

SUBMARINE POWER CABLE TRANSMISSION LINE PARAMETERS AND
PERFORMANCE

by

Aaron M. MacNeill

Submitted in partial fulfilment of the requirements
for the degree of Master of Applied Science

at

Dalhousie University
Halifax, Nova Scotia
August 2012

© Copyright by Aaron M. MacNeill, 2012

DALHOUSIE UNIVERSITY

DEPARTMENT OF ELECTRICAL AND COMPUTER ENGINEERING

The undersigned hereby certify that they have read and recommend to the Faculty of Graduate Studies for acceptance a thesis entitled “SUBMARINE POWER CABLE TRANSMISSION LINE PARAMETERS AND PERFORMANCE” by Aaron M. MacNeill in partial fulfilment of the requirements for the degree of Master of Applied Science.

Dated: August 1st 2012

Supervisor: _____

Readers: _____

DALHOUSIE UNIVERSITY

DATE: August 1st 2012

AUTHOR: Aaron M. MacNeill

TITLE: Submarine Power Cable Transmission Line Parameters and Performance

DEPARTMENT OR SCHOOL: Department of Electrical and Computer Engineering

DEGREE: MAsc CONVOCATION: May YEAR: 2013

Permission is herewith granted to Dalhousie University to circulate and to have copied for non-commercial purposes, at its discretion, the above title upon the request of individuals or institutions. I understand that my thesis will be electronically available to the public.

The author reserves other publication rights, and neither the thesis nor extensive extracts from it may be printed or otherwise reproduced without the author's written permission.

The author attests that permission has been obtained for the use of any copyrighted material appearing in the thesis (other than the brief excerpts requiring only proper acknowledgement in scholarly writing), and that all such use is clearly acknowledged.

Signature of Author

Dedication

This thesis is dedicated to my parents, whose love and guidance has made me the person that I am today. They have helped me recognize the better parts of myself and have inspired me to be more than I am.

Table of Contents

List of Tables	ix
List of Figures	x
Abstract	xiii
List of Symbols and Abbreviations Used	xiv
Acknowledgments	xv
Chapter 1: Introduction	1
1.1 Thesis Objective.....	1
1.2 Thesis Contribution.....	2
1.3 Thesis Outline.....	2
Chapter 2: Submarine Cable Construction	4
2.1 Introduction.....	4
2.2 Submarine Cable Components.....	5
2.2.1 Core Conductor.....	5
2.2.2 The Insulation.....	9
2.2.3 The Sheath.....	10
2.2.4 The Armor.....	11
2.2.5 The Sea Water.....	12
2.3 Cable Configurations.....	12
2.4 Cable Model Used For Analysis.....	14
2.5 Magnetic Field Effects on Submarine Life.....	17
2.6 Design Summary.....	17

Chapter 3: Electromagnetic Analysis	19
3.1 Introduction.....	19
3.2 The Wave Equation.....	20
3.3 The Imperfect Coaxial Cable.....	22
3.4 Surface Impedances.....	24
3.4.1 Solid Conductor.....	24
3.4.2 Indefinite Conductor.....	25
3.4.3 Hollow Cylindrical Shells.....	25
3.5 Impedance of Single Core Conductor.....	27
3.5.1 Composition of Impedances.....	27
3.5.2 Application to Submarine Cables.....	29
3.6 Impedance of Three-Core Cable.....	31
3.6.1 Magnetic Field Outside Three Conductor Bundle.....	32
3.6.2 Inductance of Three-Core Cable.....	34
3.7 Admittance of Submarine Cables.....	36
3.7.1 Admittance of Single Core Cables.....	36
3.7.2 Admittance of Three-Core Cables.....	38
3.8 Resistance of Three-Core Cables.....	41
Chapter 4: Network Analysis	42
4.1 Introduction.....	42
4.2 Two Port Networks.....	42
4.3 Steady State Performance Analysis.....	46
4.4 Transient State Performance Analysis.....	48

Chapter 5: Submarine Transmission Line Parameters Simulation and

Discussion	51
5.1 Single-Core Cable Line Parameter Analysis.....	51
5.1.1 Single-Core Cable Line Parameters Case Study.....	51
5.1.1.1 Submarine Cable Type A.....	52
5.1.1.2 Submarine Cable Type B.....	54
5.1.1.3 Submarine Cable Type C.....	55
5.1.2 Effects of the Cable Layer Thickness.....	55
5.1.2.1 Lead Sheath and Copper Armor.....	56
5.1.2.2 Lead Sheath and Steel Armor.....	62
5.1.3 Model Accuracy.....	67
5.2 Three-Core Cable Line Parameter Analysis.....	69
5.2.1 Magnetic Field Analysis.....	69
5.2.2 Three-Core Cable Line Parameters Case Study.....	72
5.2.2.1 Submarine Cable Type D.....	72
5.2.2.2 Submarine Cable Type E.....	73
5.2.2.3 Submarine Cable Type F.....	74
Chapter 6: Submarine Transmission Line Performance Analysis	75
6.1 Steady State Analysis.....	75
6.1.1 Submarine Cable Type B Performance.....	76
6.1.2 Submarine Cable Type E Performance.....	82
6.2 Transient Analysis.....	87

Chapter 7: Conclusion and Future Work	92
7.1 Conclusions.....	92
7.2 Future Work.....	93
References	94

List of Tables

Table 2-1: Electrical Material Properties.....	16
Table 2-2: Submarine Power Cable Material Choices.....	18
Table 5-1: Different Cable Geometries, Single-Core Cable.....	52
Table 5-2: Cable Type A Line Parameters.....	54
Table 5-3: Cable Type B Line Parameters.....	54
Table 5-4: Cable Type C Line Parameters.....	55
Table 5-5: Different Cable Geometries, Three-Core Cable.....	72
Table 5-6: Cable Type D Line Parameters.....	73
Table 5-7: Cable Type E Line Parameters.....	74
Table 5-8: Cable Type F Line Parameters.....	74
Table 6-1: Line Parameters Per Unit Length for Cable Type B and E.....	76

List of Figures

Figure 2-1: (a) Solid Core (b) Stranded (c) Profiled (d) Segmental.....	8
Figure 2-2: (a) Single Core Cable (b) Triple Core Cable (c) Dual Core Cable.....	13
Figure 2-3: (a) Single Core Cable Model (b) Triple Core Cable Model (c) Two Core Cable Model.....	15
Figure 3-1: Multiple Layers of Cylindrical Shell Conductors.....	28
Figure 3-2: Equivalent Layers of Cylindrical Shells of a Single Core Submarine Cable.....	30
Figure 3-3: Geometry of Three-Core Cable.....	33
Figure 3-4: Inductance Network Per Phase.....	35
Figure 3-5: Method of Images Geometry.....	39
Figure 4-1: Network Used for Two-Port Analysis.....	43
Figure 4-2: Real and Reactive Power Diagram.....	46
Figure 4-3: Equivalent Circuit For Transient Analysis.....	49
Figure 5-1: Capacitance Per Unit Length As Armor Thickness Varies, 3.1mm Sheath.....	56
Figure 5-2: Inductance Per Unit Length As Armor Thickness Varies, 3.1mm Sheath.....	57
Figure 5-3: Resistance Per Unit Length As Armor Thickness Varies, 3.1mm Sheath.....	57
Figure 5-4: Capacitance Per Unit Length As Armor Thickness Varies, 2mm Sheath.....	58
Figure 5-5: Inductance Per Unit Length As Armor Thickness Varies, 2mm Sheath.....	58
Figure 5-6: Resistance Per Unit Length As Armor Thickness Varies, 2mm Sheath.....	59

Figure 5-7: Capacitance Per Unit Length As Armor Thickness Varies, 4mm Sheath.....	59
Figure 5-8: Inductance Per Unit Length As Armor Thickness Varies, 4mm Sheath.....	60
Figure 5-9: Resistance Per Unit Length As Armor Thickness Varies, 4mm Sheath.....	60
Figure 5-10: Inductance Per Unit Length As Armor Thickness Varies, 3.1mm Sheath.....	63
Figure 5-11: Resistance Per Unit Length As Armor Thickness Varies, 3.1mm Sheath.....	63
Figure 5-12: Inductance Per Unit Length As Armor Thickness Varies, 2mm Sheath.....	64
Figure 5-13: Resistance Per Unit Length As Armor Thickness Varies, 2mm Sheath.....	64
Figure 5-14: Inductance Per Unit Length As Armor Thickness Varies, 4mm Sheath.....	65
Figure 5-15: Resistance Per Unit Length As Armor Thickness Varies, 4mm Sheath.....	65
Figure 5-16: Resistance Error of Sea Water.....	68
Figure 5-17: Reactance Error of Sea Water.....	68
Figure 5-18: Magnetic Field Decay Surrounding Three-Core Cable.....	70
Figure 5-19: Magnetic Field Decay Surrounding Single-Core Cable.....	71
Figure 6-1: Receiving End Impedance Magnitude, Cable Type B.....	77
Figure 6-2: Receiving End Impedance Angle, Cable Type B.....	77
Figure 6-3: Receiving End Voltage Magnitude, Cable Type B.....	78
Figure 6-4: Receiving End Voltage Angle, Cable Type B.....	78
Figure 6-5: Receiving End Power, Cable Type B.....	79
Figure 6-6: Receiving End Reactive Power, Cable Type B.....	79

Figure 6-7: Transmission Line Efficiency, Cable Type B.....	80
Figure 6-8: Transmission Line Voltage Regulation, Cable Type B.....	80
Figure 6-9: Receiving End Power Factor, Cable Type B.....	81
Figure 6-10: Receiving End Impedance Magnitude, Cable Type E.....	82
Figure 6-11: Receiving End Impedance Angle, Cable Type E.....	83
Figure 6-12: Receiving End Voltage Magnitude, Cable Type E.....	83
Figure 6-13: Receiving End Voltage Angle, Cable Type E.....	84
Figure 6-14: Receiving End Power, Cable Type E.....	84
Figure 6-15: Receiving End Reactive Power, Cable Type E.....	85
Figure 6-16: Transmission Line Efficiency, Cable Type E.....	85
Figure 6-17: Transmission Line Voltage Regulation, Cable Type E.....	86
Figure 6-18: Receiving End Power Factor, Cable Type E.....	86
Figure 6-19: Transient Current Flow at 0° Phase Angle.....	88
Figure 6-20: Transient Receiving End Voltage at 0° Phase Angle.....	88
Figure 6-21: Transient Apparent Power at 0° Phase Angle.....	88
Figure 6-22: Transient Current Flow at 30° Phase Angle.....	88
Figure 6-23: Transient Receiving End Voltage at 30° Phase Angle.....	90
Figure 6-24: Transient Apparent Power at 30° Phase Angle.....	90

Abstract

Submarine power production installations use the power of the ocean to generate renewable energy for the population to use. To bring this electricity back to land, use of electrical cables is required. The choice of cable will affect both the quality of received power and the security of the transmission line.

To find the inductance and capacitance of these submarine transmission lines, a study of the electric and magnetic fields that are produced due to the power flow on these cables must be performed. The armor that is used to protect the cable from underwater hazards is significant in determining the cable losses and finding the equivalent inductance and capacitance.

Finding the inductance and capacitance of the submarine cable will allow for the determination of the two port parameters of the cable. These parameters will allow for the analysis of the transient and steady state performance of the cable.

List of Abbreviations and Symbols Used

σ	Conductivity
R	Resistance
I	Electric Current
δ	Skin Depth
f	Frequency
ω	Angular Frequency
μ_0	Permeability of Free Space
μ_r	Relative Permeability
μ	Permeability of a Material
B	Magnetic Field Intensity
ϵ_0	Permittivity of Free Space
ϵ_r	Relative Permittivity
ϵ	Permittivity of a Material
E	Electric Field Intensity
Γ	Propagation Constant
Z	Impedance
Y	Admittance
L	Inductance
C	Capacitance
G	Conductance
γ	Intrinsic Propagation Constant
η	Intrinsic Impedance of a Material
ψ	Magnetic Flux
V	Voltage
Z_0	Characteristic Impedance
δ_{PF}	Power Factor
P	Real Power
Q	Reactive Power
S	Apparent Power
κ	Efficiency

Acknowledgements

I would first like to thank my research supervisor, Dr. Mohamed El-Hawary for his guidance, help, and support throughout the entirety of my masters program.

I would like to acknowledge Ghanashyam Ranjitkar from NRCAN for his support.

I would like to acknowledge Dr. William Phillips and Dr. Timothy Little for serving on my supervisory committee.

I would like to thank Shadi Shehadeh, PhD candidate, for listening and providing useful suggestions for my work.

I would like to thank my friends and colleagues, without them I would not have been able to complete my work.

Finally, I would like to express my love and gratitude to my parents. They have provided me with the means, motivation, and support to achieve my goals. Their love and support have made me the person I am today.

Chapter 1: Introduction

Submarine power production installations use the power of the ocean to generate renewable energy for the population to use. To bring this electricity back to land, use of electrical cables is required. The choice of cable will affect both the quality of received power and the security of the transmission line. There are various cable types that could be used to transmit the power from the ocean to land. In order to determine how good the various cables are at transmitting the electrical power, the line parameters of the cable must be studied. These line parameters are found from studying the magnetic and electric field that exist around the cable. It turns out that the line parameters are solely dependent on the materials used and geometry of the cable. This has the implication that by varying the materials and geometry used for the different cable layers that the quality of the power at the receiving end of the transmission line can be controlled.

1.1 Thesis Objectives

The objective of this research is to study the line parameters for various types of submarine cables that are used to transmit electrical power from the ocean to land. This is necessary in order to study the performance of the transmission link between the ocean and shore. The performance of the transmission link is determined by the efficiency, voltage regulation, and reactive power requirements of the line. In addition to studying the performance for various types of submarine cables, the effects from the various cable layers will be examined. This work will allow for the analysis of what reactive power support will be required to improve the quality of the power when it gets to shore. It will also allow for the modeling of the generators' interaction with the transmission line to

determine if resonances will occur. Modeling of offshore power generation interconnection can also be performed. This allows for designing cables that would result in optimal power flows to land and minimize magnetic field effects on the submarine life.

1.2 Thesis Contribution

In this work, the analysis of submarine power cable line parameters is considered. A MatlabTM program is developed to determine the line parameters for various submarine cable types, materials, and geometries. The author's contribution to this work includes gathering all information concerning submarine power cable design, performing the analytical analysis for the various cable types, and carrying out the numerical simulations.

1.3 Thesis Outline

The work in this thesis is organized as follows:

Chapter 2 introduces a brief description of the different kinds of submarine power cables and how they are different from overhead transmission lines. The different layers in a submarine cable are discussed and the generic geometrical model for a submarine cable is developed. The cables' magnetic field effects on undersea life are also discussed.

Chapter 3 introduces the electromagnetic field theory that is required to derive the surface impedances of cylindrical shells. This is extended to finding the total impedance of multiple cylindrical shell layers of insulation or conductors.

Chapter 4 introduces steady state two-port network theory that is used to find the receiving end voltage, power, reactive power, efficiency, and voltage regulation. It also introduces the transient response of the transmission line.

Chapter 5 finds the various line parameters for different kinds of single-core and three-core submarine cables. The effect that the different cable layers have on the impedance of the cable is also examined.

Chapter 6 finds the various steady state response values for the receiving end of the transmission line. This analysis is performed for various types of submarine cables. Finally, the transient response of the transmission line when a generating source is connected at the sending end is analyzed.

Finally, Chapter 7 presents the conclusion of the research and proposes possibilities for future endeavors in this field of study.

Chapter 2: Submarine Cable Construction

This chapter provides a brief overview of submarine cable design considerations, different cable configurations, and the cable electrical properties. From this, a generic geometrical model is developed for different possible cable configurations.

2.1 Introduction

There is a fundamental difference between transmitting electrical power through conductors suspended in air versus in underwater cables. For overhead transmission lines a bare conductor is used to transmit electrical power since air is a good natural insulator. An electrically conductive substance, such as salt water, on the other hand surrounds submarine cables. An electrical insulator must surround the core conductor of the submarine cable; this confines the current flow to the core conductor and not the seawater surrounding it. Without insulation surrounding the core conductor there would be significant electrical power loss to the body of water surrounding it. So the insulation can be thought of as keeping the electrical power flowing through the conductor and not in the body of water surrounding it. The insulation material commonly used is susceptible to water damage and must then be protected from water and humidity [2]. A metallic or polymer sheath is added around the insulation; its purpose is to keep water and water vapor from reaching the insulation [2]. Finally, a layer is required to protect the cable from uncontrolled external causes of possible damage [2]. There are many considerations in designing these different layers of the cable. The differences between cable constructions have drastic effects on the parameters for submarine power cables.

Submarine power cables are used in both AC and DC underwater power transmission systems. There are different cable configurations that can be used for the AC or DC applications. For AC, either three single core cables or a single three-core cable can be used [2]. For DC, either two single core cables or a single two-core cable can be used [2]. The choice of which cable configuration to use is an important design choice issue.

All of these design considerations will be discussed in further detail in subsequent sections. A generic geometric model for the different cable configurations is also developed. This geometric model will be used to develop the electromagnetic models used to find the inductance and capacitance of different cable configurations.

2.2 Submarine Cable Components

A submarine cable is very different from an overhead transmission line. An overhead transmission line for the most part is a bare copper or aluminum or composite design conductor. A submarine cable has many more components associated with it such as: the core conductor, the insulation, the sheath, the armor, and the fact that an electrically conductive liquid surrounds the cable [2]. The reasoning for requiring these extra components and their design considerations will be discussed in this chapter.

2.2.1 Core conductor

For any cable overhead or underwater the properties of the core conductor are vital in determining its efficiency. There are many design considerations to take into account

when choosing a conductor to use for an application. These factors include: conductor material, skin, and proximity effects, and the geometry/manufacturing of the conductor.

The choice of the conductor material has a direct relation to how large the conductor surface area must be. To compare between two commonly used conductor materials aluminum and copper; if material A is aluminum which has a resistivity of $2.82e-8$ and if material B is copper which has a resistivity of $1.68e-8$. Then it can be seen that $A_B = 0.596 * A_A$ [4]. This means that the required cross sectional area of the aluminum conductor would be significantly larger than that of the copper conductor. For transmission lines, the conductors will inherently require large cross sectional areas so as to minimize power losses and making the transmission line more efficient. So if an aluminum and copper conductor were required to carry the same current; then the aluminum conductor would require a larger cross sectional area than the copper conductor. Due to this, copper conductors are generally used in submarine cables as opposed to aluminum since the cross sectional area is desired to be smaller.

Skin effect is the tendency for high frequency electromagnetic waves to concentrate in a ring around the inner-outside edge of a conductor. This causes the current flow to mainly exist in this outer ring. This will increase the resistance of the conductor because the cross sectional area is effectively reduced. The skin depth is defined as the distance inward from the outer conductor edge in which the original wave amplitude is diminished by e^{-1} , which is approximately 37% of its value at the outer edge of the conductor. This skin depth can be found as follows [4]:

$$\delta = \frac{1}{\sqrt{\pi f \mu \sigma}} \quad (2.1)$$

Where f is the frequency, μ is the permeability, and σ is the conductivity of the conductor. For a copper conductor at 60Hz, the skin depth is approximately 8.4 mm [4]. The skin effect can have a dramatic effect on the efficiency of the transmission line due to it increasing the resistance and hence the losses in the conductor.

The proximity effect is when an external electromagnetic field attracts the electrical current to one side of the conductor. The current gets pushed to one side of the cable, which increases the resistance of the conductor by making the cross sectional area effectively smaller. Similar to skin effect, this can have a dramatic effect on the efficiency of a transmission line so placement of the cables must be taken into consideration.

The core conductor for a submarine cable can be manufactured in one of the following forms, solid core, compressed strands of copper wire, profiled, or segmental [2]. Solid core conductors are generally used for cables in the lower voltage class and require a cross sectional area of 400 mm² or lower [2]. Compressed stranded wire conductors are most often used for submarine cable conductors [2]. These types of conductors are used when larger surface areas are required. This formation can achieve a 92% filling factor [2]. The filling factor compares the effective cross sectional area of a stranded conductor to that of a solid conductor. If the outer diameters of the stranded conductor and solid conductor are equivalent, then the stranded conductor will have 92% the surface area of the solid conductor. Stranded conductors can be used to reduce the impact that the

proximity effect will have on current flow [2]. This is achieved by introducing a thin insulating medium between the conductor strands, which separates them electrically [2]. This keeps current from being pushed outside of each of the individual strands of wire. Using this type of conductor cannot reduce the skin effect [2]. A drawback of this conductor is the increased resistivity due to it being cold worked [2]. Profiled conductors are made from cake-piece-shaped wire cross sections, and can have a filling factor of 96% or larger [2]. These cables can be made to form almost any shape, and the conductor does not require cold working, which results in a lower resistivity [2]. This type of conductor is used for large HVDC submarine cables [2]. The segmental conductor, also known as the Milliken conductor, is a cable formation that will allow for the decreased impact of the skin effect [2]. It does this by taking a stranded wire conductor and cutting it into cake-slice shapes [2]. Each slice is then insulated from the neighboring slice [2]. The way the wires are twisted in the Milliken conductor cancels out the skin effect to a large extent [2]. There are many advantages and disadvantages associated with each conductor type, however, economic and practical reasoning help in narrowing down which conductor is best to use for a submarine cable application. See Figure 2-1 for diagrams of each different kind of conductor.

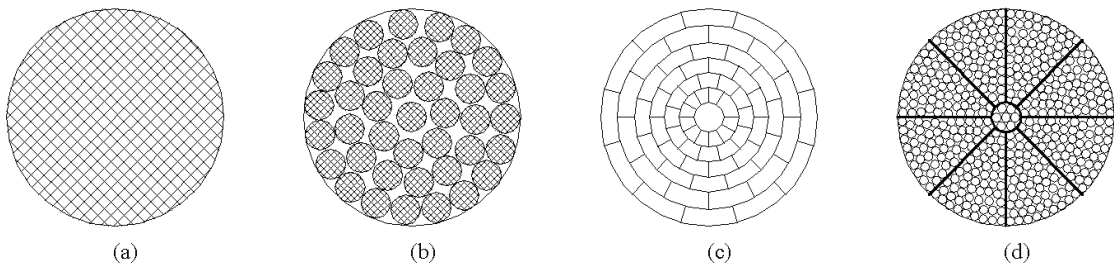


Figure 2-1 (a) Solid Core (b) Stranded (c) Profiled (d) Segmental [2]

2.2.2 The Insulation

Insulation is a layer placed between the core conductor and the sheath of the cable to provide a barrier between high and low potential surfaces. This is important because it prevents a current flow, which is orthogonal to the conductor. It is desired to have a totally longitudinal current flow, which means that all the current flows from the sending to the receiving end of the transmission line via the core conductor. The insulation material currently being used most for submarine power cables is cross-linked polyethylene or XLPE [2]. XLPE insulation has been proven over the years to be a material that is not affected by being surrounded by water [2]. When XLPE cables were first used, they had issues of water-trees that formed in the insulation [2]. The water-trees compromise the insulating properties of the dielectric and would lead to electric breakdown of the material [2]. Research in the area has proven that water trees only form if there are contaminants in the material, not because the material is affected by being submerged in water [2]. With better manufacturing techniques the water-tree issue can be reduced or eliminated [2]. XLPE has been chosen as the best insulating medium to use because it can operate at high temperatures and it is capable of providing good insulation even for high voltage applications [2]. Deviations from operating at rated temperature and rated voltage have a dramatic effect on the life expectancy of the insulation [2]. Humidity is another factor that will affect the life expectancy of the insulation material [2]. Even though the material may prevent water intrusion, it is still vulnerable to humidity [2]. The choice of sheath material affects humidity intrusion, however if humidity cannot be totally prevented from reaching the insulation material then the other layers of the cable must be very effective at preventing water intrusion [2]. Water

intrusion and operating closely to the rated values of voltage and temperature are important in maintaining the life of the insulation [2].

2.2.3 The Sheath

The sheath is a metallic layer outside the insulation, which acts as a barrier to prevent water from reaching the insulation [2]. The sheath is usually made of one of the following metals: lead, aluminum, or copper [2]. Lead is the ideal sheath metal because it can completely keep moisture away from the insulation [2]. The lead also adds weight to the cable, which can improve the seafloor stability of the cable [2]. A drawback of using lead is that it is soft and can be easily damaged during transport or laying of the cable [2]. Aluminum and copper sheaths are used depending on the application; these metals are much stronger than lead in terms of resisting mechanical fatigue [2]. The drawback of these sheaths is in how they are applied to the cable. A seam will be formed when the sheath is put on over the insulation. This will allow humidity to penetrate through the sheath [2]. If the sheath is to be grounded then the thickness and material chosen for the sheath are significant. If the sheath is grounded it will be carrying a portion of the return current, so the cross sectional area of the sheath must be approximately the same as that of the core conductor [2]. The choice of which sheath material to use is dependent on which cable configuration is going to be used, a single core conductor cable or multi core conductor cables [2]. The choice of sheath material is also dependent on which material is being used for the cables armor, as discussed in the next section. For a multi-conductor cable there are usually sheaths around each of the core conductors' insulation and a sheath around the total bundle of conductors [2].

2.2.4 The Armor

The armor is a layer or multiple layers of steel or copper round wire that comprises the outermost layers of the cable. It is used to protect the cable against any mechanical damage such as the tensional forces produced when laying the cable, or external random sources [2]. The material used for the armor depends on if the cable has one or three core conductors [2]. Steel is an iron-based material, and thus it is susceptible to having a larger magnetically induced voltage when in the presence of an alternating magnetic field. Copper is a nonmagnetic material so it is less affected when it is in a magnetic field. For a single core conductor there will be a magnetic field existing outside the core conductor. In free space the magnetic field outside a single conductor is proportional to the current flowing through the conductor, as given by the following relationship [4]:

$$B = \frac{\mu_0 I}{2\pi r} \quad (2.2)$$

Where B is the magnetic field density, I is the current flowing in the wire, and r is the radial distance away from the wire. For a balanced three-phase system the phase currents meet the following constraint:

$$I_A + I_B + I_C = I_A + I_A * e^{j\frac{2\pi}{3}} + I_A * e^{j\frac{4\pi}{3}} = 0 \quad (2.3)$$

This means that the magnitudes of all phase currents are equal but are out of phase by 120 degrees. If the three conductors in the cable are assumed to be close together, then the magnetic field outside of this bundle will cancel out as follows:

$$B_T = \frac{\mu_0}{2\pi r} \left(I_A + I_A * e^{j\frac{2\pi}{3}} + I_A * e^{j\frac{4\pi}{3}} \right) = 0 \quad (2.4)$$

The approximation that the conductors are very small and very close to each other is partially valid in that the magnetic field outside the three conductor bundle will be drastically reduced in comparison with the magnetic field that will exist outside a single

conductor cable [2]. The existence of a magnetic field outside the single core conductor means that there will be extra losses associated with the cable if steel armor is used. Ideally copper armor is used but this increases the cost of cable. The minimized magnetic field that will exist outside a three-conductor cable means that minimal losses will be associated with using steel armor [2]. The type of cable chosen and economics are the factors that determine which material will be used for the cables armor.

2.2.5 The Sea Water

The seawater surrounding the cables is most often used as the return path, or ground for the cable. Single wire earth return is the grounding system most commonly used for submarine transmission lines. The massive size of the body of water the cable will be in, in combination with the fact that sea water is a good electrical conductor means that the impedance of the water is negligibly small. If the resistivity of the material is finite and the surface area of the conductive material approaches infinity then the resistance will be zero. This makes the application of single wire ground return a viable grounding technique.

2.3 Cable Configurations

There are two different submarine cable layouts that are used for both AC and DC applications. These two layouts are either using multiple single core conductors or a single multiple core conductor. For AC applications, three single core conductors or one three-core conductor would be used [2]. For DC applications, two single core conductors

or one two-core conductor would be used [2]. Figure 2-2 shows what the cross section of a single, dual, or triple conductor cable would look like.

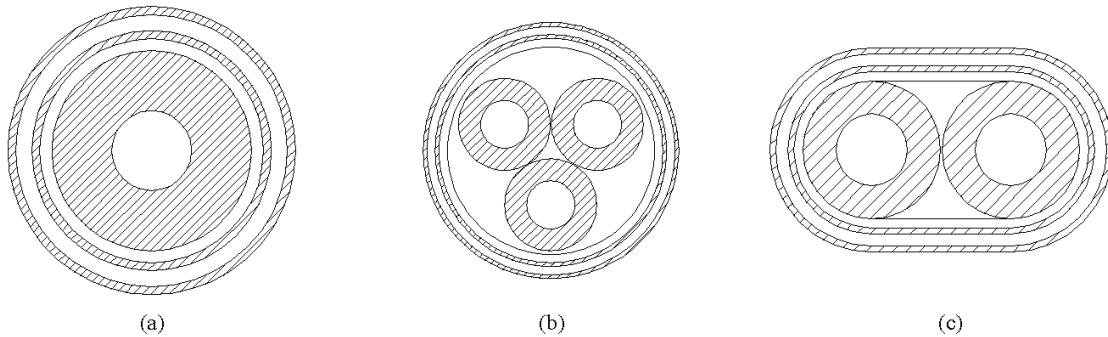


Figure 2-2 (a) Single Core Cable (b) Triple Core Cable (c) Dual Core Cable [2]

There are advantages and disadvantages associated with the choice of using either multiple or single core conductor cables. Common considerations for single and multiple core cables are: the trench characteristics, heat production/dissipation, cost, voltage class, and difficulty of laying the cable [2]. Three core conductor cables are generally more expensive than three single core counterpart; they are only made for use in medium voltage applications; they do not dissipate heat as well as three separate cables; they have a limited bending radius because the cable has a large diameter; they only require a single underwater trench to lay the cable; unforeseen incidents can ruin the entire cable resulting in a costly complete replacement of the cable [2]. Single core conductor cables are cheaper and can be used for high voltage applications; they dissipate heat better than three core cables; they are more flexible due to the cable having a smaller diameter; they require three underwater trenches to lay the cable; unforeseen incidents are unlikely to damage more than one of the cables at a time [2]. For AC cables a consideration for choosing a single or multiple core cable are the eddy current losses in the steel armor.

Eddy currents are electrical currents that are induced in electrical conductors, such as steel, due to the presence of a varying magnetic field [4,11,15]. In a three-core conductor the magnetic field around the steel armor will for the most part cancel out. This results in reduced eddy currents in the steel armor, which means that there will be little energy loss in the armor. For a single conductor with steel armor there would be no magnetic field cancellation, thus eddy currents will be induced and cause larger losses of energy in the armor [2,15]. Due to this, the three-core conductor will have fewer losses associated with it. When single core cables are laid in the water, they are separated by significant distance so as to minimize the probability of multiple cables being damaged by the same unforeseen incident [2]. Usually with the single core cables a fourth back up cable will be laid to mitigate the effects of failure of one of the other phases [2].

2.4 Cable Model Used for Analysis

The above considerations for the design and choice of a submarine cable help to determine which materials will be used for the different layers of the cable and which configuration will be used. A general geometric model for the cross section of the different cable configurations can be developed as shown in Figure 2-3.

The assumptions made when using this model are as follows [2,4,5]: the cables materials are homogenous, the core conductor is solid, the armor is a solid annulus, and the cable is surrounded by an infinite seawater medium.

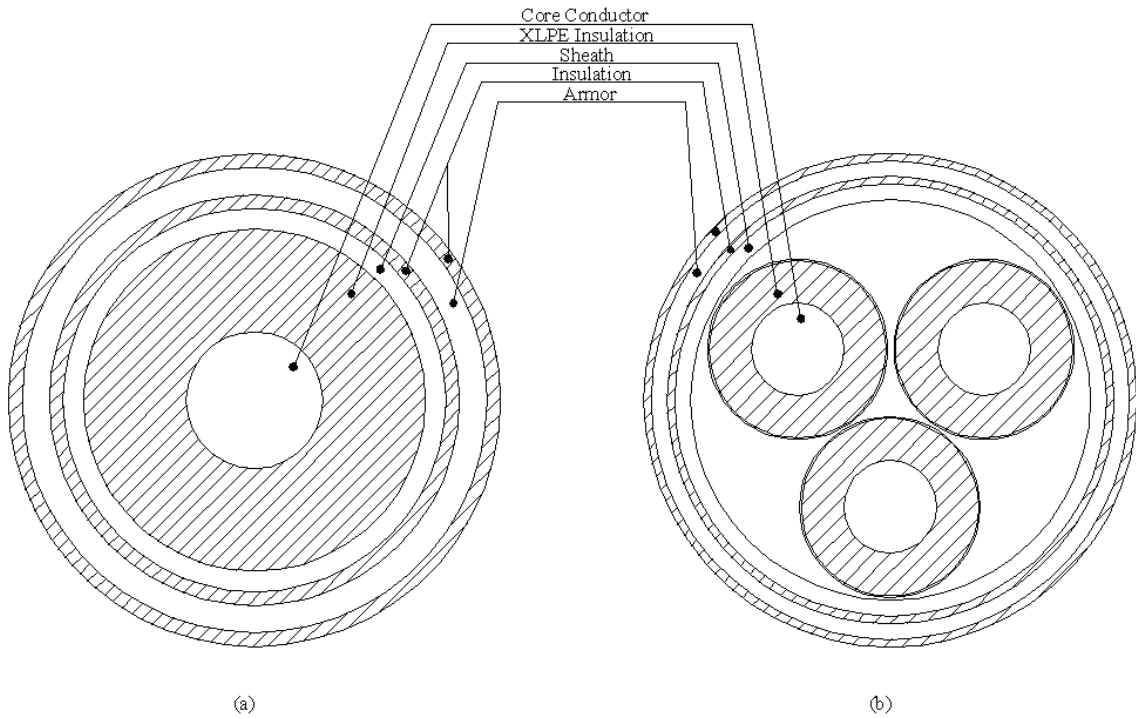


Figure 2-3 (a) Single Core Cable Model (b) Triple Core Cable Model [2]

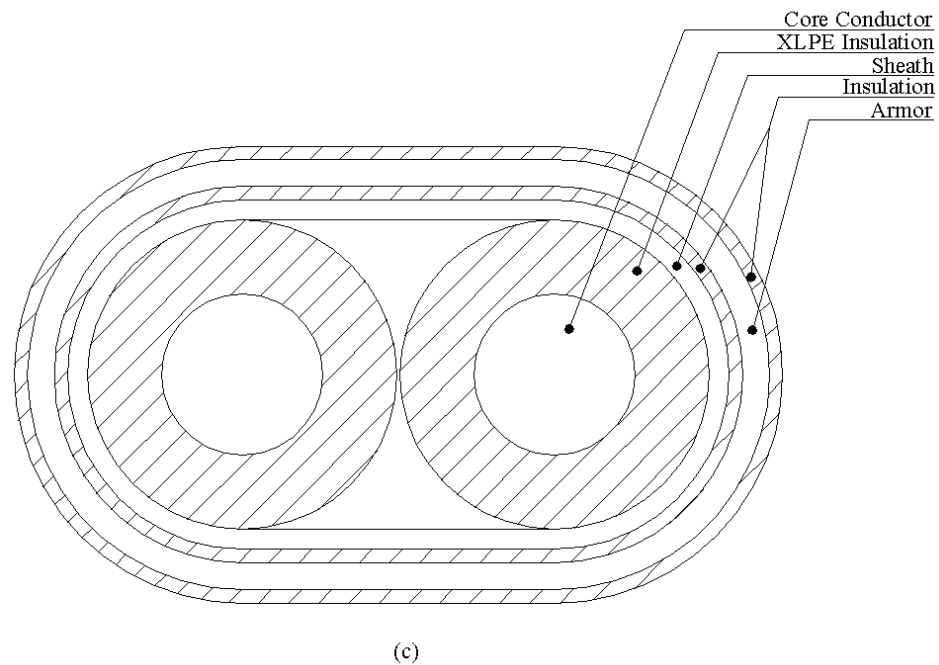


Figure 2-3 (c) Two Core Cable Model [2]

Assuming that the conductor is solid can be accounted for by using an effective resistivity of the core conductor material assuming that the solid core conductor has the same diameter as the actual one. Assuming that cable armor forms a solid annulus is a good approximation because the armor wires are pressed together rather closely and it is highly likely that there is electrical conductivity between all of the wires. The assumption of an infinite sea can be made when analyzing the transmission line parameters [5]. A cable half in water and half in soil can be approximated as being a cable totally surrounded by water [5]. Assuming the materials have uniform composition is important to allow assigning standard values for the resistivity, permittivity and permeability. In Table 2-1 typical values of electrical properties of various materials used in a submarine cable are shown.

Table 2-1: Electrical Material Properties [2,4]

	Conductors				Armor	Insulation	
	Copper	Aluminum	Lead	Sea Water	Steel	XLPE	Rubber
Conductivity	5.96e7	3.5e7	4.55e6	4.8	1e7	1e-14	1e-14
Permittivity	1	1	1	70	1	2.5	7
Permeability	1	1	1	1	100	1	1

The values of permittivity and permeability in this table are the relative value, ϵ_r and μ_r respectively. These relative permittivity and permeability values are related to the actual material properties as follows [4]:

$$\epsilon = \epsilon_0 * \epsilon_r \quad (2.8)$$

$$\mu = \mu_0 * \mu_r \quad (2.9)$$

Where the values ϵ_0 and μ_0 are called the permittivity and the permeability of free space respectively, these values are constants with the following values $\epsilon_0=8.85e-12$ and $\mu_0=1.2566e-6$ [4]. The properties of the materials govern how the electric fields and magnetic fields will

interact with the different materials, thus it is important to have good approximations for these values.

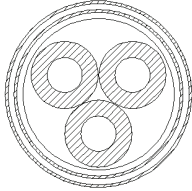
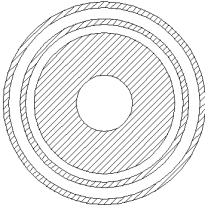
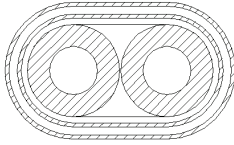
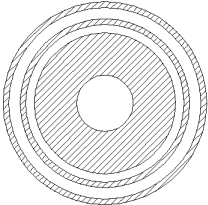
2.5 Magnetic Field Effects on Submarine Life

With large developments in offshore power production, the number of submarine cables will be increasing. This means that the presence of artificial, man-made, magnetic fields present in the ocean is increasing. These artificial magnetic fields, which are superimposed on the Earth's magnetic field, may influence spatial patterns in submarine life [17,18]. For submarine life that uses the Earth's natural magnetic field to navigate, the added magnetic field from cables could cause confusion of spatial orientation for submarine life. The magnetic field from the Earth is characterized by a DC magnetic field that has a flux of $60\mu\text{T}$ at the poles where the field lines are vertical, and a flux of $30\mu\text{T}$ at the equator where the field lines are horizontal [17]. Using a high permeability metal for the cables armor, bundling the conductor, smaller current loading, and burying the cables are a means to reduce the magnetic field that will be experienced by submarine life living in the water. The AC and DC magnetic fields affect submarine life in different ways. The DC magnetic field affects submarine life more significantly [18]. The magnetic field affects different species of submarine life in different ways, so a study of marine life in the area where a cable will be installed must be conducted [17].

2.6 Design Summary

In designing a submarine cable, there are many design considerations to account for. A summary of the design considerations mentioned earlier is shown in Table 2-2.

Table 2-2: Submarine Power Cable Material Choices [2]

	<u>AC</u>		<u>DC</u>	
	<u>Three Conductor</u>	<u>Single Conductor</u>	<u>Two Conductor</u>	<u>Single Conductor</u>
				
<u>Core Conductor</u>	Solid Stranded Profiled Segmental	Solid Stranded Profiled Segmental	Solid Stranded Profiled Segmental	Solid Stranded Profiled Segmental
<u>Insulator</u>	XLPE	XLPE	XLPE	XLPE
<u>Sheath</u>	Copper Aluminum Lead Polymer	Copper Aluminum Lead	Copper Aluminum Lead	Copper Aluminum Lead
<u>Aarmor</u>	Steel	Copper Steel	Steel	Steel

Chapter 3: Electromagnetic Analysis

This chapter provides an overview of the required electromagnetic analysis to derive expressions for the resistance, inductance, and capacitance for submarine cable configurations. The study of the wave equation, imperfect coaxial cables, and surface impedance of cylindrical shells provides useful insights as to how equivalent impedances can be found for a multi layered cable. This chapter provides the means to evaluate a cables line parameters based on the geometry of the cable and material properties.

3.1 Introduction

Submarine power cable total resistance, inductance, and capacitance found through electromagnetic analysis depend on the cables geometry and material properties. The circular symmetry of the magnetic field around a single core cable results in the ability to determine the exact surface impedance of cylindrical shell conductors [6]. This technique can be applied repeatedly to account for multiple layers of concentric cylindrical shells [5]. This allows us to find the net impedance of a multilayered cable. The asymmetry of the magnetic and electric field of a three-core cable results in greater complexity. Approximations of the impedances for the different cable layers can be used to find the total impedance of the cable. The analysis used to find the impedance of a three-core cable requires a numerical solution procedure because direct closed form expressions are difficult to compute.

3.2 The Wave Equation

In a linear, isotropic, homogenous, lossy dielectric, which is charge free, Maxwell's equations take on the following form [4,6,11].

$$\nabla E_S = 0 \quad (3.1)$$

$$\nabla H_S = 0 \quad (3.2)$$

$$\nabla \times E_S = -j\omega\mu H_S \quad (3.3)$$

$$\nabla \times H_S = (\sigma + j\omega\varepsilon) \quad (3.4)$$

Where ω is the angular frequency at which the wave is oscillating at, μ is the permeability of the material, ε is the permittivity of the material, and σ is the conductivity of the material. The divergence of a vector, ∇A , is defined in the cylindrical coordinate system as follows:

$$\nabla A = \frac{1}{\rho} \frac{\partial A_\rho}{\partial \rho} (\rho A_\rho) + \frac{1}{\rho} \frac{\partial A_\phi}{\partial \phi} + \frac{\partial A_z}{\partial z} \quad (3.5)$$

The curl of a vector, $\nabla \times A$, is defined in the cylindrical coordinate system as follows:

$$\nabla \times A = \widehat{a}_\rho \left[\frac{1}{\rho} \frac{\partial A_z}{\partial \phi} - \frac{\partial A_\phi}{\partial z} \right] + \widehat{a}_\phi \left[\frac{\partial A_\rho}{\partial z} - \frac{\partial A_z}{\partial \rho} \right] + \widehat{a}_z \frac{1}{\rho} \left[\frac{\partial(\rho A_\phi)}{\partial \rho} - \frac{\partial A_\rho}{\partial \phi} \right] \quad (3.6)$$

From these definitions, Maxwell's equations can be expressed in the following form [6]:

$$\frac{\partial H_z}{\rho \partial \phi} - \frac{\partial H_\phi}{\partial z} = (\sigma + j\omega\varepsilon) E_\rho \quad (3.7)$$

$$\frac{\partial H_\rho}{\partial z} - \frac{\partial H_z}{\partial \rho} = (\sigma + j\omega\varepsilon) E_\phi \quad (3.8)$$

$$\frac{1}{\rho} \left[\frac{\partial(\rho H_\phi)}{\partial \rho} - \frac{\partial H_\rho}{\partial \phi} \right] = (\sigma + j\omega\varepsilon) E_z \quad (3.9)$$

$$\frac{\partial E_z}{\rho \partial \phi} - \frac{\partial E_\phi}{\partial z} = (-j\omega\mu) H_\rho \quad (3.10)$$

$$\frac{\partial E_\rho}{\partial z} - \frac{\partial E_z}{\partial \rho} = (-j\omega\mu) H_\phi \quad (3.11)$$

$$\frac{1}{\rho} \left[\frac{\partial(\rho E_\phi)}{\partial \rho} - \frac{\partial E_\rho}{\partial \phi} \right] = (-j\omega\varepsilon)H_z \quad (3.12)$$

In the application of straight conductors it is known that fields are independent of the ϕ direction. This results in all partial derivatives with respect to this direction becoming zero. The equations that are left describe two specific cases, when the magnetic field is circular and when the electric field is circular [6]. It is known that the magnetic field around a straight conductor is circular in nature so the following set of Maxwell's equations are used [6]:

$$\frac{\partial H_\phi}{\partial z} = -(\sigma + j\omega\varepsilon)E_\rho \quad (3.13)$$

$$\frac{1}{\rho} \left[\frac{\partial(\rho H_\phi)}{\partial \rho} \right] = (\sigma + j\omega\varepsilon)E_z \quad (3.14)$$

$$\frac{\partial E_\rho}{\partial z} - \frac{\partial E_z}{\partial \rho} = (-j\omega\mu)H_\phi \quad (3.15)$$

Taking equations (3.13) and (3.14) and substituting them into equation (3.15) results in the following [6]:

$$\frac{\partial}{\partial \rho} \left[\frac{1}{\rho} \frac{\partial(\rho H_\phi)}{\partial \rho} \right] + \frac{\partial^2 H_\phi}{\partial z^2} = (\sigma\omega\mu j - \omega^2\varepsilon\mu)H_\phi \quad (3.16)$$

From here on out the term $(\sigma\omega\mu j - \omega^2\varepsilon\mu)$ will be denoted by γ^2 and is called the intrinsic propagation constant. The solution of equation (3.16) can be found by splitting it into two particular solutions, one solution as a function of z and the other solution as a function of ρ . It is known that the solution to each component has a term $e^{-\Gamma z}$ so it can be seen that the partial derivatives of any term with respect to z will have a $-\Gamma e^{-\Gamma z}$ term to replace it. This results in modified versions of equations (3.13), (3.14), and (3.15) as follows [6]:

$$\Gamma H_\phi = (\sigma + j\omega\varepsilon)E_\rho \quad (3.17)$$

$$\frac{1}{\rho} \left[\frac{\partial(\rho H_\phi)}{\partial \rho} \right] = (\sigma + j\omega\varepsilon)E_z \quad (3.18)$$

$$\Gamma E_\rho + \frac{\partial E_z}{\partial \rho} = (j\omega\mu)H_\phi \quad (3.19)$$

3.3 The Imperfect Coaxial Cable

In a coaxial cable with center core of radius b and outer conductor inner radius a ; equations (3.17), (3.18), and (3.19) can be combined together along with the fact that the circular magnetic field inside a coaxial cable, H_ϕ , takes the following form [4,6]:

$$H_\phi = \frac{I}{2\pi\rho} \quad (3.20)$$

Using equations (3.17) to (3.20) a solution for E_z takes the following form [6]:

$$E_z(\rho) = \frac{1}{2\pi} \left[j\omega\mu - \frac{\Gamma^2}{\sigma + j\omega\varepsilon} \right] I * \log\left(\frac{\rho}{b}\right) + A \quad (3.21)$$

From this equation it can be seen that E_z is proportional to I by a constant value that is only related to the geometry of the cable and the material properties. Looking at this equation when $\rho = b$ and $\rho = a$ will be equated to be the surface impedances for the inner conductor and outer conductor of the coaxial cable respectively [6].

$$E_z(b) = Z_b I \quad (3.22)$$

$$E_z(a) = Z_a I \quad (3.23)$$

Substituting equations (3.22) and (3.23) into equation (3.21) [6]:

$$A = Z_b I \quad (3.24)$$

$$\frac{1}{2\pi} \left[j\omega\mu - \frac{\Gamma^2}{\sigma + j\omega\varepsilon} \right] I * \log\left(\frac{a}{b}\right) + A = -Z_a I \quad (3.25)$$

Substituting equation (3.24) into (3.25) and solving using the knowledge of what the capacitance and inductance are between the coaxial conductors and that $\Gamma^2 = YZ$ results in the following definition to describe the total impedance of a coaxial cable [6,11].

$$Z = Z_a + Z_b + j\omega L_e \quad (3.26)$$

What this equation does, is it describes the total impedance of a coaxial cable as the sum of the two conductors' surface impedances and the impedance of the insulation separating them. As will be shown later on, this method can be applied to coaxial cylinders with multiple layers of conductors. Equations (3.17) to (3.19) can also be used to solve for a differential equation describing H_ϕ . This equation takes the following form [4,6,8]:

$$\frac{\partial^2 H_\phi}{\partial \rho^2} + \frac{1}{\rho} \frac{\partial H_\phi}{\partial \rho} - \frac{H_\phi}{\rho^2} = (\gamma^2 - \Gamma^2) H_\phi \quad (3.27)$$

In this equation the term $\gamma^2 - \Gamma^2$ can be simplified to just be equal to γ^2 since this value is significantly larger than Γ^2 . The solution to this differential equation is a first order Bessel function where [6,7],

$$H_\phi = AI_1(\gamma\rho) + BK_1(\gamma\rho) \quad (3.28)$$

Two properties of the first order Bessel functions can be used [6,7]

$$\frac{d}{dx}(x^n I_n) = x^n I_{n-1} \quad (3.29)$$

$$\frac{d}{dx}(x^n K_n) = -x^n K_{n-1} \quad (3.30)$$

Using the result of equation (3.28) and the two properties of (3.29) and (3.30) then equation (3.18) can be solved to find E_z in a similar form found in equation (3.28) [6]:

$$E_z = \eta[AI_0(\gamma\rho) - BK_0(\gamma\rho)] \quad (3.31)$$

$$\eta = \frac{\gamma}{\sigma + j\omega\epsilon} \quad (3.32)$$

Where the complex constant η will be referred to as the intrinsic impedance of the material.

3.4 Surface Impedances

Based on the analysis of Maxwell's equations for the particular case of a coaxial cable, it can be seen that the net impedance of a cable can be decomposed into the sum of the surface impedances of the conductor layers and the impedance of the insulation separating them. This technique can be further generalized to find the net (effective) impedance of a coaxial cable with many different layers of conductors and insulators.

3.4.1 Solid Conductor

From the results obtained in equations (3.28) and (3.31) a special case of surface impedance can be found for solid core conductor. Using the same geometry as before, where b is defined as the radius of the inner solid conductor of the coaxial cable, equation (3.28) can be written as [5]:

$$\frac{I}{2\pi b} = AI_1(\gamma b) \quad (3.33)$$

In this case the constant B is equal to zero because as the radius ρ approaches zero, the value of $K_1(\gamma\rho)$ will go to infinity [5]. Thus from equation (3.33) it can be seen that the constant A can be solved for which can then be applied to equation (3.31) [5]:

$$E_z = \frac{\eta}{2\pi b} \frac{I_0(\gamma b)}{I_1(\gamma b)} I \quad (3.34)$$

From this, the impedance of the core conductor can be found to be ratio of the electric field in the z direction to the current flowing through the conductor. The units of this impedance are ohms per meter.

$$Z_{solid\ core} = \frac{\eta}{2\pi b} \frac{I_0(\gamma b)}{I_1(\gamma b)} \quad (3.35)$$

3.4.2 Infinite Conductor

In the case of an infinite conductor with an internal radius, a, and outer radius which extends to infinity, the internal impedance of the conductor can be found in a manner similar to that used for a solid core conductor [5]. The difference this time is that the internal radius of the cylindrical shell is finite while the external radius tends to infinity. Due to this, the Bessel functions of the first kind approach infinity. This requires that the constant A approaches zero [5]. Using a similar methodology as for solid core conductors, the internal impedance can be found to be [5]:

$$Z_i = \frac{\eta}{2\pi a} \frac{K_0(\gamma a)}{K_1(\gamma a)} \quad (3.36)$$

3.4.3 Hollow cylindrical shells

In the case of a hollow conductor whose inner and outer radii are a and b respectively and has arbitrary current flowing on the internal and external surface of the conductor; and if the assumption is made that the total current flowing in the hollow conductor is equal to $I_a + I_b$ where the current component I_a flows inside the conductor and the rest flows outside [6]. The total current enclosed by the inner surface of the hollow conductor is $-I_a$ and the current enclosed by the outer surface of the conductor is I_b [6]. From this assumption and the use of the result of equations (3.20) and (3.28) [6]:

$$-\frac{I_a}{2\pi a} = AI_1(\gamma a) + BK_1(\gamma a) \quad (3.37)$$

$$\frac{I_b}{2\pi b} = AI_1(\gamma b) + BK_1(\gamma b) \quad (3.38)$$

From this the constants A and B can be found, and then substituted into equation (3.31) and from this the longitudinal electromotive intensity can be found at any point in the conductor. It can be shown that the values of A and B are [6]:

$$A = \frac{1}{I_1(\gamma b)K_1(\gamma a) - I_1(\gamma a)K_1(\gamma b)} \left[\frac{K_1(\gamma b)}{2\pi a} I_a + \frac{K_1(\gamma a)}{2\pi b} I_b \right] \quad (3.39)$$

$$B = \frac{1}{I_1(\gamma b)K_1(\gamma a) - I_1(\gamma a)K_1(\gamma b)} \left[-\frac{I_1(\gamma b)}{2\pi a} I_a - \frac{I_1(\gamma a)}{2\pi b} I_b \right] \quad (3.40)$$

Substituting this into equation (3.31) and finding the electric field intensity at both surface a and b and after some rearranging, equation (3.40) reduces to [6]:

$$E_z(a) = \eta \left[\frac{I_0(\gamma a)K_1(\gamma b) + K_0(\gamma a)I_1(\gamma b)}{I_1(\gamma b)K_1(\gamma a) - I_1(\gamma a)K_1(\gamma b)} \frac{I_a}{2\pi a} + \frac{I_0(\gamma a)K_1(\gamma a) + K_0(\gamma a)I_1(\gamma a)}{I_1(\gamma b)K_1(\gamma a) - I_1(\gamma a)K_1(\gamma b)} \frac{I_b}{2\pi b} \right] \quad (3.41)$$

$$E_z(b) = \eta \left[\frac{I_0(\gamma b)K_1(\gamma b) + K_0(\gamma b)I_1(\gamma b)}{I_1(\gamma b)K_1(\gamma a) - I_1(\gamma a)K_1(\gamma b)} \frac{I_a}{2\pi a} + \frac{I_0(\gamma b)K_1(\gamma a) + K_0(\gamma b)I_1(\gamma a)}{I_1(\gamma b)K_1(\gamma a) - I_1(\gamma a)K_1(\gamma b)} \frac{I_b}{2\pi b} \right] \quad (3.42)$$

Recalling the Bessel function identity [6,7]:

$$I_0(x)K_1(x) + K_0(x)I_1(x) = \frac{1}{x} \quad (3.43)$$

Using this identity the equations for the electric field intensity can be simplified to [6]

$$E_z(a) = \eta \left[\frac{I_0(\gamma a)K_1(\gamma b) + K_0(\gamma a)I_1(\gamma b)}{I_1(\gamma b)K_1(\gamma a) - I_1(\gamma a)K_1(\gamma b)} \frac{I_a}{2\pi a} + \frac{1}{I_1(\gamma b)K_1(\gamma a) - I_1(\gamma a)K_1(\gamma b)} \frac{I_b}{2\pi b a} \right] \quad (3.44)$$

$$E_z(b) = \eta \left[\frac{1}{I_1(\gamma b)K_1(\gamma a) - I_1(\gamma a)K_1(\gamma b)} \frac{I_a}{2\pi a b} + \frac{I_0(\gamma b)K_1(\gamma a) + K_0(\gamma b)I_1(\gamma a)}{I_1(\gamma b)K_1(\gamma a) - I_1(\gamma a)K_1(\gamma b)} \frac{I_b}{2\pi b} \right] \quad (3.45)$$

From these two equations it is clear that there exists an internal surface impedance, external surface impedance and mutual surface impedance for a hollow shell conductor. These impedances will be denoted as Z_i , Z_e , and Z_m respectively; they are [5,6]:

$$Z_i = \frac{\eta}{2\pi a} \frac{I_0(\gamma a)K_1(\gamma b) + K_0(\gamma a)I_1(\gamma b)}{I_1(\gamma b)K_1(\gamma a) - I_1(\gamma a)K_1(\gamma b)} \quad (3.46)$$

$$Z_m = \frac{\eta}{2\pi ab[I_1(\gamma b)K_1(\gamma a) - I_1(\gamma a)K_1(\gamma b)]} \quad (3.47)$$

$$Z_e = \frac{\eta}{2\pi b} \frac{I_0(\gamma b)K_1(\gamma a) + K_0(\gamma b)I_1(\gamma a)}{I_1(\gamma b)K_1(\gamma a) - I_1(\gamma a)K_1(\gamma b)} \quad (3.48)$$

3.5 Impedance of Single Core Conductor

The model equations of the surface impedances of a hollow cylindrical shell conductor can be applied to find the total impedance of multiple layers of concentric cylindrical conductor and insulation. Knowledge of the electric fields and electric currents between the conducting and insulating layers allows us to determine how to convert the surface impedances for each individual cylindrical shell into a single equivalent impedance for the total set of layers.

3.5.1 Composition of Impedances

To determine a total equivalent impedance for layers of hollow cylindrical shell layers of conductor or insulation the composition of impedances method can be applied. This method allows for multiple hollow cylindrical shell layers to be combined into an equivalent single hollow cylindrical shell. To understand how this can be accomplished a simple example can be analyzed. Figure 3-1 is a model of two annular conductors, C1 and C2, separated by an insulator, C0. The model in Figure 3-1 will be analyzed to see how an equivalent impedance can represent the three different hollow cylindrical shell layers.

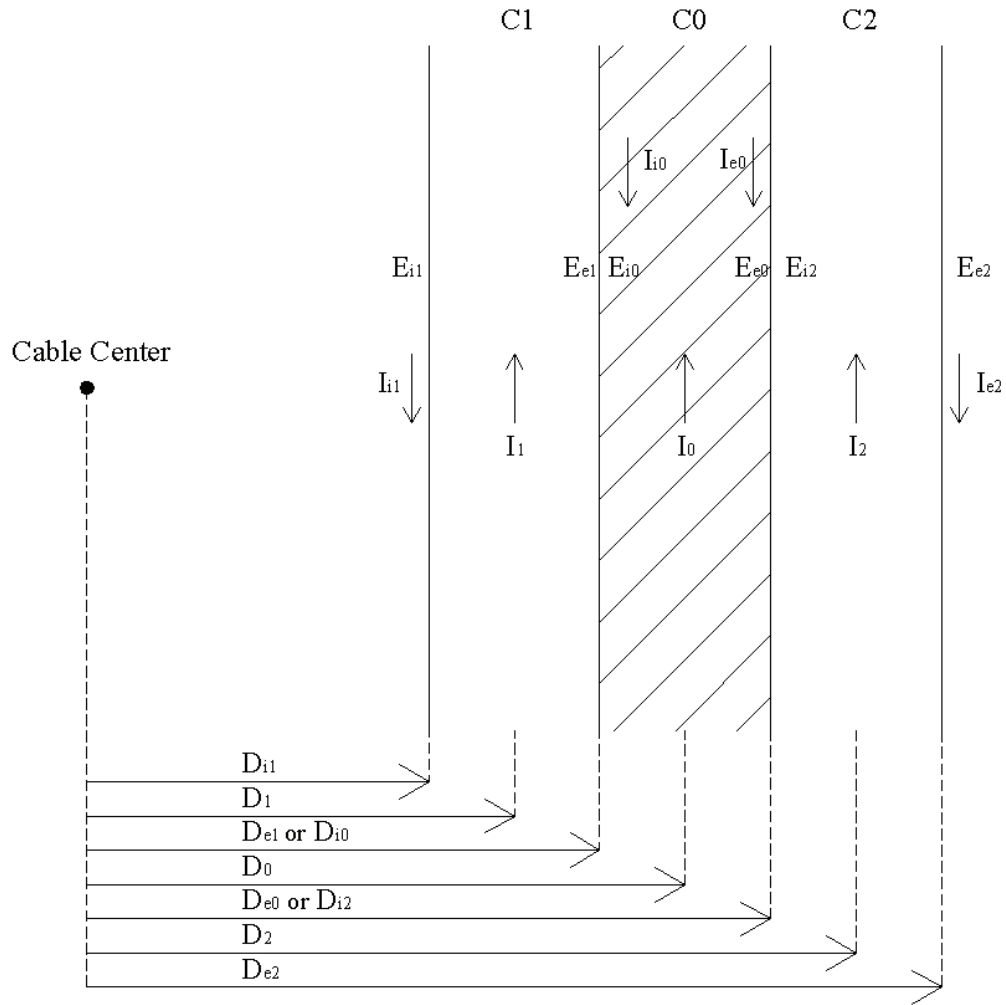


Figure 3-1: Multiple Layers of Cylindrical Shell Conductors [5]

From Figure 3-1 it is possible to make the following statements concerning the current and electric field intensities at the different surfaces [5]: $E_{e1} = E_{i0}$, $E_{e0} = E_{i2}$, $I_0 = 0$, and $I_1 + I_2 = I_{i1} + I_{e2}$. Also using the relation between the electric field intensity and voltage the following is true [5]:

$$E_{i0} - E_{e0} = \frac{dV_i}{dr} - \frac{dV_e}{dr} \quad (3.49)$$

Where r is the radial direction in Figure 1. This equation when simplified reduces to [5]:

$$E_{i0} - E_{e0} = \frac{j\omega\mu}{2\pi} \ln(D_{e0})I_{i0} - \frac{j\omega\mu}{2\pi} \ln(D_{i0})I_{i0} \quad (3.50)$$

$$E_{i0} - E_{e0} = \frac{j\omega\mu}{2\pi} \ln\left(\frac{D_{e0}}{D_{i0}}\right)I_{i0} \quad (3.51)$$

$$E_{i0} - E_{e0} = j\omega I_{i0} L_{C_0} \quad (3.52)$$

Equations (3.42) to (3.48) can be simplified and represented in this general form [5]:

$$E_i = Z_i I_i + Z_m I_e \quad (3.53)$$

$$E_e = Z_m I_i + Z_e I_e \quad (3.54)$$

Then a set of these equations can be written for each layer, and then by applying the relations of currents and electric field intensities of the common surfaces and the result of equation (3.52) the following can be obtained [5], which represents all of the three layers as if it were one equivalent material with a single equivalent internal, external, and mutual surface impedance [5].

$$E_{i1} = I_{i1} \left[Z_{i1} - \frac{Z_{m1}^2}{j\omega L + Z_{e1} + Z_{i2}} \right] + I_{e2} \left[\frac{Z_{m1} Z_{m2}}{j\omega L + Z_{e1} + Z_{i2}} \right] \quad (3.55)$$

$$E_{e2} = I_{i1} \left[\frac{Z_{m2} Z_{m1}}{j\omega L + Z_{e1} + Z_{i2}} \right] + I_{e2} \left[Z_{e2} - \frac{Z_{m2}^2}{j\omega L + Z_{e1} + Z_{i2}} \right] \quad (3.56)$$

From this combination of impedances it is clear that the 3 layers of conductors and insulators can be grouped into an equivalent set of impedances that represents all three layers. Now that this has been simplified to be an equivalent single hollow conductor equation (3.26) can be used to find the total impedance of that equivalent hollow conductor [5].

3.5.2 Application to Submarine Cables

The composition of impedances explained earlier can be applied to submarine power cables. The geometric model developed in chapter 2 will be used to determine the

different layers of materials that are used to construct a submarine cable. Figure 3-2 shows the different layers associated with a submarine cable.

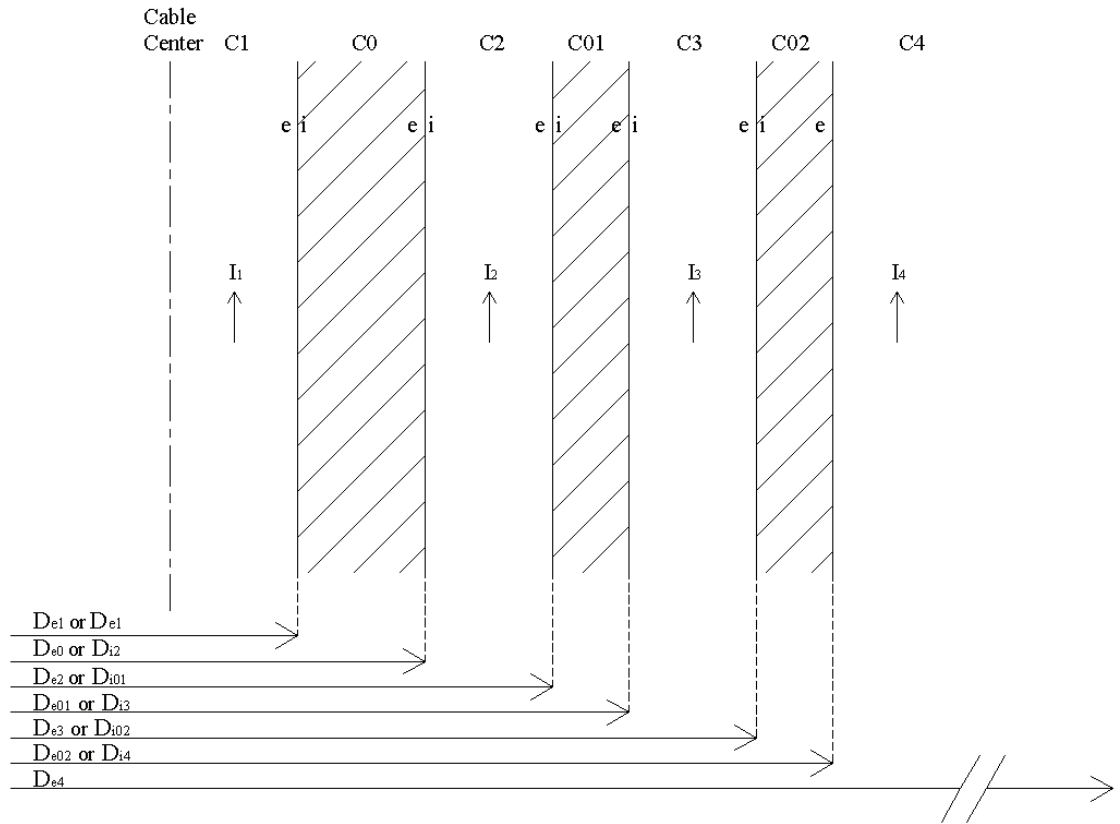


Figure 3-2: Equivalent Layers of Cylindrical Shells of a Single Core Submarine Cable

The first layer labeled C1 is the core conductor of the cable, C0 is the XLPE insulation, C2 is the sheath, C01 is insulation between the sheath and armor, C3 is the armor, C02 is the insulation between armor and the sea water, and C4 is the sea water. The exterior and interior side of each of the layers is labeled. This cable has the two special cases of impedances that were discussed earlier, a solid core conductor and an infinite conductor. By using the method of composition of impedances it can be determined that the equivalent impedance per unit length of this kind of cable is as follows:

$$Z = Z_{e1} + j\omega L_0 + Z_{i2} - \left\{ \frac{Z_{m2}^2}{Z_{e2} + j\omega L_{01} + \frac{Z_{m3}^2}{(Z_{e3} + j\omega L_{02} + Z_{i4})}} \right\} \quad (3.57)$$

Each component of this equation can be found from equations (3.46), (3.47), and (3.48). This equation allows finding the exact equivalent resistance and inductance of a single core submarine cable. The value for Z_{e1} can be found from the special case of a solid core conductor, equation (3.35); also the value for Z_{i4} can be found from the special case of an indefinite conductor, equation (3.36). The impedances found for each of the cables do not account for the mutual inductance between all of other phase conductors. To account for this, the mutual inductance between the other phases can be lumped into the impedance of the sea, Z_{i4} . If transposed lines are assumed then the inductance that exists between the separated cables will be [3]:

$$L_{an} = 2 * 10^{-7} \ln \left(\frac{\sqrt[3]{D_{ab}D_{ac}D_{bc}}}{r_{cond}} \right) \quad (3.58)$$

When this is added to the sea impedance component, the total inductance per unit length for a single core submarine cable can be determined.

3.6 Impedance of Three-Core Cable

Another commonly used cable configuration for submarine power system applications is a three-core conductor cable. This type of cable is more difficult to analyze using exact means of evaluating impedances. The magnetic and electric fields produced by each of the core conductors interact with each other and form two dimensional variable fields. The method used to compute the impedance in the previous sections was all based on the idea that the magnetic fields were variable in only a single direction. Determining the

magnetic field that exists outside the three-conductor bundle can assist in finding the equivalent inductance and resistance per unit length of the cable.

3.6.1 Magnetic Field Outside Three Conductor Bundle

The magnetic field that exists outside a bundle of three conductors is equal to the sum of the magnetic field components contributed by each conductor. This makes the magnetic field variable in two of its dimensions. The geometric description of the three-conductor bundle in Figure 3-3 will be used to analyze the magnetic field contribution from each of the conductors. Using the notation of this figure, it is desired to find the magnetic field at arbitrary circle of radius R from the center of the bundle. To use equation (3.20) for each conductor then the equivalent radii for each phase must be found. These are denoted as ρ_a , ρ_b , and ρ_c in Figure 3-3. These radii depend on the location on the circle of radius R . In a cylindrical coordinate system, the phase radii are dependent on ϕ , the azimuth from the origin.

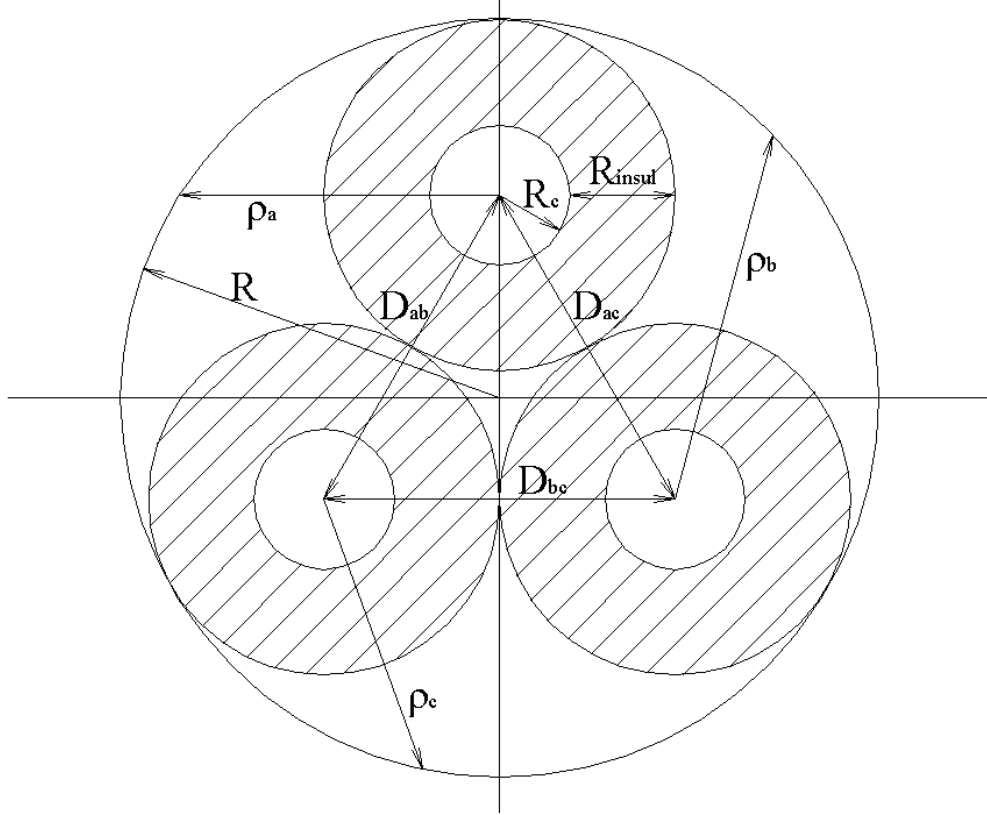


Figure 3-3: Geometry of Three-Core Cable

Using the geometric notation in Figure 3-3, the following equations can be developed to describe the radius from the phases to any point on the circle of radius R:

$$\rho_a = \sqrt{\left(R\sin(\phi) - \frac{2}{\sqrt{3}}(R_{insul} + R_c)\right)^2 + (-R\cos(\phi))^2} \quad (3.59)$$

$$\rho_b = \sqrt{\left(R\sin(\phi) + \frac{\sqrt{3}}{3}(R_{insul} + R_c)\right)^2 + ((R_{insul} + R_c) - R\cos(\phi))^2} \quad (3.60)$$

$$\rho_c = \sqrt{\left(R\sin(\phi) + \frac{\sqrt{3}}{3}(R_{insul} + R_c)\right)^2 + (-(R_{insul} + R_c) - R\cos(\phi))^2} \quad (3.61)$$

These phase radii can be used to find the equivalent magnetic field at the circle of arbitrary radius R, so long as the circle of radius R encompasses all three-core conductors entirely. The expressions for the magnetic field can now be formulated to be as follows:

$$B = \frac{\mu}{2\pi} \left[\frac{I_a}{\rho_a} + \frac{I_b}{\rho_b} + \frac{I_c}{\rho_c} \right] \quad (3.62)$$

Where the $e^{j\omega t}$ term has been suppressed. If the power system is balanced, then the magnitudes of the phase currents are equal but have a phase separation of 120 degrees from each other. This can be expressed as follows:

$$I_a + I_b + I_c = I \left[e^{j0} + e^{j\frac{2\pi}{3}} + e^{j\frac{4\pi}{3}} \right] \quad (3.63)$$

These relations can be used to help find the inductance of the different layers of the submarine cable. This will provide an approximate solution because the exact solution is difficult to compute because the magnetic field is non-uniform in two dimensions as opposed to one dimension as in the single core conductor case.

3.6.2 Inductance of Three-Core Cable

The inductance of a three-core cable can be determined by finding the magnetic flux through the surfaces of the different cable layers. The magnetic flux is related to the magnetic field as follows [4]:

$$\psi = \oiint B \, dS \quad (3.64)$$

$$\psi = \frac{I}{2\pi} \int_{\rho=a}^{\rho=b} \int_{\phi=0}^{\phi=2\pi} \left[\frac{1}{\rho_a} + \frac{1}{\rho_b} + \frac{1}{\rho_c} \right] d\rho d\phi \quad (3.65)$$

The lumped parameter Inductance can be determined from the relationship between the flux and current, where [4]:

$$L = \frac{N\Psi}{I} \quad (3.66)$$

In the case of a transmission line, the number of loops, N, will be just one. From this the inductances of each of the layers of the cable can be found. The inductances of each of the layers and the mutual inductances between the conductors can be used to determine

the total inductance of the transmission line. All of the Inductive components forms an inductor mesh network as can be seen in Figure 3-4.

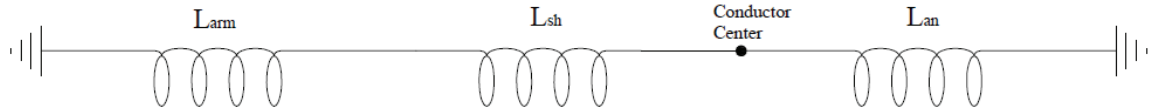


Figure 3-4: Inductance Network Per Phase

In Figure 3-4 the values L_{arm} represent the inductance of the armor layer, L_{sh} represents the inductance of the sheath layer, and L_{an} represents the equivalent inductance to ground from the self and mutual inductances of each of the phase conductors. The inductance of the cable layers is evaluated numerically using equation (3.64) where the radial integral bounds are defined by the geometry and thickness of each of the layers. A closed form solution of this integral, given the magnetic field that exists, is not easily obtained. The approximate self and mutual inductance of each phase conductor can be found from the following equation [3]:

$$L_{an} = 2 * 10^{-7} \ln \left(\frac{D_{AB}}{e^{\frac{1}{4}} r_{cond}} \right) \quad (3.67)$$

The Equivalent inductance for all three components can be found to equal the following:

$$L_{eq} = \frac{(L_{sh} + L_{arm}) L_{an}}{L_{sh} + L_{arm} + L_{an}} \quad (3.68)$$

This value of equivalent inductance will give the average inductance per meter of each of the phase conductors. It has been assumed that the phase conductors are transposed, which results in balanced inductance values for each of the phases [3].

3.7 Admittance of Submarine Cables

Admittance has two components, capacitive susceptance (ωC), and conductance (G). The capacitance C is related to the electric field that exists between two conducting bodies, and the conductance is related to the radial resistance of a material exterior to a conductor. If a conductor is totally surrounded by a grounded perfectly conducting medium, then no electric field can penetrate through this barrier [4,14]. This is the principle of electrostatic shielding. The significance of this principle is that for many of the submarine cables the sheath, which surrounds the cables insulation, is grounded. This will act as an electrostatic shield and will keep the electric field within the area surrounded by the grounded plane. This in turn affects which layers of the cable contribute to the capacitance. The conductance of a cable is a measure of the radial resistance to ground from the core conductor. For overhead transmission lines this would be the resistance of the air separating the conductors from the ground. For submarine cables it would be the resistance of the insulation that separates the core conductor from ground. Since the XLPE insulation is a very highly resistive material, the conductance will be very small. The capacitance and conductance of single and three-core submarine cables are found very differently due to how there are different ways to ground the inner layers of the cables.

3.7.1 Admittance of Single Core Cables

The capacitance and admittance of a single core submarine cable can be determined from the case of an imperfect coaxial cable. Single-core submarine cable sheaths are grounded; this acts as an electrostatic shield, and keeps the electric field totally contained

within the insulation between the core conductor and the sheath [4,14]. Also the conductance, which is the reciprocal of the resistance to ground, would be the radial resistance of the insulation. In the case of a non-ideal coaxial cable, with conductor radius b and outer conductor with inner radius a ; then the admittance can be formulated as follows from equation (3.17) and (3.20) [6]:

$$E_{\rho} = \frac{\Gamma I}{2\pi(\sigma + j\omega\epsilon)\rho} \quad (3.69)$$

The potential between the inner conductor and the inner surface of the outer conductor is related to the electromotive intensity as follows [4,6]:

$$V = \int_b^a E_{\rho} d\rho \quad (3.70)$$

$$V = \frac{\ln\left(\frac{a}{b}\right)}{2\pi(\sigma + j\omega\epsilon)} I_{\rho} \quad (3.71)$$

The potential between the two surfaces divided by the radial current flow is equal to the admittance of the coaxial cable per unit length [6].

$$Y = \frac{2\pi(\sigma + j\omega\epsilon)}{\ln\left(\frac{a}{b}\right)} \quad (3.72)$$

This can be further split down into its conductance, the real part of the equation, and the capacitive susceptance ωC , the imaginary part of the equation.

$$G = \frac{2\pi\sigma}{\ln\left(\frac{a}{b}\right)} \quad (3.73)$$

$$C = \frac{2\pi\omega\epsilon}{\ln\left(\frac{a}{b}\right)} \quad (3.74)$$

These equations can be applied to a single core submarine cable. The mutual capacitance between the phases is negligibly small if it exists at all. This is due to the electrostatic shielding of the core conductor due to the grounded sheath encompassing the conductor.

3.7.2 Admittance of Three-Core Cables

The admittance of a three-core cable can be found the same way as for the single-core conductors depending on the sheathing configuration used with the cable. The sheathing of three-core cables is done the following way; there is a sheath around each conductor and then a sheath around the bundle [2]. All of the sheaths are interconnected. The outer sheath is grounded, however the sheaths around the individual conductors may be metal or may be plastic [2]. Thus the ground plane could have a different geometry. In the case where the individual conductor sheaths are metallic, the admittance for each phase can be found the same way as for the single-core conductors. If the sheath around the individual conductors is a non-electrical conductor then a different approach must be used to find the admittance. The following assumptions are used in the formulation of the admittance, the conductors are transposed and the entire medium between the conductors and sheath is XLPE insulation. Figure 3-3 shows the geometry of the conductors and sheath that will be used in the analysis to find the admittance. The total capacitance per phase can be found in two parts, the capacitance between each conductor and the sheath, and the capacitance between each conductor and the remaining phase conductors [3]. The equivalent capacitance to ground due to the other phases can be found using the following equation [3]:

$$C_{an} = \frac{2\pi\epsilon}{\ln\left(\frac{2(R_c + R_{insul})}{R_c}\right)} \quad (3.75)$$

The capacitance between each phase and the sheath can be found by using the method of images. If a single conductor in the bundle is analyzed, and the geometry set up as in Figure 3-5, then the method of images can be used to find the capacitance between the conductor and sheath.

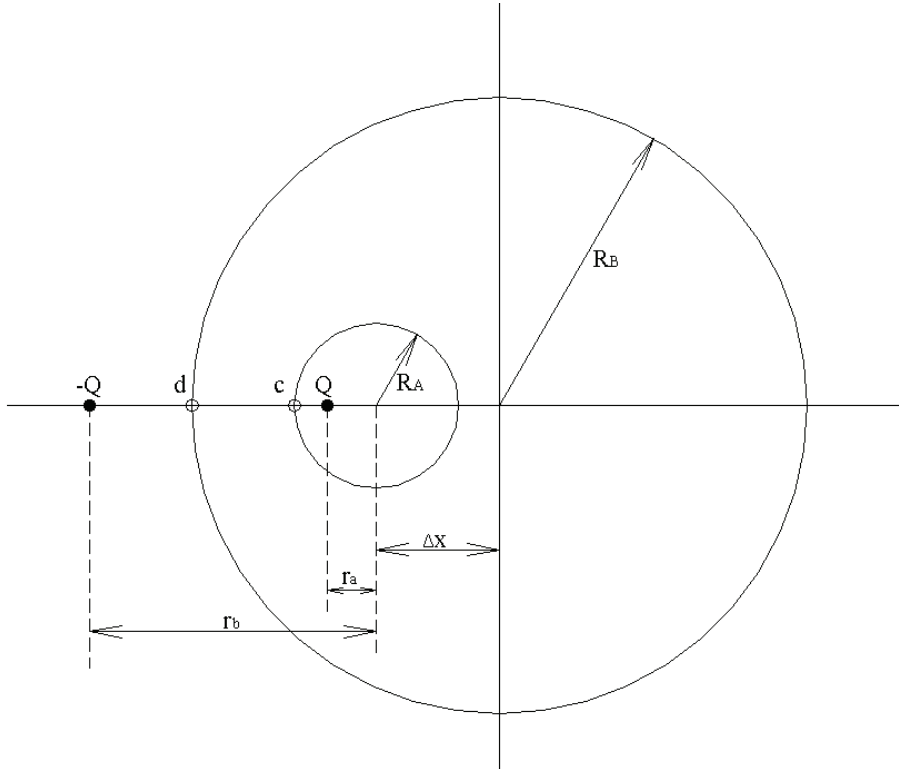


Figure 3-5: Method of Images Geometry [16]

For cylindrical conductors, using the notation of Figure 3-5, the following equations can be used to determine where charges Q and $-Q$ must be placed to make both the conductor and sheath equipotential surfaces [16]:

$$r_a = \frac{R_A^2}{r_b} \quad (3.76)$$

$$r_a + \Delta x = \frac{R_B^2}{r_b + \Delta x} \quad (3.77)$$

Substituting equations (3.76) and (3.77) and solving for the variable r_a [16]

$$r_a = \frac{(R_B^2 - R_A^2 - \Delta x^2) + /- \sqrt{(R_B^2 - R_A^2 - \Delta x^2)^2 - 4(R_A^2 \Delta x^2)}}{2\Delta x} \quad (3.78)$$

The electric field produced by a line charge is [4,16]

$$E = \frac{Q}{2\pi\epsilon l\rho} \quad (3.79)$$

The electric potential at a point is related to the electric field as follows [4,16]:

$$V = \int E dl \quad (3.80)$$

From this relation the electric potential at points c and d can be found as follows [16]:

$$V_c = \int_{\rho=r_a}^{\rho=R_A} \frac{Q}{2\pi\epsilon l p} dp - \int_{\rho=R_a}^{\rho=r_b} \frac{Q}{2\pi\epsilon l p} dp \quad (3.81)$$

$$V_c = \frac{Q}{2\pi\epsilon l} \ln \left(\frac{R_A - r_a}{r_b - R_A} \right) \quad (3.82)$$

$$V_d = \int_{\rho=r_a+\Delta x}^{\rho=R_B} \frac{Q}{2\pi\epsilon l p} dp - \int_{\rho=R_b}^{\rho=r_b+\Delta x} \frac{Q}{2\pi\epsilon l p} dp \quad (3.83)$$

$$V_d = \frac{Q}{2\pi\epsilon l} \ln \left(\frac{R_B - r_a - \Delta x}{r_b - R_B + \Delta x} \right) \quad (3.84)$$

Substitute equation (3.76) into equation (3.82) for r_b , and substitute (3.77) into equation (3.84) for r_b . This results in equations for voltage only dependent on the value of r_a , which was solved for in equation (3.78) based on the geometry of the cable and sheath.

After making these substitutions it can be seen that [16]:

$$\Delta V = V_d - V_c = \frac{Q}{2\pi\epsilon l} \ln \left(\frac{R_A}{R_B} \left(1 + \frac{\Delta x}{r_a} \right) \right) \quad (3.85)$$

Since the capacitance is related to the charge divided by the voltage differential, the following equation will be the capacitance per unit length between the conductor and sheath [16]:

$$C = \frac{2\pi\epsilon}{\ln \left(\frac{R_A}{R_B} \left(1 + \frac{\Delta x}{r_a} \right) \right)} \quad (3.86)$$

Where the value of r_a is evaluated by equation (3.78). With reference to Figure 3-3,

$\Delta x = \frac{2}{\sqrt{3}}(R_c + R_{insul})$, $R_A = R_c$, and $R_B = R$. Since the capacitance between the

conductor and sheath and the capacitance between the conductor and other phases are

both equivalent admittances to ground, it means they can be added to form the net capacitance per unit length per phase of the cable.

3.8 Resistance of Three-Core Cables

Finding the AC resistance of the core conductor, and equating the energy loss in the different cable layers to an equivalent resistance finds the total resistance of a submarine cable. For the three-core submarine cable it will be assumed that since the magnetic field seen by the different cable layers is insignificant that the AC resistance of the core conductors can approximate the resistance of the cable [4,5,15]. The AC resistance can be found from the following equation [4]:

$$R_{ac} = \sqrt{\frac{\pi f \mu}{\sigma}} \frac{l}{2\pi R_{cond}} \quad (3.87)$$

It should be noted that this equation only applies for cables with radius greater than 8.6mm; otherwise just the DC resistance should be used [4].

Chapter 4: Network Analysis

This chapter offers a brief review of the network analysis required to model the performance of the submarine power system. Cables can be analyzed using two-port network theory, using the values of inductance, capacitance, and resistance to find relationships between the input (Sending end) and output (receiving end) of a transmission line. There are limitations on the information that the two-port network analysis can provide. The system is assumed to have reached its steady state and so a transient response must be used such that the response of the system during transients can be evaluated. This chapter will cover both the means to evaluate the two port network parameters and some of the various transient responses of the system.

4.1 Introduction

Network analysis uses the values of inductance, capacitance, and resistance found from the electromagnetic analysis to find the two port parameters, which define the relationship between the input to a network and the output. When the system is assumed to be in the steady state, this two-port network analysis can be performed. When the system is in a transient state a complete network analysis must be performed.

4.2 Two-Port Networks

To begin the two-port network analysis an equivalent circuit for the transmission line will be used. Figure 4-1 shows this equivalent circuit, which has the equivalent per phase per

unit length capacitance, inductance, and resistance. For two port networks it is required to obtain a solution of the following form [3,10]:

$$V_s = AV_r + BI_r \quad (4.1)$$

$$I_s = CV_r + DI_r \quad (4.2)$$

Where V_s and I_s are the sending end voltage and current, V_r and I_r are the receiving end voltage and current. The values for A, B, C, and D are the values that relate the input to the output.

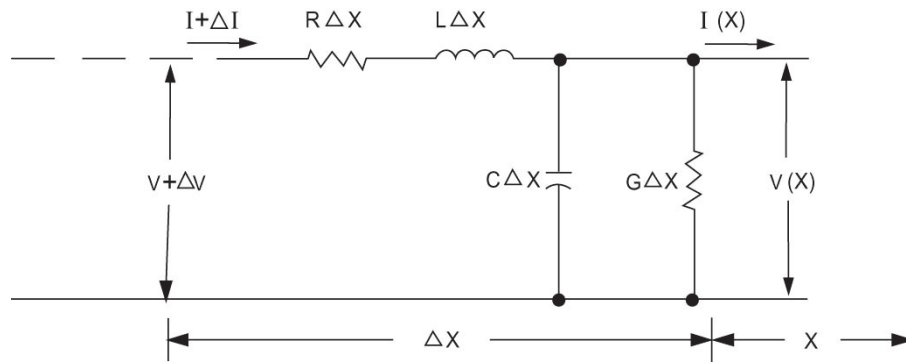


Figure 4-1: Network Used for Two-Port Analysis [3]

For the analysis of this network it is assumed that the transmission lines are operating under sinusoidal conditions, balanced loads/line parameters, and operating in steady state. For the analysis to find the two port network parameters, the following changes to notation in Figure 4-1 must be made, $V_s = V + \Delta V$, $V_r = V$, $I_s = I + \Delta I$, and $I_r = I$. The transmission line is assumed to exist down the length of the z-axis, so an incremental portion dz of the line is taken for analysis [3]. Using Kirchhoff's voltage and current relations results in the following set of equations relating the input to the output of the network [3]:

$$[V(z) + \Delta V] - V(z) = [I(z) + \Delta I][R + j\omega L]\Delta z \quad (4.3)$$

$$[I(z) + \Delta I] - I(z) = V(z)[G + j\omega C]\Delta z \quad (4.4)$$

These equations reduce to be the following [3]:

$$\Delta V = I(z)[R + j\omega L]\Delta z \quad (4.5)$$

$$\Delta I = V(z)[G + j\omega C]\Delta z \quad (4.6)$$

As the value for Δz approaches zero, these equations take on the following form [3]:

$$\frac{dV(z)}{dz} = [R + j\omega L]I(z) \quad (4.7)$$

$$\frac{dI(z)}{dz} = [G + j\omega C]V(z) \quad (4.8)$$

Taking the derivative of equation (4.5) and substituting into equation (4.6) results in the following equation [3]:

$$\frac{d^2V(z)}{dz^2} = [R + j\omega L][G + j\omega C]V(z) \quad (4.9)$$

Taking the derivative of equation (4.6) and substituting into equation (4.5) results in the following equation [3]:

$$\frac{d^2I(z)}{dz^2} = [R + j\omega L][G + j\omega C]I(z) \quad (4.10)$$

Making the substitution of the propagation factor, $\Gamma^2 = [R + j\omega L][G + j\omega C]$ into these equations results in the following set of differential equations [3,4].

$$\frac{d^2V(z)}{dz^2} = \Gamma^2 V(z) \quad (4.11)$$

$$\frac{d^2I(z)}{dz^2} = \Gamma^2 I(z) \quad (4.12)$$

The solutions to these differential equations take on the following form [3,4]:

$$V(z) = C_1 e^{\Gamma z} + C_2 e^{-\Gamma z} \quad (4.13)$$

$$I(z) = \frac{C_1 e^{\Gamma z} - C_2 e^{-\Gamma z}}{Z_0} \quad (4.14)$$

Where the value of the characteristic impedance $Z_0 = \sqrt{\frac{R+j\omega L}{G+j\omega C}}$ has been substituted into the result. The constants C_1 and C_2 can be evaluated by looking at the sending end of the transmission line when $z=0$. This results in the following relationship between the constants [3]:

$$V(0) = C_1 + C_2 \quad (4.15)$$

$$Z_0 I(0) = C_1 - C_2 \quad (4.16)$$

From these two equations the values for the constants can be found such that they are a function of the voltage and current at the sending end of the transmission line. Substituting these into equations (4.11) and (4.12) the following result can be obtained [3]:

$$V(z) = \frac{1}{2} ([V(0) + Z_0 I(0)] e^{\Gamma z} + [V(0) - Z_0 I(0)] e^{-\Gamma z}) \quad (4.17)$$

$$I(z) = \frac{1}{2} \left(\left[I(0) + \frac{V(0)}{Z_0} \right] e^{\Gamma z} + \left[I(0) - \frac{V(0)}{Z_0} \right] e^{-\Gamma z} \right) \quad (4.18)$$

These functions can be replaced with the hyperbolic sin and hyperbolic cosine functions such that they assume the following form [3]:

$$V(z) = V(0) \cosh(\Gamma z) + Z_0 I(0) \sinh(\Gamma z) \quad (4.19)$$

$$I(z) = I(0) \cosh(\Gamma z) + \frac{V(0)}{Z_0} \sinh(\Gamma z) \quad (4.20)$$

Equations (4.19) and (4.20) can be compared to equations (4.1) and (4.2) to conclude the following about the ABCD parameters of the two port network [3]:

$$A(z) = \cosh(\Gamma z) \quad (4.21)$$

$$B(z) = Z_0 \sinh(\Gamma z) \quad (4.22)$$

$$C(z) = \frac{1}{Z_0} \sinh(\Gamma z) \quad (4.23)$$

$$D(z) = \cosh(\Gamma z) \quad (4.24)$$

4.3 Steady State Performance Analysis

Having found the two-port network parameters for the transmission line; a performance analysis for the transmission line can be performed. For this problem it is assumed that the generator output voltage V_s , apparent power S_s , and power factor δ_{PF} are known. See Figure 4-2 for a diagram of how these values are related to each other.

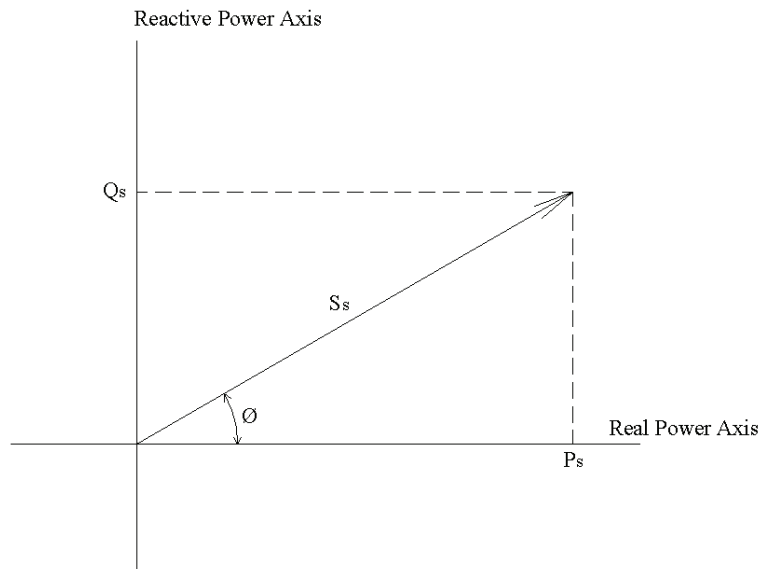


Figure 4-2: Real and Reactive Power Diagram [10]

From Figure 4-2, the power factor is defined as follows [10]:

$$\delta_{PF} = \cos(\phi) \quad (4.25)$$

The power factor will always be a positive number, since this is so a further definition must be associated with this value. When the power factor is said to be lagging the angle ϕ is positive [10]. When the power factor is said to be leading the angle ϕ is negative [10]. Effectively what this means is that when the power factor is leading the generator is absorbing reactive power from the system, and when the power factor is lagging the

generator providing reactive power to the system. From this definition the following statements can be made about the real and reactive power based on the power factor and apparent power [10]:

$$P_s = S_s \delta_{PF} \quad (4.26)$$

If the power factor is lagging [10]

$$Q_s = S_s \sin(\cos(\delta_{PF})) \quad (4.27)$$

If the power factor is leading [10]

$$Q_s = -S_s \sin(\cos(\delta_{PF})) \quad (4.28)$$

Since these are the known parameters then equations (4.1) and (4.2) can be rearranged as follows:

$$I_r = \frac{I_s A - C V_s}{D A - B C} \quad (4.29)$$

$$V_r = \frac{D V_s - B I_s}{D A - B C} \quad (4.30)$$

The following equation relates the sending end current to the sending end voltage and apparent power:

$$I_s = \left(\frac{S_s \delta_{PF} + / - j S_s \sin(\cos(\delta_{PF}))}{V_s} \right)^* \quad (4.31)$$

It is assumed that the sending end voltage has a phase of zero for now since it is used as the reference bus voltage. Knowing the sending end voltage and current, the receiving end voltage and current can be found from equations (4.29) and (4.30). From finding the receiving end voltage and current, the transmission line efficiency, output impedance, output apparent power, and power factor can be determined as follows [3]:

$$\eta = \frac{Re(S_r)}{Re(S_s)} * 100\% \quad (4.32)$$

$$Z_r = \frac{V_r}{I_r} \quad (4.33)$$

$$S_r = V_r(I_r)^* \quad (4.34)$$

$$\delta_{PF} = \cos\left(\text{atan}\left(\frac{\text{Re}(S_r)}{\text{Im}(S_r)}\right)\right) \quad (4.35)$$

Another important figure of merit in determining the transmission lines performance is the voltage regulation. The voltage regulation is a measure of a percentage voltage change if the receiving end of a transmission line goes from having a rated load on it to no load at all. The equation defining the voltage regulation is as follows [3]:

$$\text{Regulation} = \frac{V_{no\ load} - V_{rated}}{V_{rated}} * 100\% \quad (4.36)$$

The no load voltage can be found from equations (4.1) and (4.2) by setting the receiving end current zero and solving for the receiving end voltage. The receiving end no load voltage is defined as follows:

$$V_{no\ load} = \frac{V_s}{A} \quad (4.37)$$

The resulting equation for the voltage regulation now takes the following form:

$$\text{Regulation} = \frac{V_s - V_r}{AV_r} * 100\% \quad (4.38)$$

These values provide important information about the quality and quantity of power that is provided to the receiving end of the transmission line. These values will help in determining if reactive power support is necessary or not for a submarine transmission line.

4.4 Transient State Performance Analysis

The transmission line transient analysis is important in determining the initial power draw of the transmission line and also in determining the transient state over voltage

magnitudes. Figure 4-3 shows the equivalent circuit that will be used for determining the transient response of the network.

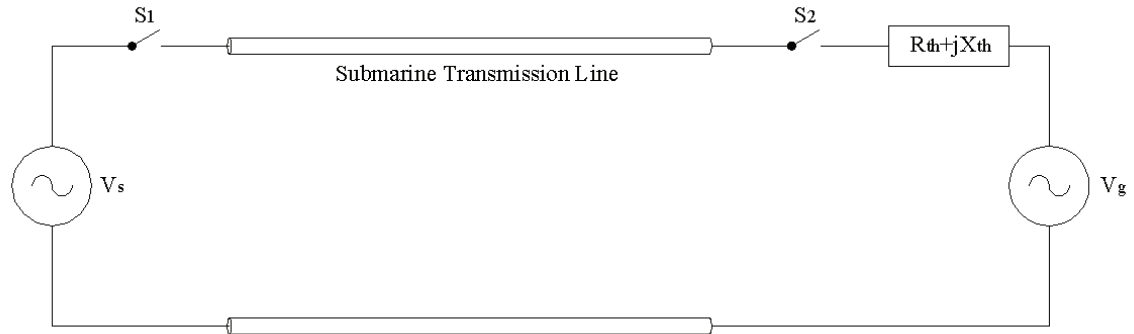


Figure 4-3: Equivalent Circuit For Transient Analysis

The section labeled ‘Submarine Transmission Line’ in Figure 4-3 was used to replace the equivalent network for the transmission line in Figure 4-1. Switches S1 and S2 are the location of switches that connect the generator to the transmission line and connect transmission line to the grid respectively. The grid has been broken down into a Thevenin equivalent circuit, represented by a sinusoidal voltage source and a series impedance. For the purposes of this analysis, the equivalent impedance of the network the transmission line is connected to is unknown, so different values will be assumed for the thevenin equivalent impedance in the transient analysis. The phase angle for the grid equivalent voltage source is assumed to be zero, while the source voltage phase angle is assumed to be δ_s . The equation describing the system when switch S1 is closed and S2 is open are as follows [9,12,13]:

$$|V_s| \sin(\omega t + \delta_s) - L \frac{di(t)}{dt} - Ri(t) - \left(\frac{1}{c} \int i(t) dt + v(t_0) \right) = 0 \quad (4.39)$$

Taking the Laplace transform of this equation:

$$|V_s| \frac{\sin(\delta_s)s + \omega \cos(\delta_s)}{s^2 + \omega^2} - [LsI(s) - i(0)] - RI(s) - \frac{1}{sC}I(s) - v(0) = 0 \quad (4.40)$$

Prior to switch S1 being closed all the initial currents and voltages are zero. Solving equation (4.40) for the current results in the following transfer function:

$$I(s) = \frac{s^2 \left[\sin(\delta_s) \frac{|V_s|}{L} \right] + s \left[\cos(\delta_s) \frac{|V_s|}{L} \omega \right]}{(s^2 + \omega^2) \left(s^2 + \frac{R}{L}s + \frac{1}{LC} \right)} \quad (4.41)$$

Taking the inverse Laplace transform of this equation will determine the resulting generator current in the time domain. Multiplying this by the generator voltage will yield the transient and steady state power flow that the transmission line will require. This transient power flow represents the energy that is required to charge the transmission line.

Chapter 5: Submarine Transmission Line Parameter Simulation and Discussion

This chapter presents the simulation and discussion of the calculated transmission line parameters for various typically used submarine power cables. In addition to this, the effects that the geometry/materials of the different cable layers has on the line parameters are simulated and discussed.

5.1 Single Core Cable Line Parameter Analysis

Analyzing single-core submarine cable line parameters involves a study of specific cases of cables that are commonly manufactured, as well as an analysis of how the different cable layers affect the line parameters. The subsequent sections analyze specific cases of manufactured cables as well as the relationship between how the material properties and thickness of the cable layers affect line parameters. The results of the analysis are then compared to those of overhead transmission lines. This comparison shows how dramatically different these kinds of cables are from overhead lines and how important the choice of materials and cable layering is for submarine cable design.

5.1.1 Single-Core Cable Line Parameters Case Study

To begin analyzing the submarine transmission line parameters, some examples of cable geometry must be considered. For this analysis some manufacturer specifications for different single-core cable geometries are used. The following different cable geometries will be used in the line parameter simulations:

Table 5-1: Different Cable Geometries, Single-Core Cable [1]

Cable Type	Conductor Radius [mm]	Insulation Thickness [mm]	Sheath Thickness [mm]	Armor Thickness [mm]
A	13.1	24	2.9	5
B	14.9	32	3.1	5
C	23.7	27	3.1	5

It is assumed that the insulation layers between the sheath and armor, and the armor and seawater are 1mm in thickness. It has also been assumed that the individual cable phases are in the H configuration, the three phases are in line, and have been spaced apart by 10m. For the overhead transmission lines it has been assumed to have the same phase configuration with spacing of 10 m. All of the phase conductors are elevated 10 m above ground. This height was chosen such that the capacitance for the overhead lines would be larger than it would be for a practical overhead transmission line. The core conductor properties are the same as that used for the submarine cables. This allows a direct comparison between the two different cable types.

5.1.1.1 Submarine Cable Type A

From the geometry of Table 5-1 for Cable Type A, assuming a lead sheath and copper armor; the line parameters for the submarine cable type A can be found to be as follows: an inductance per unit length of 0.28235 mH/km, capacitance per unit length of 0.16644 μ F/km, and a resistance per unit length of 46.7447 m Ω /km. For comparison purposes the following are the inductance, capacitance, and resistance for an overhead transmission line: an inductance per unit length of 1.42mH/km, capacitance per unit length of

8.73nF/km, and a resistance per unit length of 24.2 m Ω /km. These results show that the line parameters for this cable have larger capacitance and resistance but smaller inductance than the overhead transmission lines. The results are reconciled with a comparison of the two-wire network and the coaxial cable network. The coaxial cable has inherently a smaller inductance and larger capacitance than the two-wire network. The difference between overhead and submarine lines is similar to this, so the same kind of results would be expected. The resistance of the submarine cable is larger because of the induced currents in the different layers of the cable.

The analysis of submarine cable type A is performed again with steel armor replacing the copper armor. The resulting line parameters after making this change is as follows: an inductance per unit length of 0.4418mH/km, capacitance per unit length of 0.16644 μ F/km, and resistance per unit length of 176.4 m Ω /km. The resistance and capacitance were larger than the overhead values while the inductance was smaller. However in comparing the steel armor to the copper armor it can be seen that the resistance and inductance have increased significantly. The capacitance remains the same regardless of the metal used for the armor. This result is justified by recognizing that the addition of a ferrous-based metal increases the permeability of that layer of the cable, so the inductance for that cylindrical shell will be increased. The resistance increases because the magnetic field produced by the core conductor will induce currents in the steel armor. These induced currents are proportional to the permeability of the material and since steel is an iron-based metal the permeability is large. This results in the magnetic field inducing larger currents in iron than a material like copper, which has a very small value

of permeability. This causes a loss of energy and will be reflected as an increase in the net resistance of the cable. The results obtained are summarized in Table 5-2.

Table 5-2: Cable Type A Line Parameters

Line Parameter	Copper Armor	Steel Armor	Overhead Lines
Inductance [mH/km]	0.2823	0.4418	1.42
Capacitance [μ F/km]	0.16644	0.16644	0.00873
Resistance [m Ω /km]	46.7447	176.4	24.2

5.1.1.2 Submarine Cable Type B

From the geometry in Table 5-1 for Cable Type B, assuming a lead sheath and copper armor, the Line parameters can be found as follows: an inductance per unit length of 0.29713 mH/km, capacitance per unit length of 0.1522 μ F/km, and resistance per unit length of 38.1557 m Ω /km. For an overhead transmission line the line parameters are as follows: an inductance per unit length of 1.398 mH/km, capacitance per unit length of 8.9142 nF/km, and resistance per unit length of 21.294 m Ω /km. When the armor for Cable Type B is switched from copper to steel the line parameters become as follows: a inductance per unit length of 0.41495 mH/km, capacitance per unit length of 0.1522 μ F/km, and resistance per unit length of 139.44 m Ω /km. These results for the line parameters for Cable Type B are summarized in Table 5-3.

Table 5-3: Cable Type B Line Parameters

Line Parameter	Copper Armor	Steel Armor	Overhead
Inductance [mH/km]	0.29713	0.41495	1.398
Capacitance [μ F/km]	0.1522	0.1522	0.0089142
Resistance [m Ω /km]	38.1557	139.44	21.294

5.1.1.3 Submarine Cable Type C

From the geometry in Table 5-1 for Cable Type C, assuming a lead sheath, and copper armor. The Line parameters can be found to be as follows: an inductance per unit length of 0.2071 mH/km, capacitance per unit length of 0.2275 μ F/km, and resistance per unit length of 25.092 m Ω /km. For an overhead transmission line the line parameters are as follows: an inductance per unit length of 1.305 mH/km, capacitance per unit length of 9.6304 nF/km, and resistance per unit length of 13.387 m Ω /km. When the armor for Cable Type C is switched from copper to steel the line parameters become as follows: a inductance per unit length of 0.3163 mH/km, capacitance per unit length of 0.2275 μ F/km, and resistance per unit length of 119.24 m Ω /km. These results for the line parameters for Cable Type C are summarized in Table 5-4.

Table 5-4: Cable Type C Line Parameters

Line Parameter	Copper Armor	Steel Armor	Overhead
Inductance [mH/km]	0.2071	0.3163	1.305
Capacitance [μ F/km]	0.2275	0.2275	0.0096304
Resistance [m Ω /km]	25.092	119.24	13.387

5.1.2 Effects of the Cable Layer Thickness

In order to analyze the effects that the different cable layering thickness' have on the line parameters, a typical submarine cable geometry must be assumed. The geometry of the different layers will be varied around this assumed geometry. After choosing this geometric model the following simulations will be performed: the armor, sheath, and insulation thickness will be varied while the sheath material is chosen to be lead, and the armor material used is both copper and steel. The effect of having a copper sheath versus

a lead sheath is not of interest because it will have negligible effects on the total cable resistance, capacitance, and inductance.

5.1.2.1 Lead Sheath and Copper Armor

From Table 5-1, the cable geometry for Cable Type B will be used as the assumed geometric model. To test the effect that each of the layers has on the line parameters, the following simulation will be done: a sheath thickness will be chosen, five insulation layer thickness' will be chosen, and the cables armor thickness will be varied. This will allow for conclusions to be drawn concerning the effect that the different cable layers have on line parameters. Figures 5-1 to 5-9 show the results of the simulation.

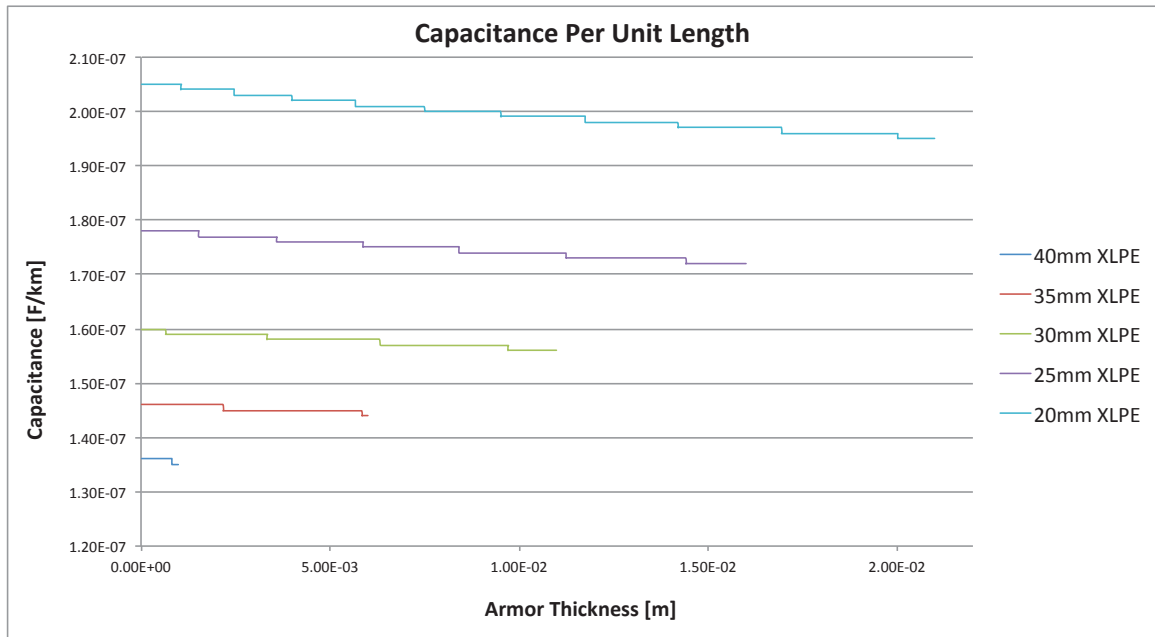


Figure 5-1: Capacitance Per Unit Length As Armor Thickness Varies, 3.1mm Sheath

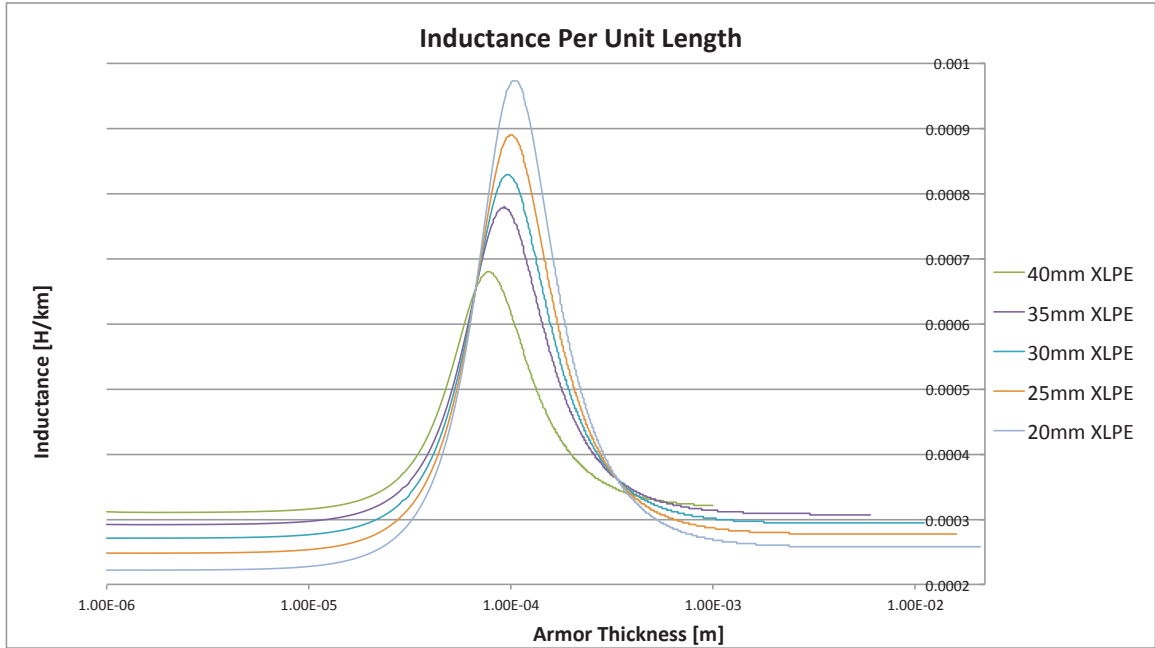


Figure 5-2: Inductance Per Unit Length As Armor Thickness Varies, 3.1mm Sheath

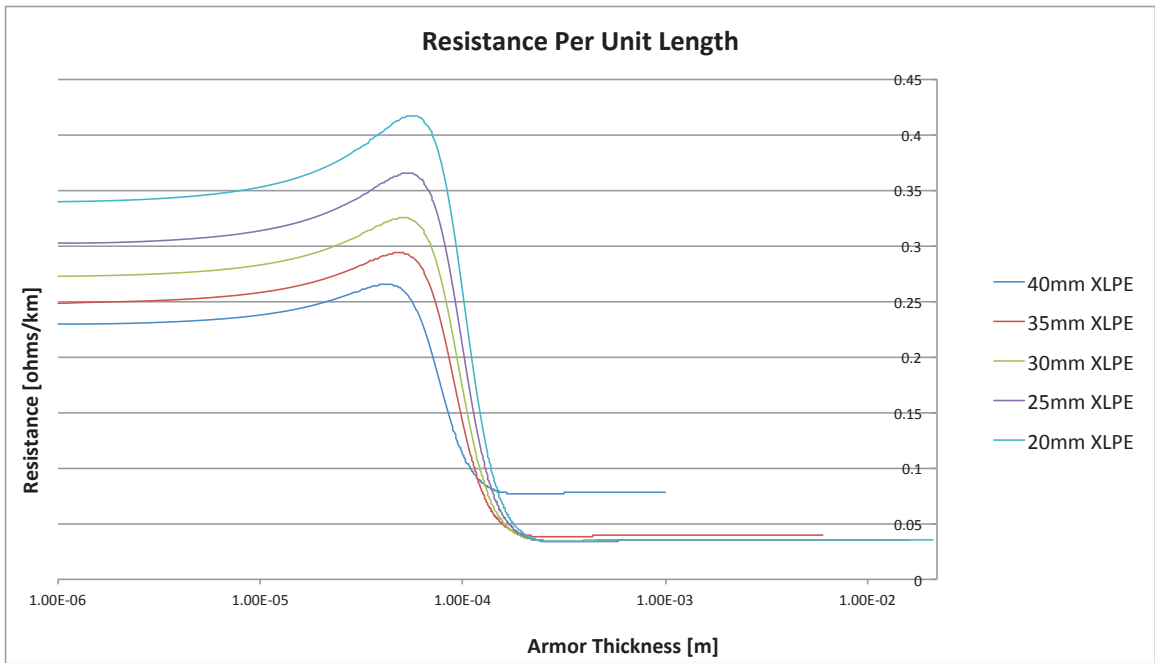


Figure 5-3: Resistance Per Unit Length As Armor Thickness Varies, 3.1mm Sheath

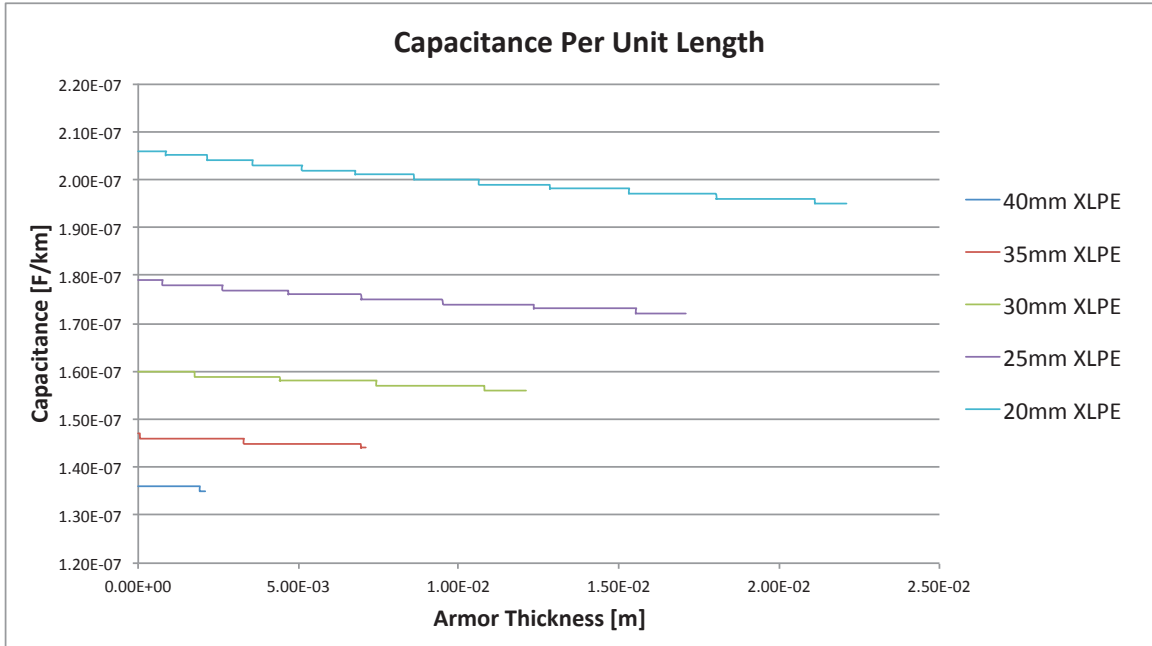


Figure 5-4: Capacitance Per Unit Length As Armor Thickness Varies, 2mm Sheath

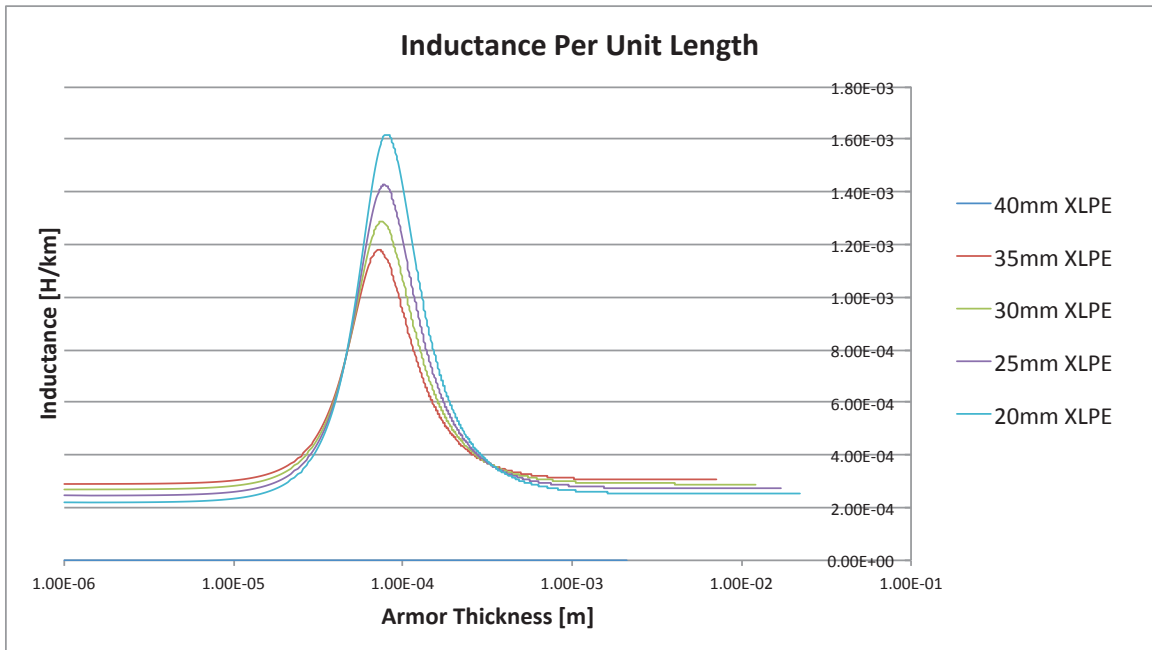


Figure 5-5: Inductance Per Unit Length As Armor Thickness Varies, 2mm Sheath

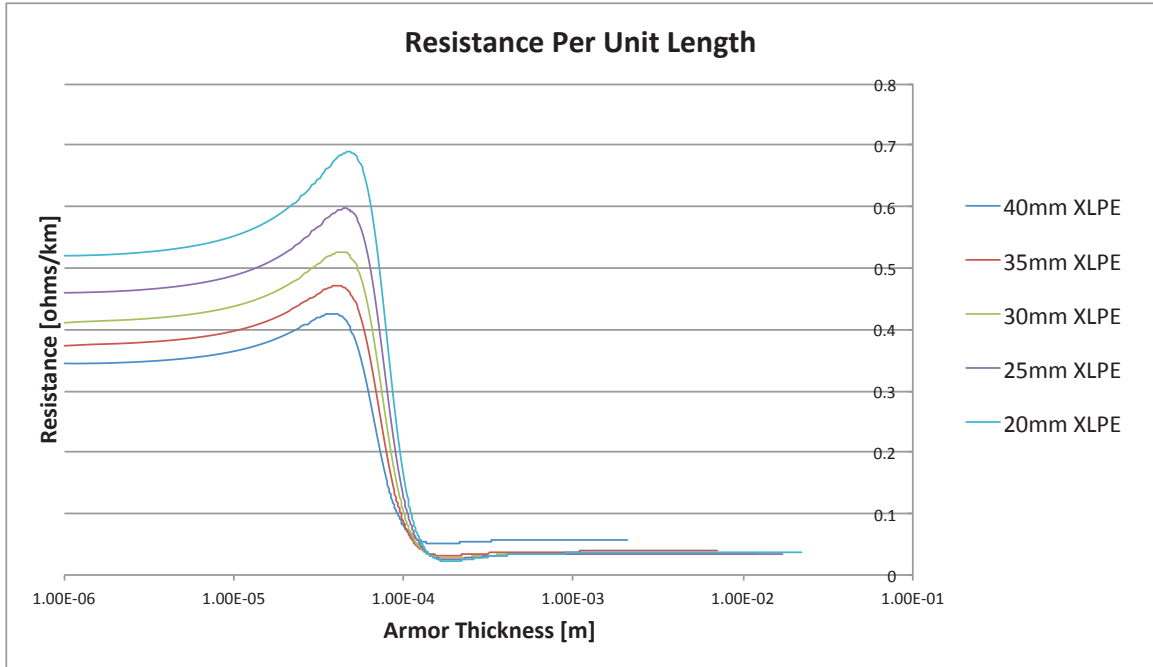


Figure 5-6: Resistance Per Unit Length As Armor Thickness Varies, 2mm Sheath

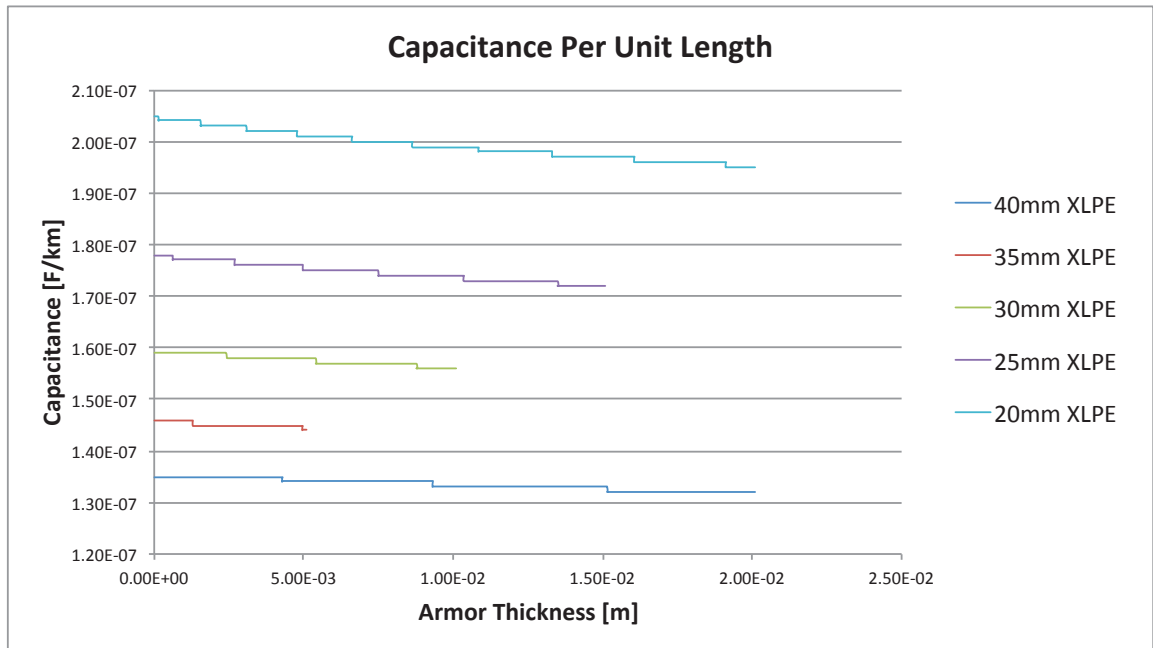


Figure 5-7: Capacitance Per Unit Length As Armor Thickness Varies, 4mm Sheath

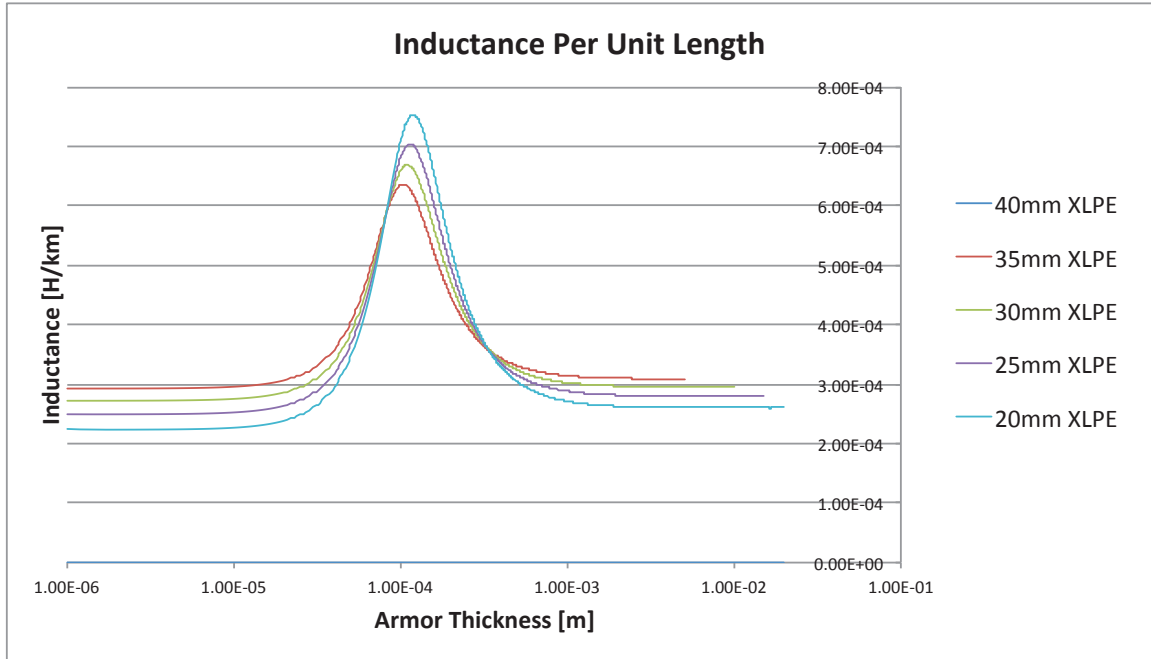


Figure 5-8: Inductance Per Unit Length As Armor Thickness Varies, 4mm Sheath

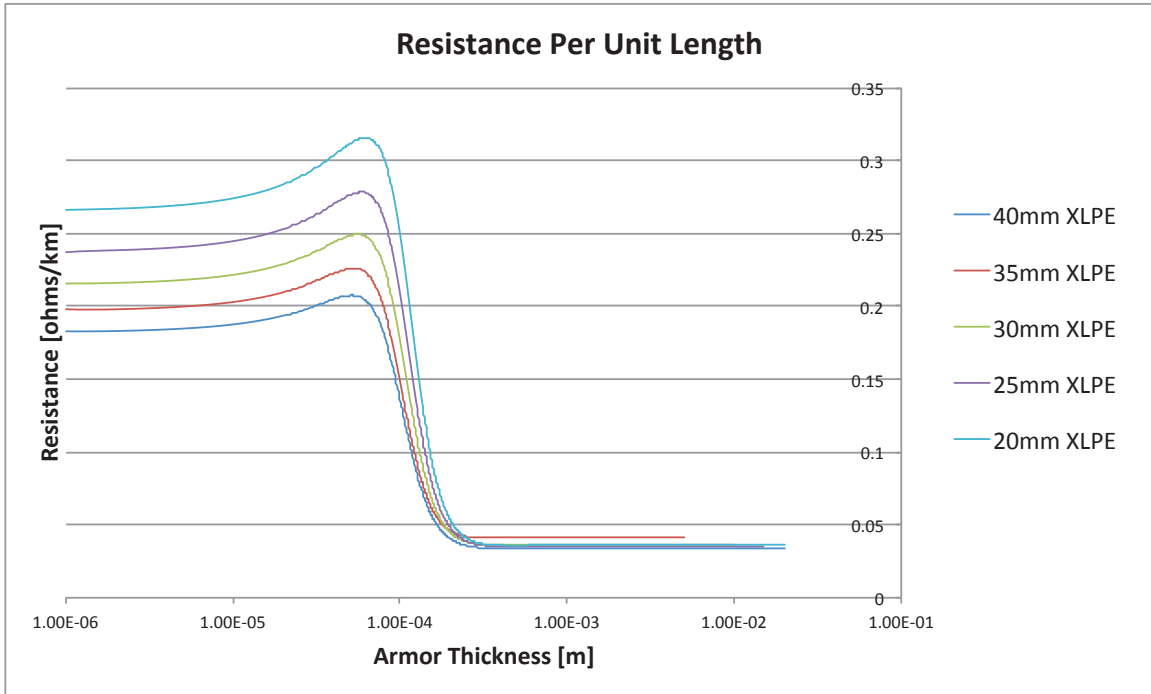


Figure 5-9: Resistance Per Unit Length As Armor Thickness Varies, 4mm Sheath

The results for the net cable capacitance have the following characteristics: the total capacitance decreases approximately linearly with increasing armor thickness. The insulation thickness affects the capacitance significantly; it shifts the capacitance inversely proportional to the insulation thickness. Thinner insulation results in larger capacitance and thicker insulation results in smaller capacitance. The sheath thickness variation does not affect the capacitance of the cable.

The results for the net cable inductance have the following characteristics: as the armor thickness is small the inductance is constant, as the thickness is further increased the inductance reaches a maximum, as the thickness is further increased the inductance will begin to decrease and reach another constant value. The constant inductance value when the armor is thin is smaller than when the inductance armor is thick. The insulation thickness affects the magnitude of the constant inductance when the armor is thin or thick, the magnitude of the maximum inductance, and which armor thickness results in the maximum inductance. As the thickness of insulation is increased the constant inductances when the armor is thick or thin also increase; the maximum value of inductance is decreased, and the armor thickness that causes this maximum value of inductance is decreased. As the sheath thickness is increased the constant values of inductance when the armor is thin or thick are approximately the same. The maximum value of inductance is lower and the armor thickness that causes this maximum value of inductance is decreased.

The results for the net cable resistance have the following characteristics: when the armor thickness is small the resistance is constant. As the thickness is increased the resistance increases to a maximum; as the thickness is further increased the resistance begins to decrease to a minimum; as the thickness is further increased the resistance increases and approaches a constant value. When the armor is thin the constant value of resistance is larger than when the armor is thick. As the insulation thickness is increased the constant resistance value when the armor is thin decreases, when the armor is thick the resistance values are approximately the same. Increasing the insulation thickness decreases how much the maximum resistance overshoots the resistance when the armor is thin; the increasing insulation thickness causes the maximum resistance value to occur for a smaller armor thickness. The sheath thickness being increased causes a drop in resistance for all armor thicknesses, it also decreases the maximum resistance overshoot from the resistance value when the armor is thin. The location of the resistance minimum is not affected significantly by sheath or insulation thicknesses.

5.1.2.2 Lead Sheath and Steel Armor

The material used for the armor will be changed from copper to steel. The same simulation will be performed where a sheath thickness will be chosen, five insulation thicknesses chosen, and the armor thickness varied. The results of this simulation can be found in Figures 5-10 to 5-15. It can be noted that the capacitance does not depend on the metal used for the sheath and armor since the permittivity of metals is approximately equal to that of free space, because of this the capacitance will not be simulated again for this change in armor material.

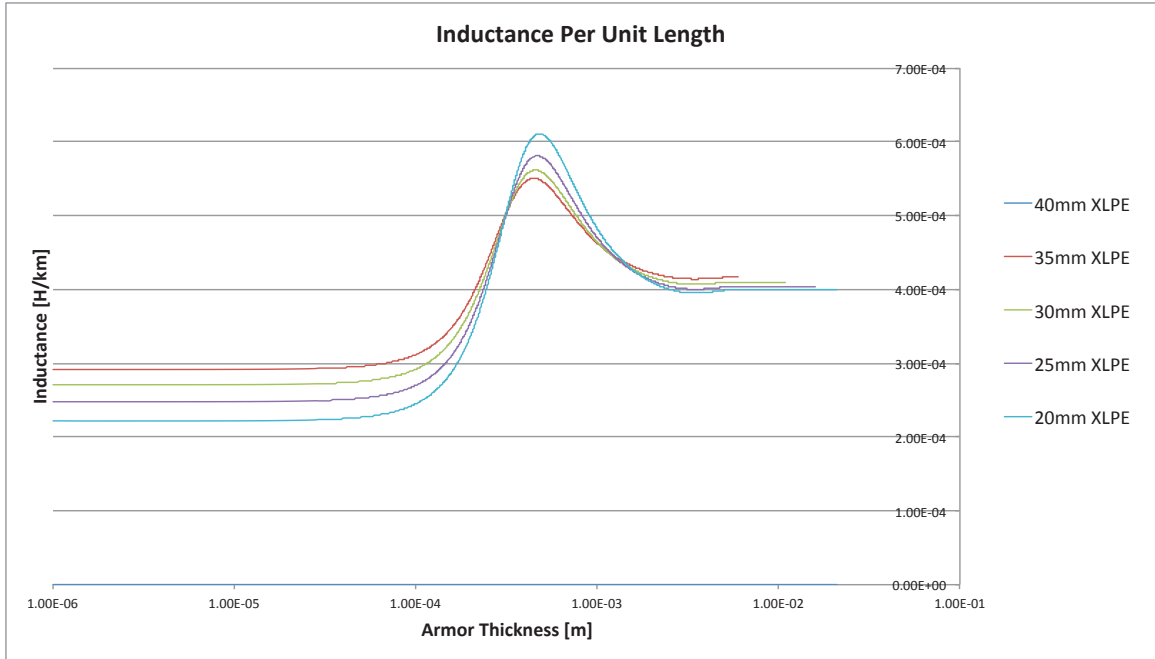


Figure 5-10: Inductance Per Unit Length As Armor Thickness Varies, 3.1mm Sheath

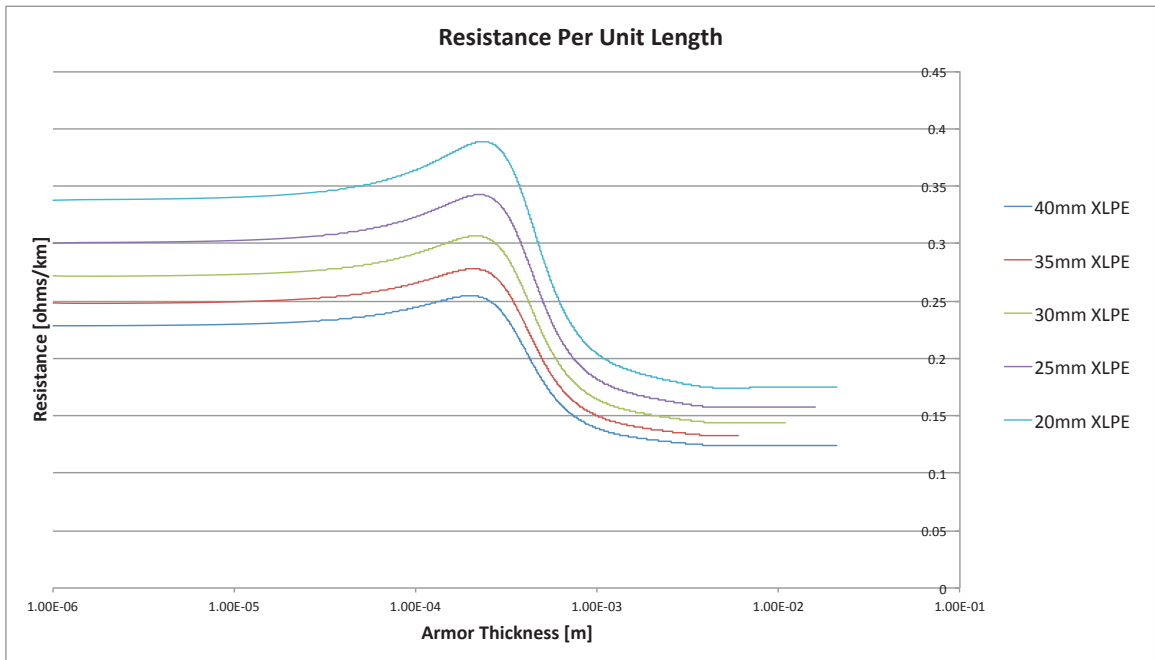


Figure 5-11: Resistance Per Unit Length As Armor Thickness Varies, 3.1mm Sheath

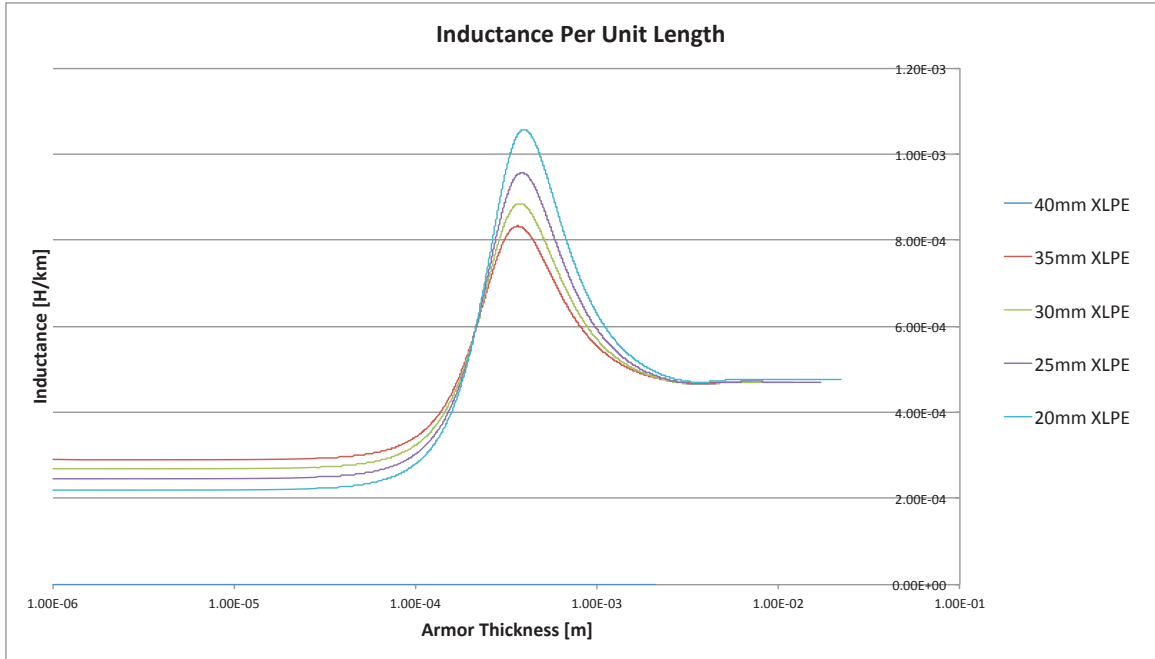


Figure 5-12: Inductance Per Unit Length As Armor Thickness Varies, 2mm Sheath

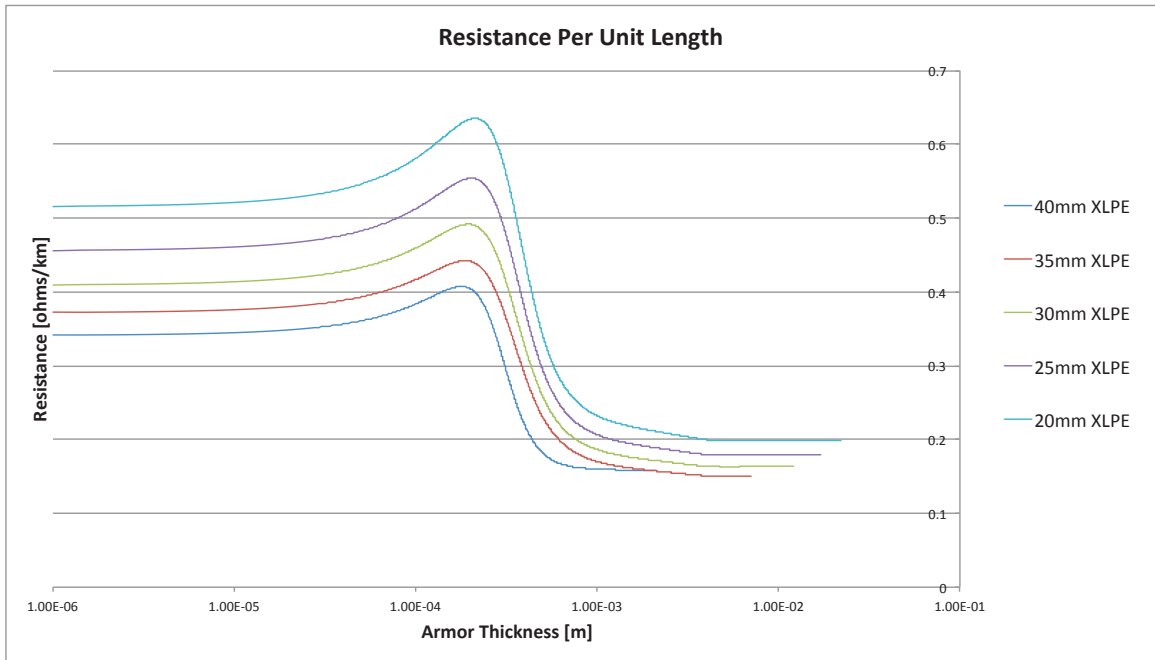


Figure 5-13: Resistance Per Unit Length As Armor Thickness Varies, 2mm Sheath

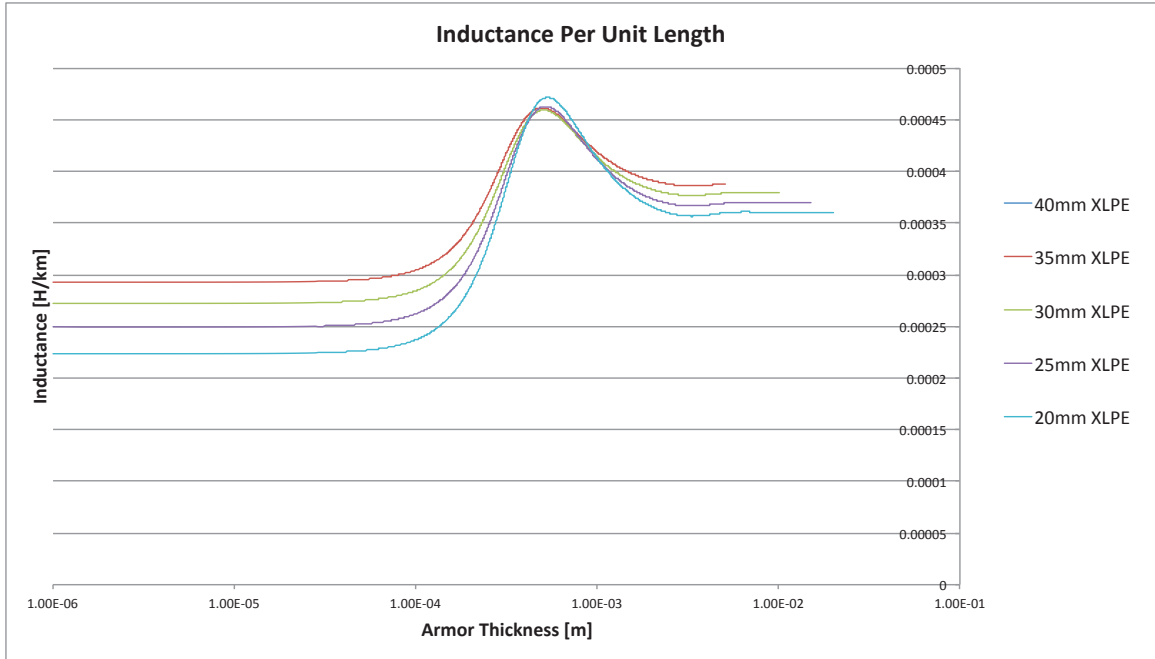


Figure 5-14: Inductance Per Unit Length As Armor Thickness Varies, 4mm Sheath

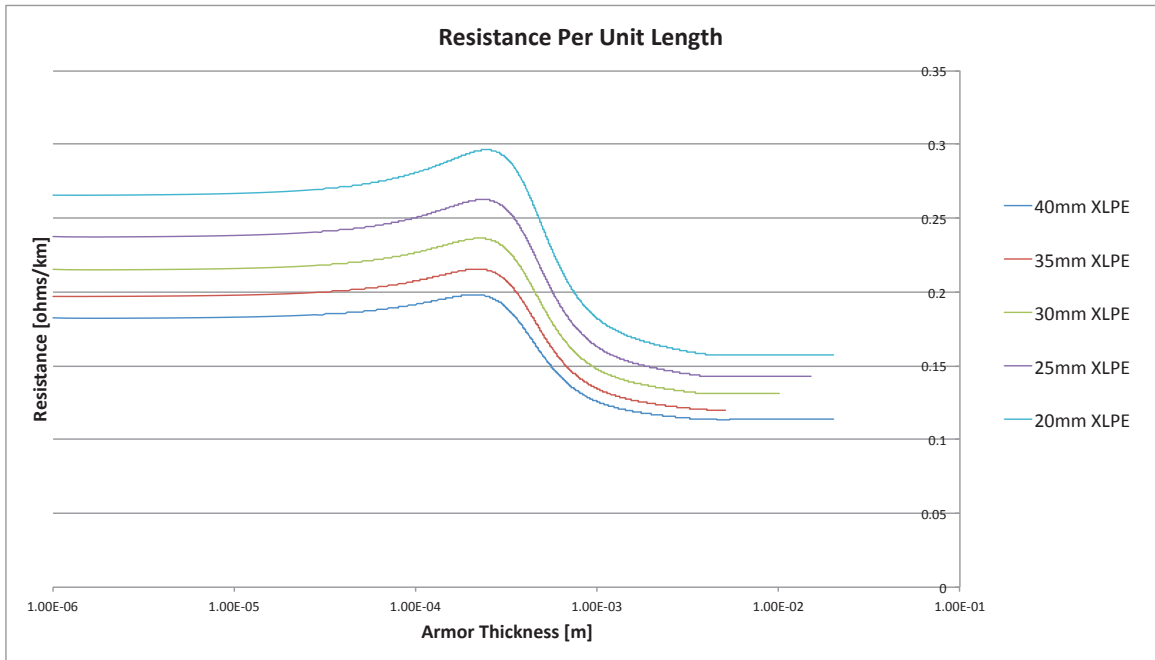


Figure 5-15: Resistance Per Unit Length As Armor Thickness Varies, 4mm Sheath

The results for the net cable inductance have the following characteristics: as the armor thickness is small the inductance is constant, as the thickness is further increased the inductance reaches a maximum, as the thickness is further increased the inductance will begin to decrease and reach another constant value. The constant inductance value when the armor is thin is smaller than when the inductance armor is thick. The insulation thickness affects the magnitude of the constant inductance when the armor is thin or thick, the magnitude of the maximum inductance, and which armor thickness results in the maximum inductance. As the thickness of insulation is increased the constant inductances when the armor is thin or thick increases; the maximum value of inductance is decreased, and the armor thickness that causes this maximum value of inductance is decreased. As the sheath thickness is increased the constant value of inductance when the armor is thin remains approximately the same, when the armor is thick the constant inductance decreases; the maximum value of inductance is decreased and the armor thickness that causes this maximum value of inductance is decreased.

The results for the net cable resistance have the following characteristics: when the armor thickness is small the resistance is constant. As the thickness is increased the resistance increases to a maximum; as the thickness is further increased the resistance increases and approaches a constant value. When the armor is thin the constant value of resistance is larger than when the armor is thick. As the insulation thickness is increased the constant resistance value when the armor is thin or thick decreases. Increasing the insulation thickness decreases how much the maximum resistance overshoots the resistance when the armor is thin; the increasing insulation thickness causes the maximum resistance

value to occur for a smaller armor thickness. The sheath thickness being increased causes a drop in resistance for all armor thicknesses, it also decreases the maximum resistance overshoot from the resistance value when the armor is thin.

Comparing both sets of results the following can be observed: when the armor is thin for both copper and steel armor the inductance and resistance have the same constant values. The maximum value of inductance and resistance is larger with copper armor. When the armor is thick the constant inductance and resistance is larger with steel armor.

5.1.3 Model Accuracy

In this analysis an assumption was made concerning the geometry of the seawater surrounding the cable. It was assumed that the water surrounding the cable was infinite. To find what an effectively infinite body of seawater is the proper assumption which models the sea impedance can be compared to the approximate model. The result can then be decomposed into two components quantifying the error associated with sea resistance and reactance. Subtracting the exact value of resistance or reactance from the approximate and dividing this difference by the exact value of resistance or reactance can find the percent error. This error will define the conditions for when the model used to analyze the submarine cables is accurate. Figures 5-16 and 5-17 show the percentage error of sea resistance and reactance respectively for different depths of seawater. From these figures it can be seen that the approximate model is accurate when the water depth is greater than 140m.

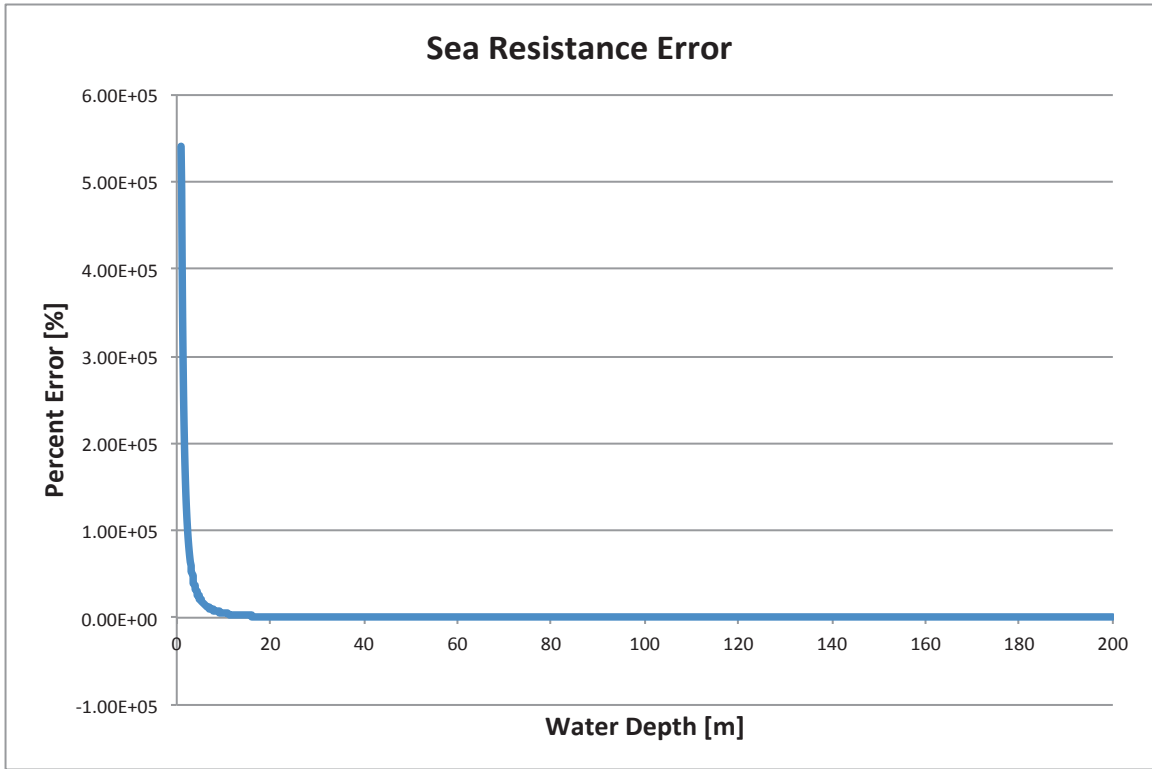


Figure 5-16: Resistance Error of Sea Water

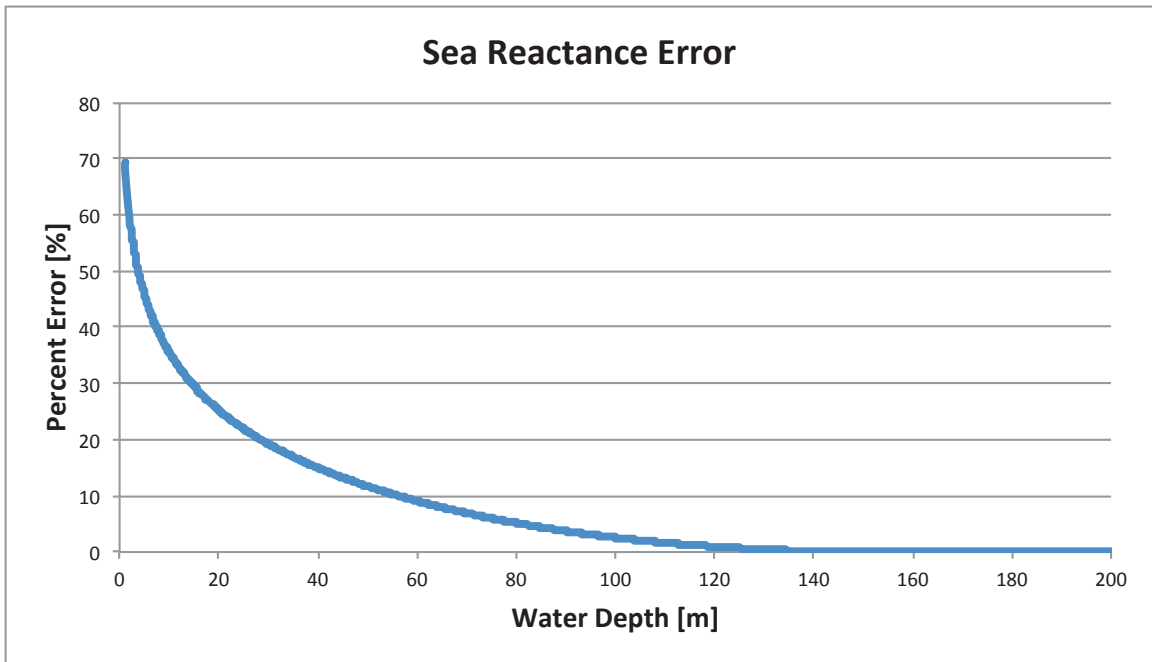


Figure 5-17: Reactance Error of Sea Water

5.2 Three-Core Cable Line Parameter Analysis

Analyzing three-core submarine cable line parameters involves a study of specific cases of cables that are commonly manufactured, as well as an analysis of how different cable layers affect the values of line parameters. In analyzing line parameters for a three-core submarine cable, a model for the magnetic field must first be developed. The subsequent sections analyze specific cases of manufactured cables as well as the relationship between how the material properties and thickness of the cable layers affect the line parameters.

The results of the analysis are then compared to overhead transmission lines. This comparison shows how dramatically different these kinds of cables are from overhead lines and single-core submarine cables. It is also illustrated how important the choice of materials and cable layering is for submarine cable design. The comparison between submarine cables and overhead lines is crucial in technical and economic studies of offshore wind platform options. In addition comparisons between submersed turbine/generator tidal/wave platform systems and in-water column options.

5.2.1 Magnetic Field Analysis

For three-core submarine cables, due to the complexity of the magnetic field that exists outside the three-core bundle, alternative means must be employed. With knowledge of the magnetic field, the inductance contribution from each of the cable layers can be found and distributed to have an equivalent per phase value. Figure 5-18 shows the magnetic field that exists inside the three-core cable. In this figure the different curves correspond to concentric circles at distances away from the three conductor and insulation bundle. The x-axis of Figure 5-18 corresponds to angular location on one of these concentric

circles. Figure 5-19 shows the magnetic field that exists outside of a single-core cable; each curve corresponds to a specific radial distance away from the cable center.

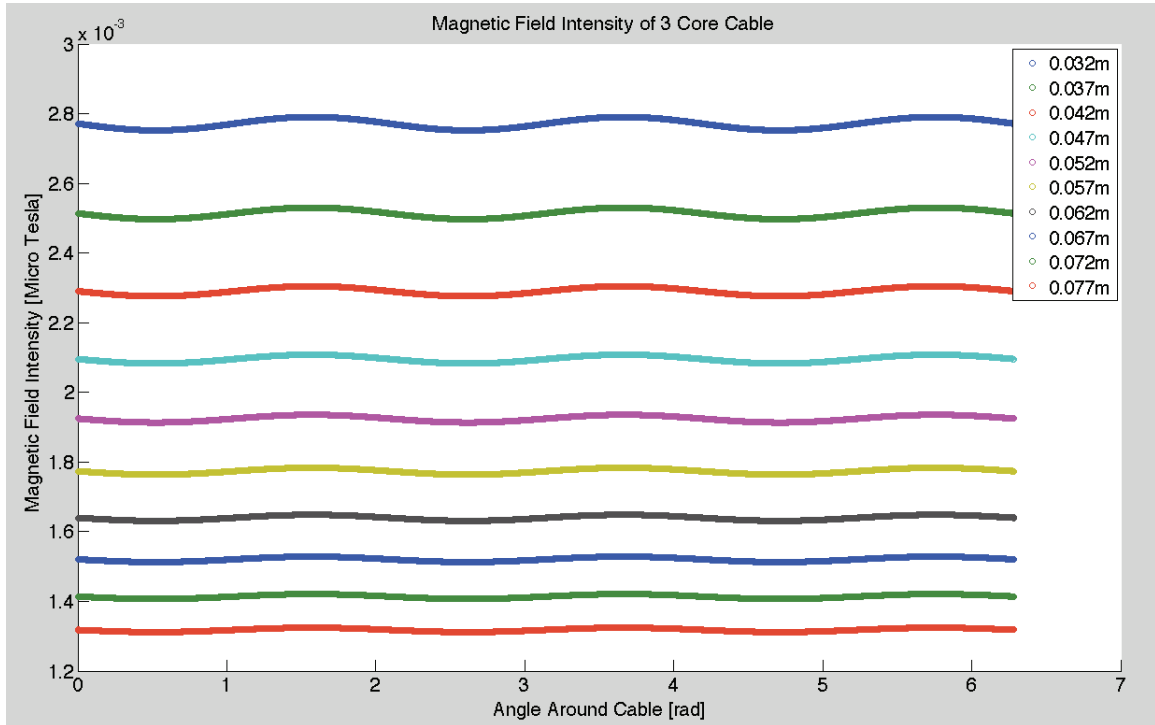


Figure 5-18: Magnetic Field Decay Surrounding Three-Core Cable

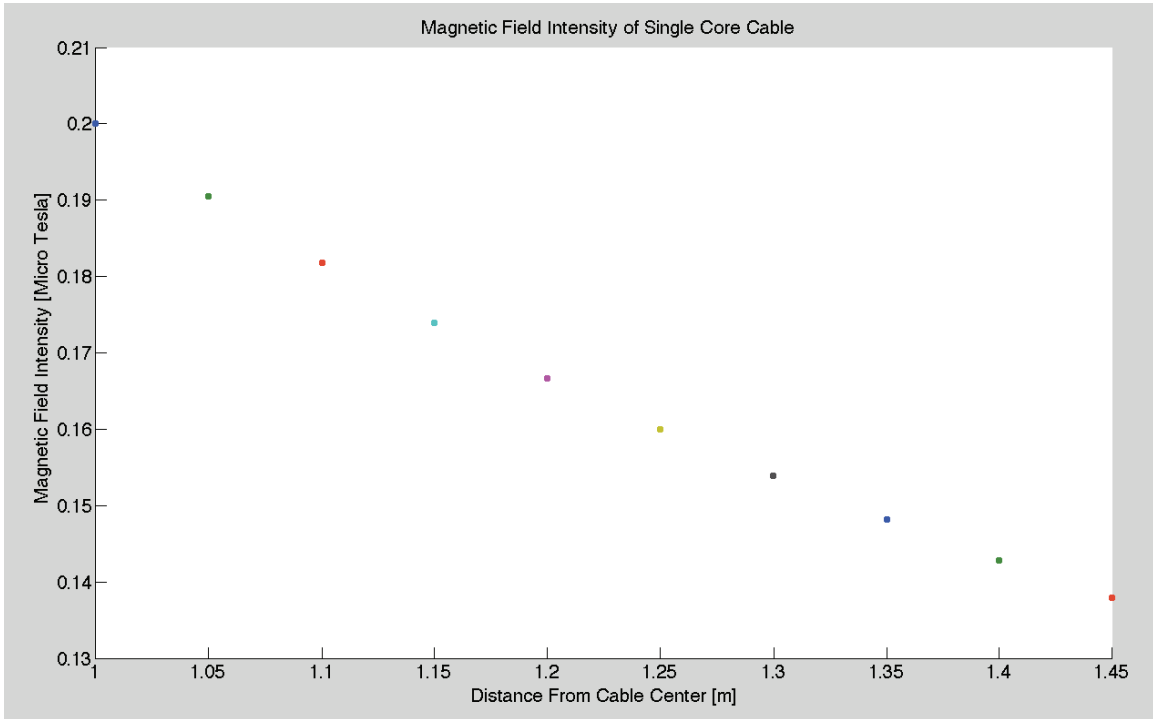


Figure 5-19: Magnetic Field Decay Surrounding Single-Core Cable

The magnitude of line current flowing through each conductor has been assumed to be 1 A. In each plot, the similarly colored point or curve corresponds to the same distance away from the cable center. It can be seen that the magnetic field outside the three-core cable bundle decays much faster than the case of a single-core cable. This is due to the fact that the sum of the currents in all of the phase conductors equals zero. So as the distance from the cable increases the magnetic field will decay much faster for the three-core cable than the single-core cable. This model for the magnetic field will be used in calculating the inductance and resistance of the different three-core cables.

5.2.2 Three Core Cable Line Parameters Case Study

To begin analyzing submarine transmission line parameters, some examples of cable geometry must be assumed. For this analysis some manufacturer specifications for different three-core cable geometries are used. The following different cable geometries will be used in the line parameter simulations:

Table 5-5: Different Cable Geometries, Three-Core Cable [1]

Cable Type	Conductor Radius [mm]	Insulation Thickness [mm]	Sheath Thickness [mm]	Radius Over Bundle [mm]	Armor Thickness [mm]
D	5.6	8	1.3	29.3	5
E	10.2	9	1.6	41.37	5
F	18.95	8	2.2	58.07	5

It is assumed that the insulation layers between the sheath and armor, and the armor and seawater are 1 mm in thickness. It has also been assumed that the individual cable phases are in the H configuration and have been spaced apart by 10 m. For the overhead transmission lines it has been assumed to have the same phase configuration with spacing of 10 m. All of the phase conductors are elevated 10 m from the ground. The core conductor properties are the same as that used for the submarine cables. This will provide a direct comparison between the two different cable types.

5.2.2.1 Submarine Cable Type D

Submarine cables that have three core conductors typically only use steel as the armor material due to the magnetic field incurring minimal losses in the steel. From the

geometry in Table 5-5 for Cable Type D, assuming a lead sheath and steel armor. The Line parameters can be found to be as follows: an inductance per unit length of 0.355mH/km, a capacitance per unit length of 1.567 μ F/km, and resistance per unit length of 0.189 Ω /km. For a set of overhead cables the line parameters will be as follows: an inductance per unit length of 1.5475mH/km, a capacitance per unit length of 7.79nF/km, and a resistance per unit length of 0.189 Ω /km. A summary of these line parameters is given in Table 5-6.

Table 5-6: Cable Type D Line Parameters

Line Parameter	Submarine Cable	Overhead Cable
Inductance [mH/km]	0.355	1.5475
Capacitance [μ F/km]	0.1567	0.00779
Resistance [m Ω /km]	189	189

5.2.2.2 Submarine Cable Type E

From the geometry in Table 5-5 for Cable Type E, assuming a lead sheath and steel armor. The Line parameters can be found to be as follows: an inductance per unit length of 0.308mH/km, a capacitance per unit length of 0.22 μ F/km, and resistance per unit length of 32.75m Ω /km. For a set of overhead cables the line parameters will be as follows: an inductance per unit length of 1.427mH/km, a capacitance per unit length of 8.504nF/km, and a resistance per unit length of 32.75 m Ω /km. A summary of these line parameters is found in Table 5-6.

Table 5-7: Cable Type E Line Parameters

Line Parameter	Submarine Cable	Overhead Cable
Inductance [mH/km]	0.308	1.427
Capacitance [μ F/km]	0.22	0.008504
Resistance [m Ω /km]	32.75	32.75

5.2.2.3 Submarine Cable Type F

From the geometry in Table 5-5 for Cable Type F, assuming a lead sheath and steel armor. The Line parameters can be found to be as follows: an inductance per unit length of 0.253mH/km, a capacitance per unit length of 0.395 μ F/km, and resistance per unit length of 17.63m Ω /km. For a set of overhead cables the line parameters will be as follows: an inductance per unit length of 1.304mH/km, a capacitance per unit length of 9.394nF/km, and a resistance per unit length of 17.63 m Ω /km. A summary of these line parameters is found in Table 5-7.

Table 5-8: Cable Type F Line Parameters

Line Parameter	Submarine Cable	Overhead Cable
Inductance [mH/km]	0.253	1.304
Capacitance [μ F/km]	0.395	0.009394
Resistance [m Ω /km]	17.63	17.63

Chapter 6: Submarine Transmission Line Performance Analysis

The performance of a transmission line is important in determining what the output voltage and power (at the receiving end) of a transmission link will be like, given an input (sending end) conditions. The steady state response and transient response are two aspects that must be considered when dealing with line performance. The steady state response consists of analyzing the output voltage, active power, power factor, efficiency, and voltage regulation when the line is operating under sinusoidal steady state conditions. These values determine how the transmission line transforms power from the sending end to receiving end, and how sensitive the receiving end voltage is to load variations. The transient analysis is important to determine the voltage overshoot and oscillations that may occur under switching conditions. These two sets of results determine how well the transmission line performs.

6.1 Steady State Analysis

The steady state analysis of a transmission line involves finding the two-port parameters from the line parameters. Once the two-port parameters have been found, the receiving end voltage, power, line regulation, and efficiency can be found given the conditions at the sending end. This determines how the transmission line transforms the input power and voltage, how much energy is dissipated, and how sensitive the receiving end voltage is when the load changes. The steady state analysis will be done for three cable types, one single-core cable with copper armor, the same single-core cable except with steel armor, and one three-core cable. The cables that will be analyzed are the ones used in

chapter 5 when studying line parameters, Cables Type B and E. These steady state values will be plotted against the equivalent overhead transmission line values. Table 6-1 shows the line parameters, which will be used for each of the cable types.

Table 6-1: Line Parameters Per Unit Length for Cable Type B and E

Cable Type	Inductance [mH/km]	Capacitance [μ F/km]	Resistance [m Ω /km]
B, copper	0.29713	0.1522	38.1557
B, steel	0.41495	0.1522	139.44
B, overhead	1.398	0.0089142	21.294
E, three-core	0.308	0.22	32.75
E, overhead	1.427	0.008504	32.75

For steady state analysis, only two cable types will be analyzed. The performance indices which will be obtained for various transmission line lengths are the following: receiving end impedance and impedance angle, receiving end voltage and voltage angle, receiving end power, receiving end reactive power, receiving end power factor, receiving end efficiency, and the receiving end voltage regulation.

6.1.1 Submarine Cable Type B Performance

Figures 6-1 through 6-9 show the plots for these performance indices for various line lengths of cable type B.

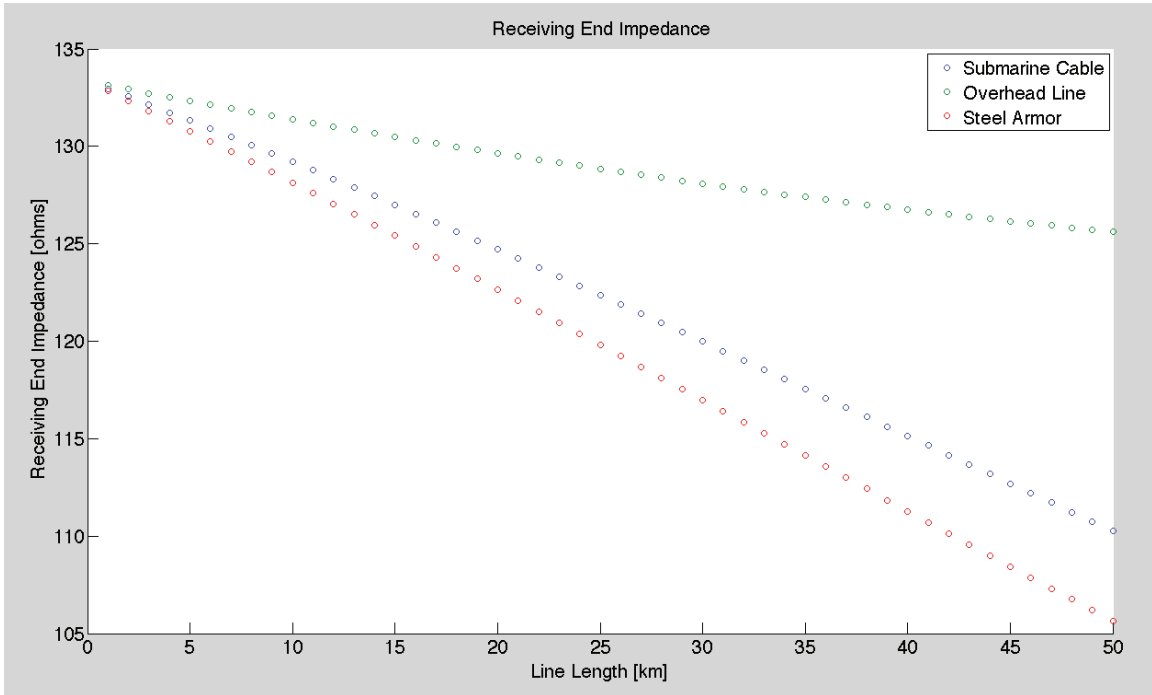


Figure 6-1: Receiving End Impedance Magnitude, Cable Type B

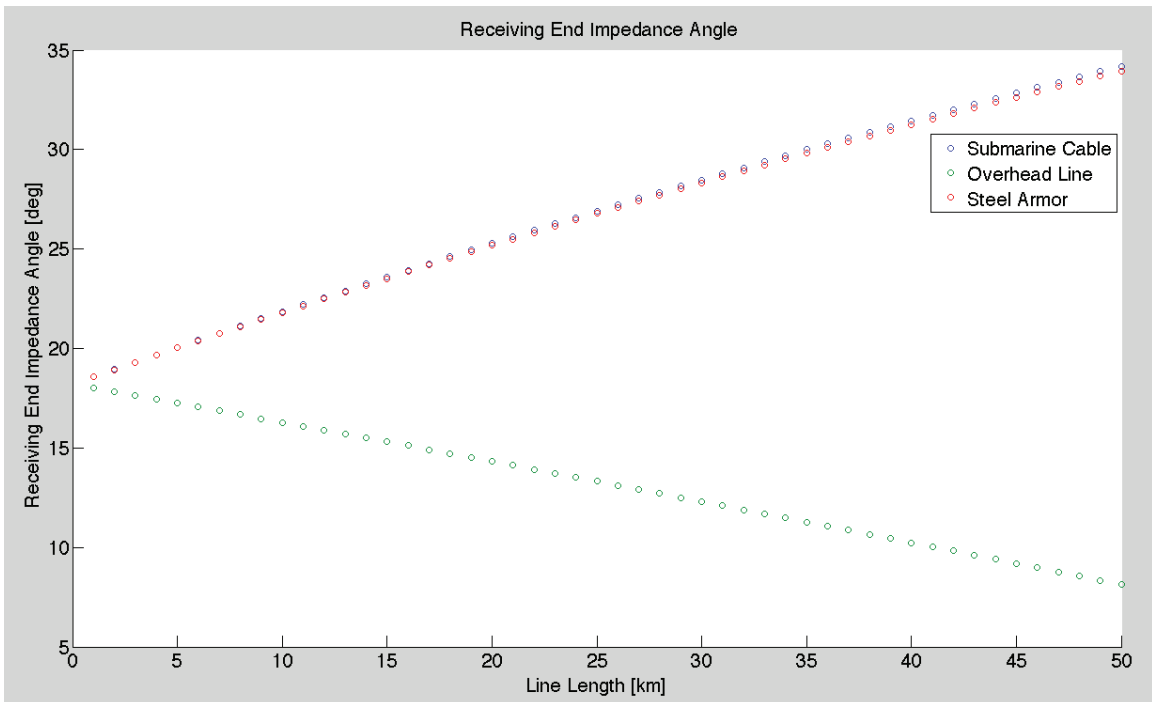


Figure 6-2: Receiving End Impedance Angle, Cable Type B

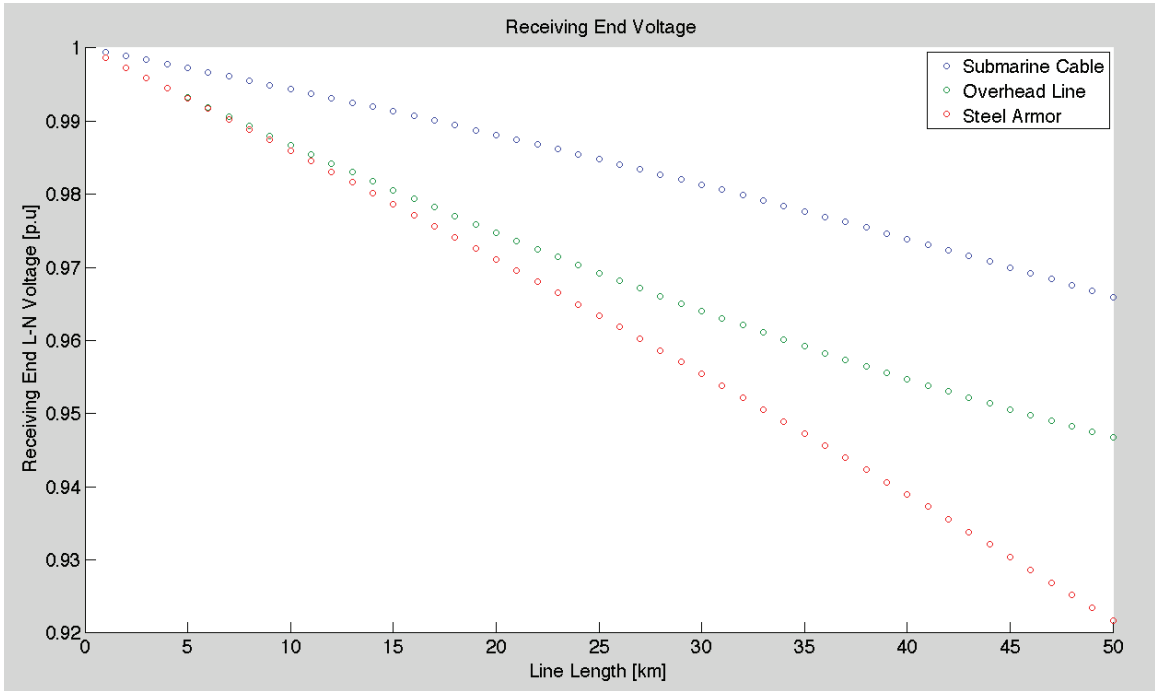


Figure 6-3: Receiving End Voltage Magnitude, Cable Type B

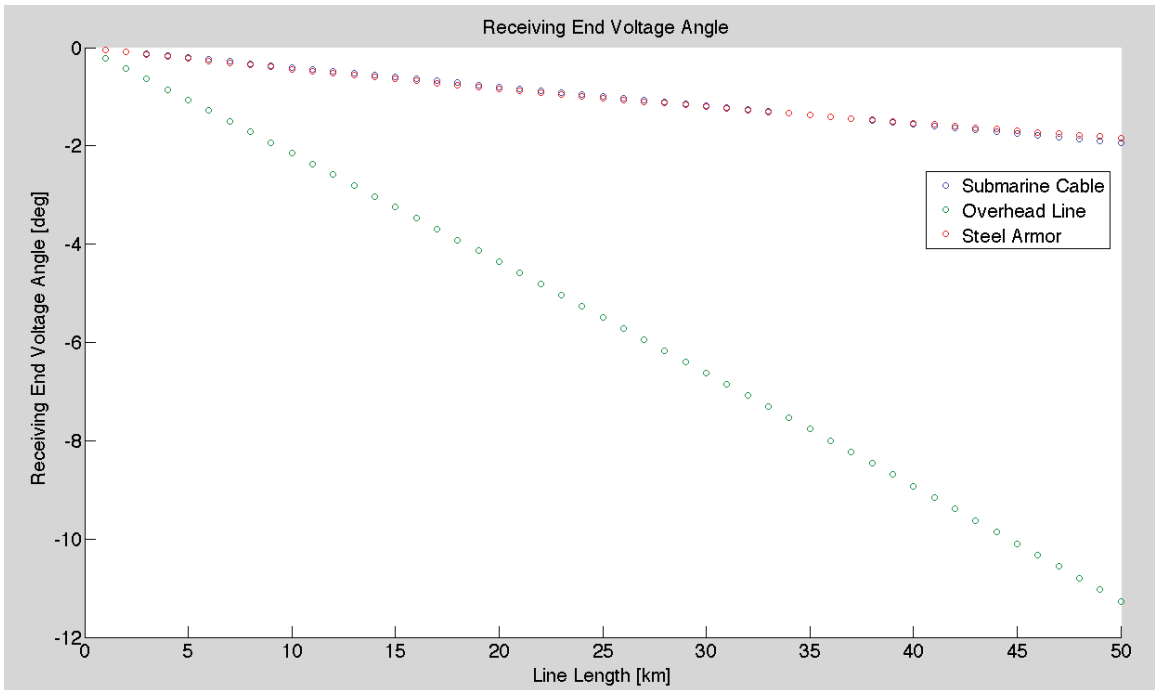


Figure 6-4: Receiving End Voltage Angle, Cable Type B

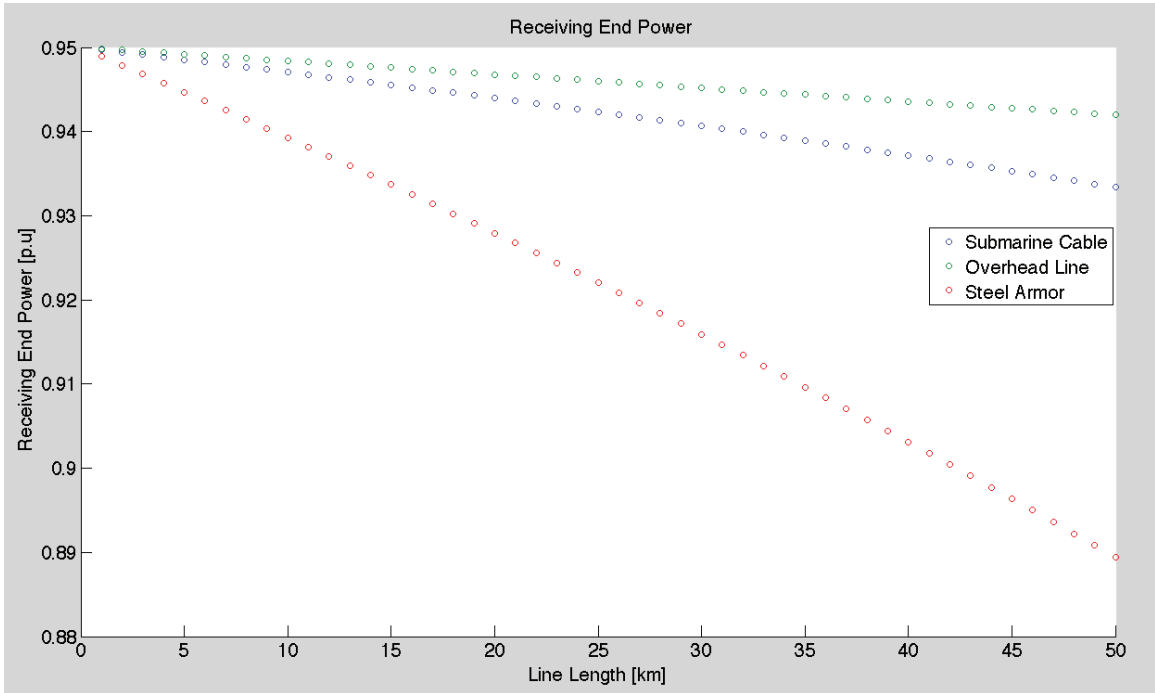


Figure 6-5: Receiving End Power, Cable Type B

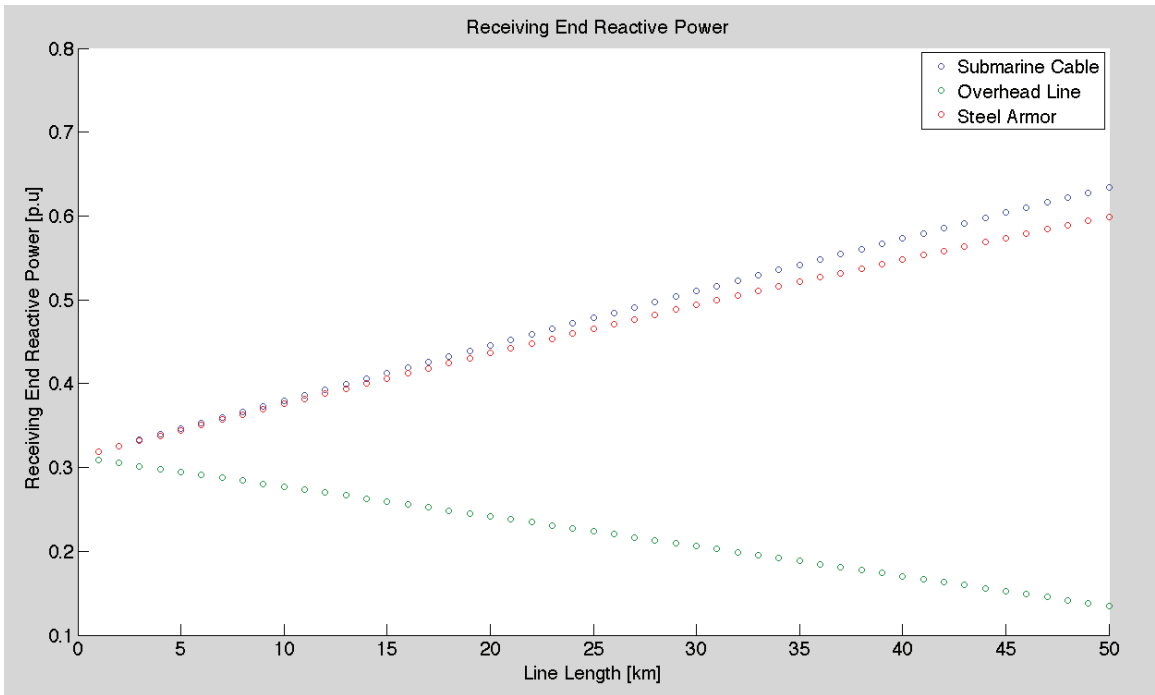


Figure 6-6: Receiving End Reactive Power, Cable Type B

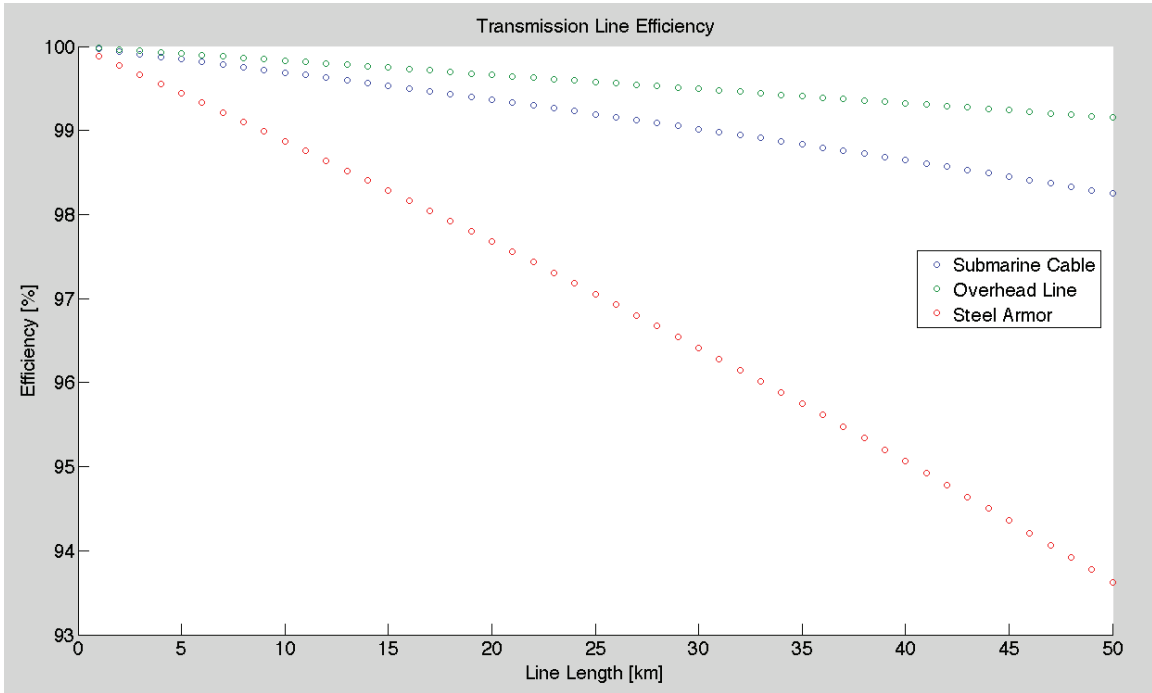


Figure 6-7: Transmission Line Efficiency, Cable Type B

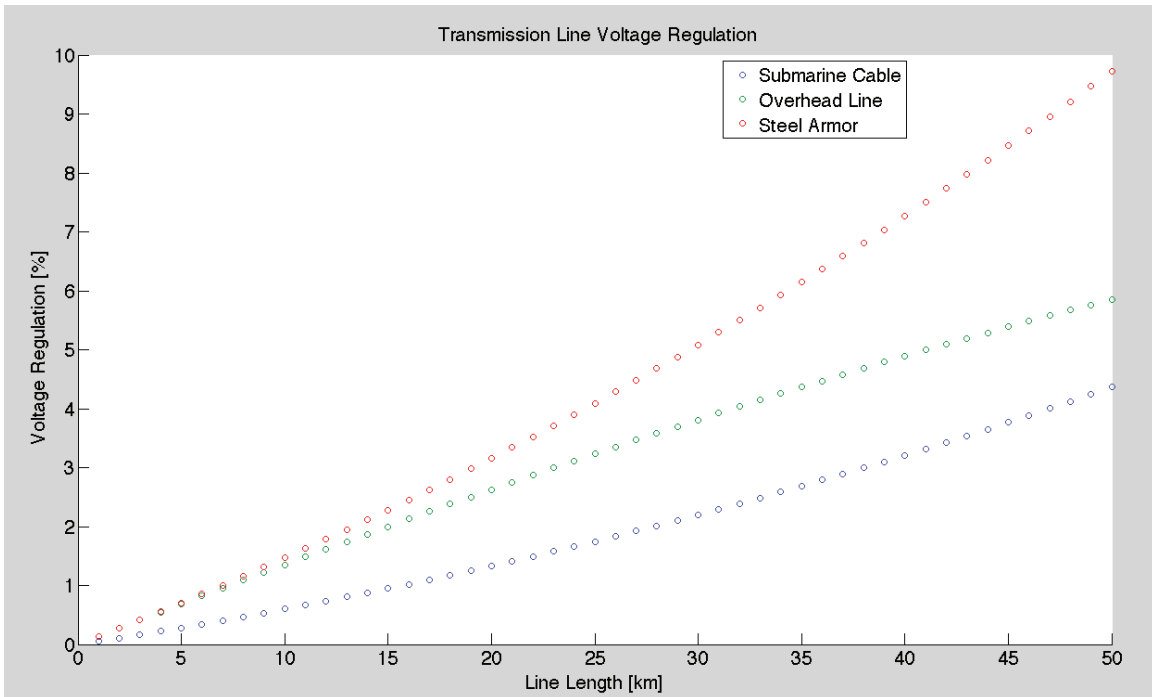


Figure 6-8: Transmission Line Voltage Regulation, Cable Type B

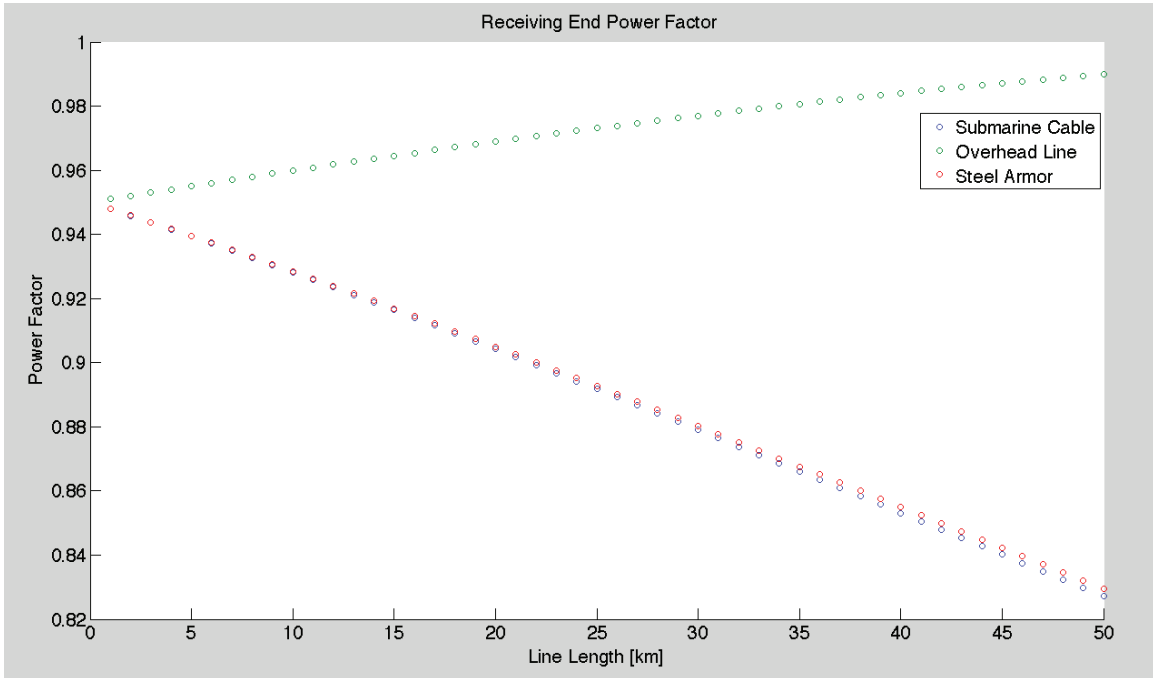


Figure 6-9: Receiving End Power Factor, Cable Type B

The specifications of the sending end are: the sending end three phase voltage of 20 kV, the sending end power was 3 MVA with a 0.95 power factor lagging, voltage frequency of 60Hz. From the results obtained, the following conclusions can be made: the receiving end voltage magnitude for copper armor submarine cables is less affected by transmission line length than iron armor submarine cables and overhead transmission lines; where iron armored submarine cables have the largest receiving end voltage drop. The receiving end voltage angle for copper and iron armor submarine cables is approximately the same for the different line lengths; the voltage angle for overhead lines decreases significantly. Overhead transmission lines are most efficient while iron armor submarine cables are significantly less efficient. The submarine cables provide reactive power to the output, which means that they are capacitive dominant transmission lines. The overhead line absorbs reactive power, which means it is an inductive dominant transmission line. The

voltage regulation for the iron armor submarine cable is the worst, while the voltage regulation for the copper armor submarine cable is best.

6.1.2 Submarine Cable Type E Performance

For Cable Type E the various performance indexes can be seen in Figures 6-10 through 6-18 for various transmission line lengths.

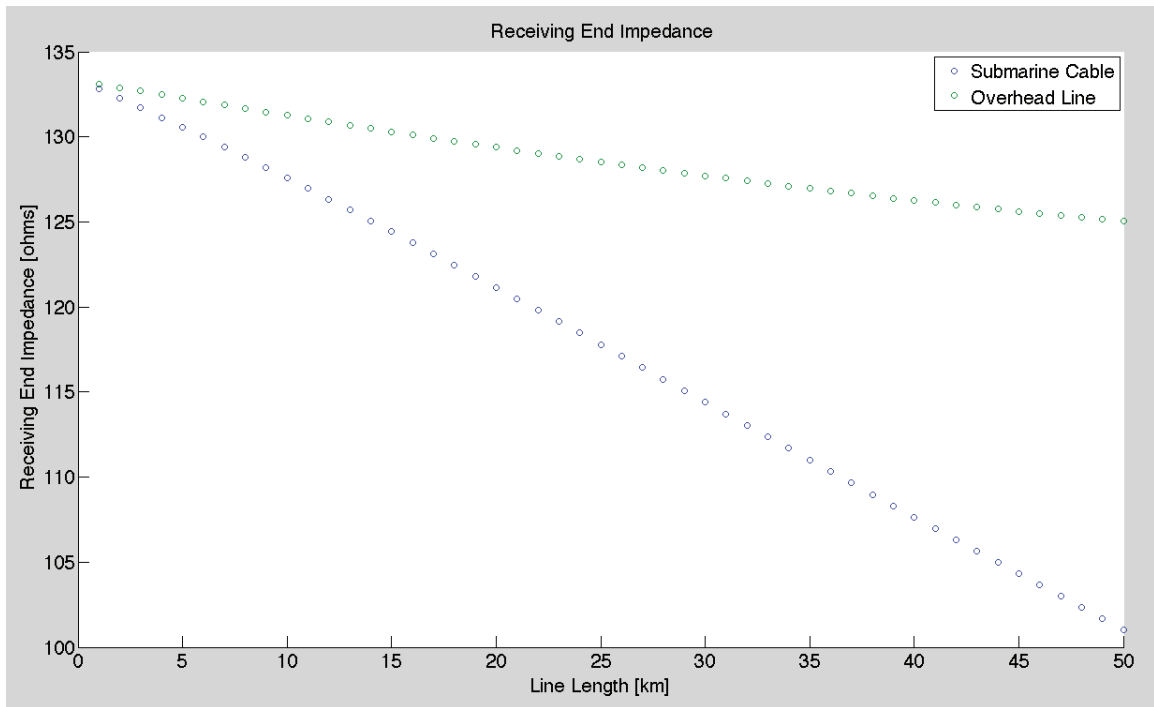


Figure 6-10: Receiving End Impedance Magnitude, Cable Type E

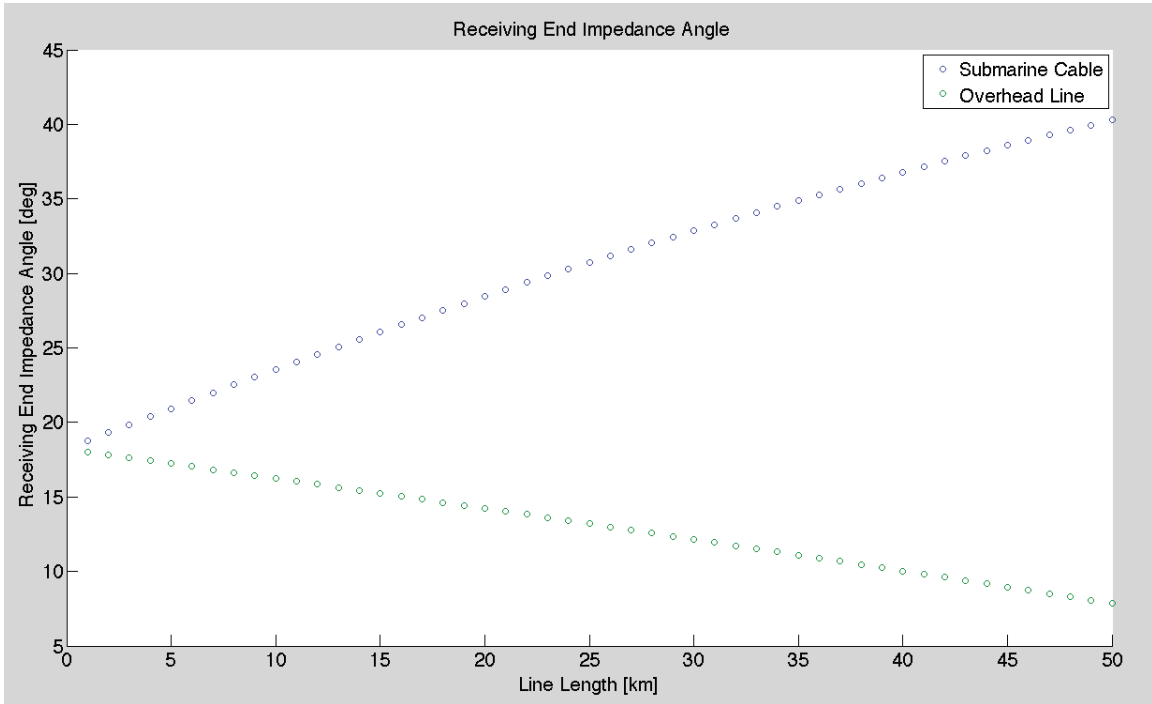


Figure 6-11: Receiving End Impedance Angle, Cable Type E

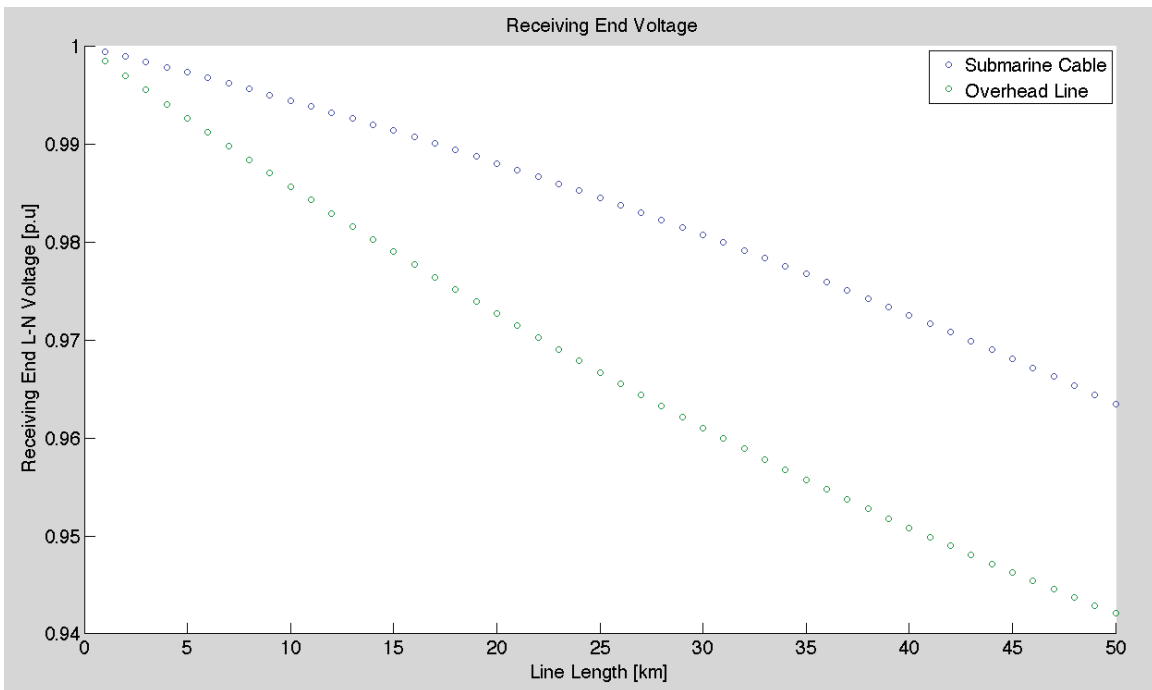


Figure 6-12: Receiving End Voltage Magnitude, Cable Type E

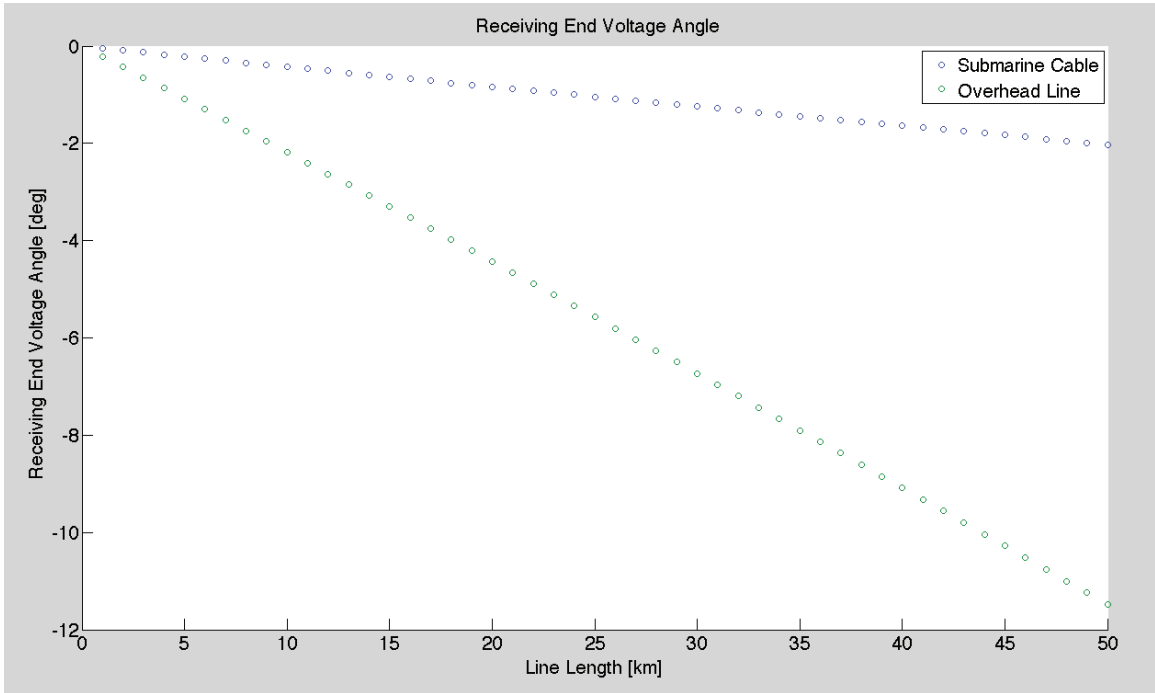


Figure 6-13: Receiving End Voltage Angle, Cable Type E

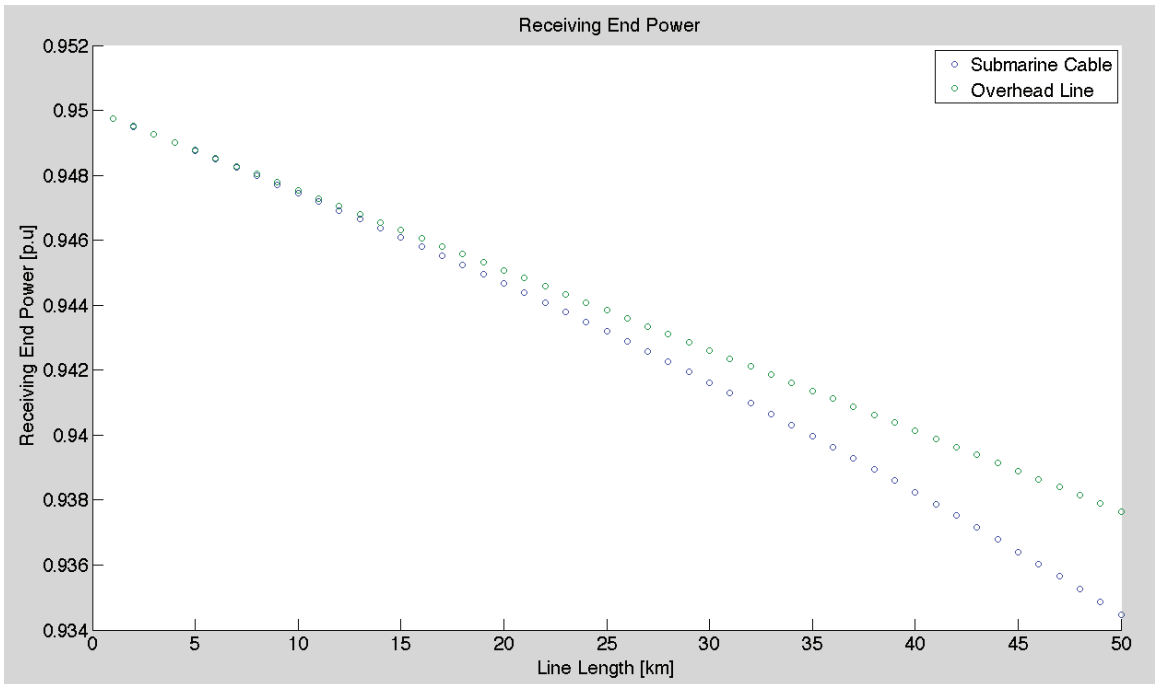


Figure 6-14: Receiving End Power, Cable Type E

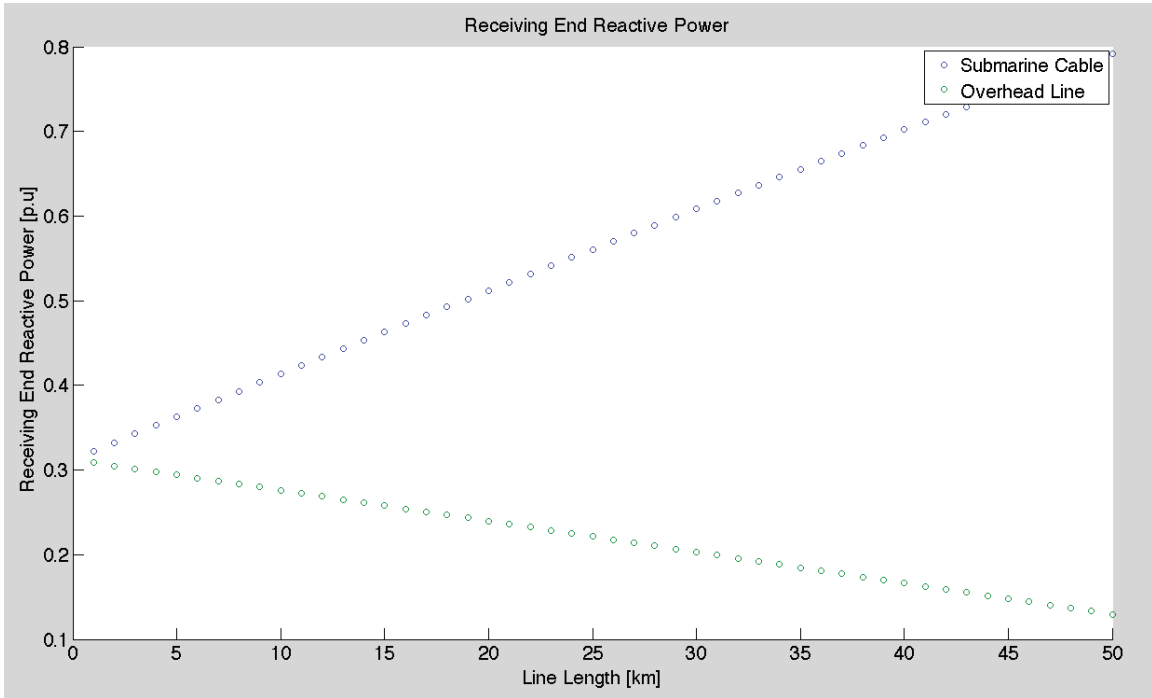


Figure 6-15: Receiving End Reactive Power, Cable Type E

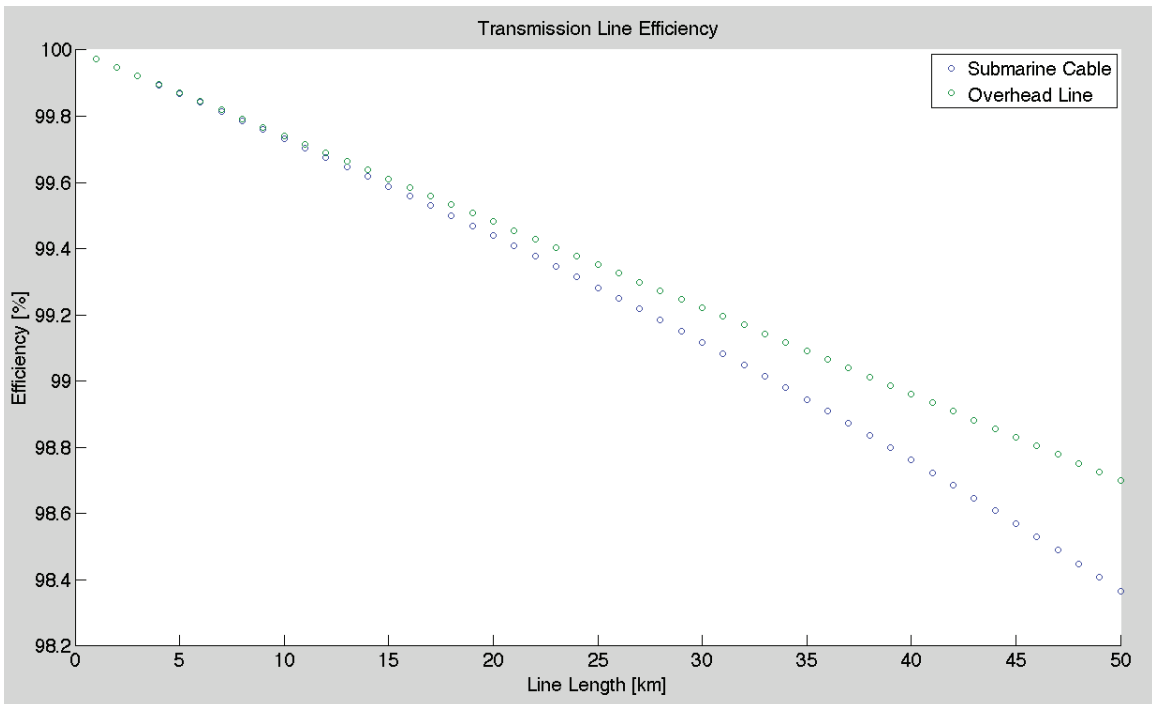


Figure 6-16: Transmission Line Efficiency, Cable Type E

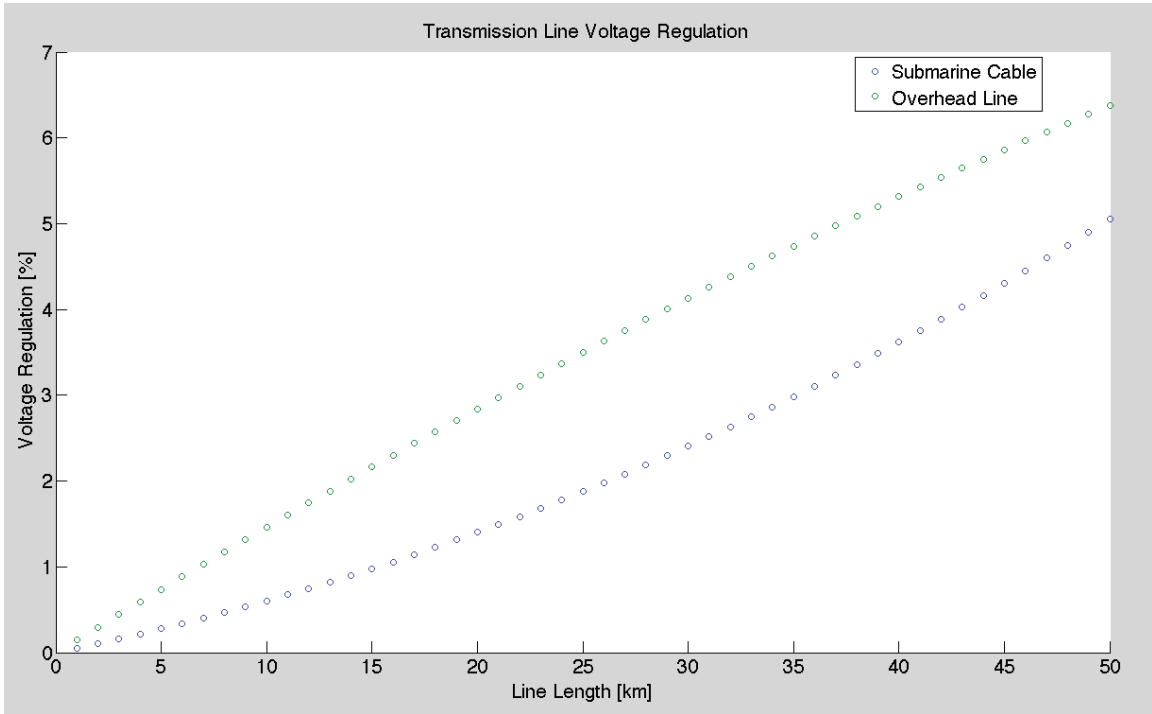


Figure 6-17: Transmission Line Voltage Regulation, Cable Type E

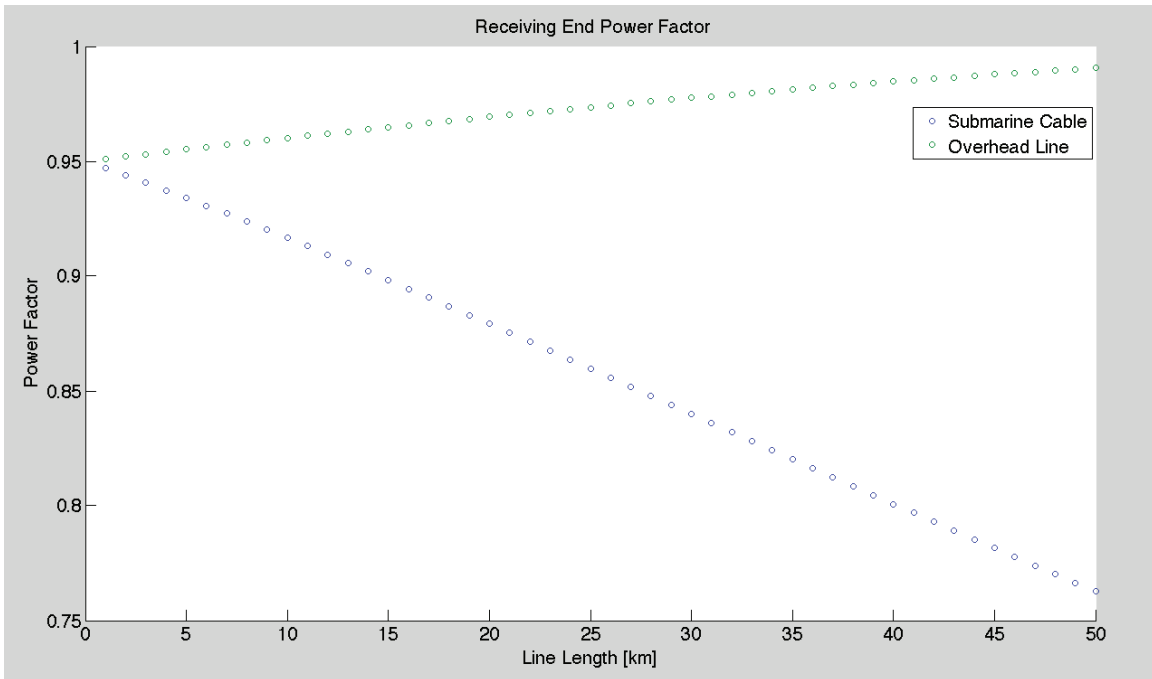


Figure 6-18: Receiving End Power Factor, Cable Type E

This result shows that three core submarine cables are less efficient than overhead transmission lines however have a better voltage regulation. Similar results are obtained as when the single-core cables were compared to the overhead transmission lines.

6.2 Transient Analysis

The transient analysis is performed for the transmission line to determine what inrush of power is required to charge the transmission line, and what the corresponding spike in voltage will be. The transient flow of power for the transmission line has been modeled under the following assumptions, three-phase generator voltage of 20kV, line length of 30km, generator voltage phase angle of 0 degrees. Figures 6-19 to 6-21 show the transient responses of the system. The second transient response that is performed is when the generator voltage phase angle is 30 degrees. This means that the generator is connected to the transmission line when the voltage is non-zero. This will result in a more drastic transient response with large transient power draw and voltage overshoot. Figures 6-22 to 6-24 show this transient response when the generator voltage phase angle is 30 degrees.

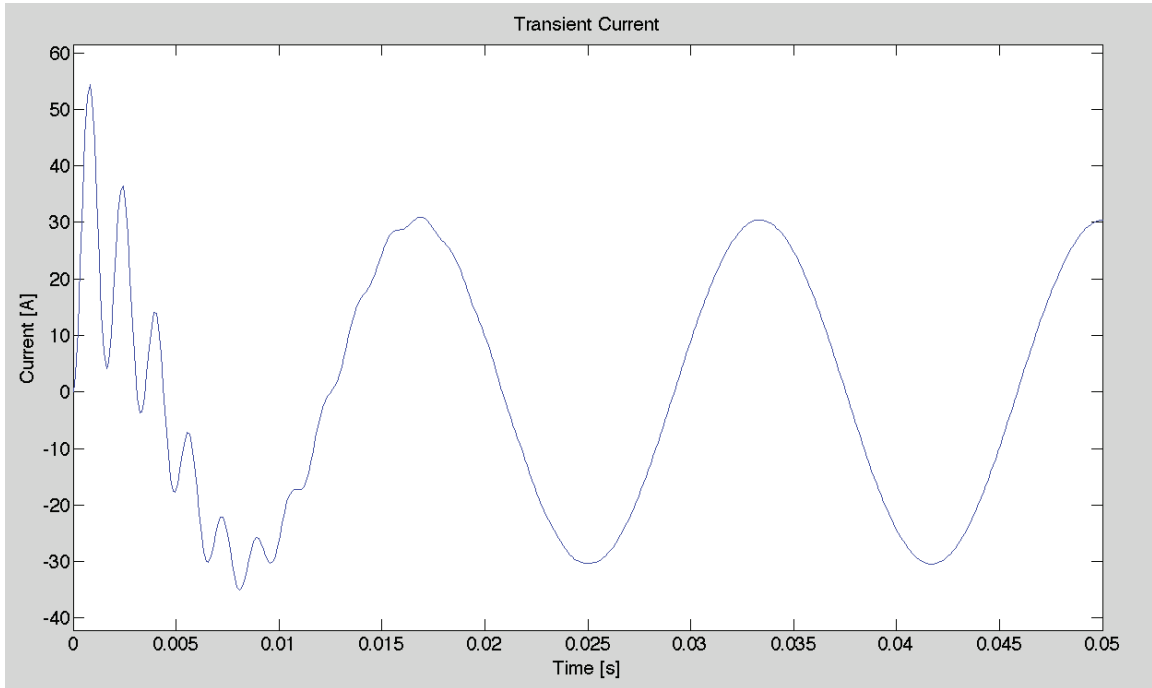


Figure 6-19: Transient Current Flow at 0° Phase Angle

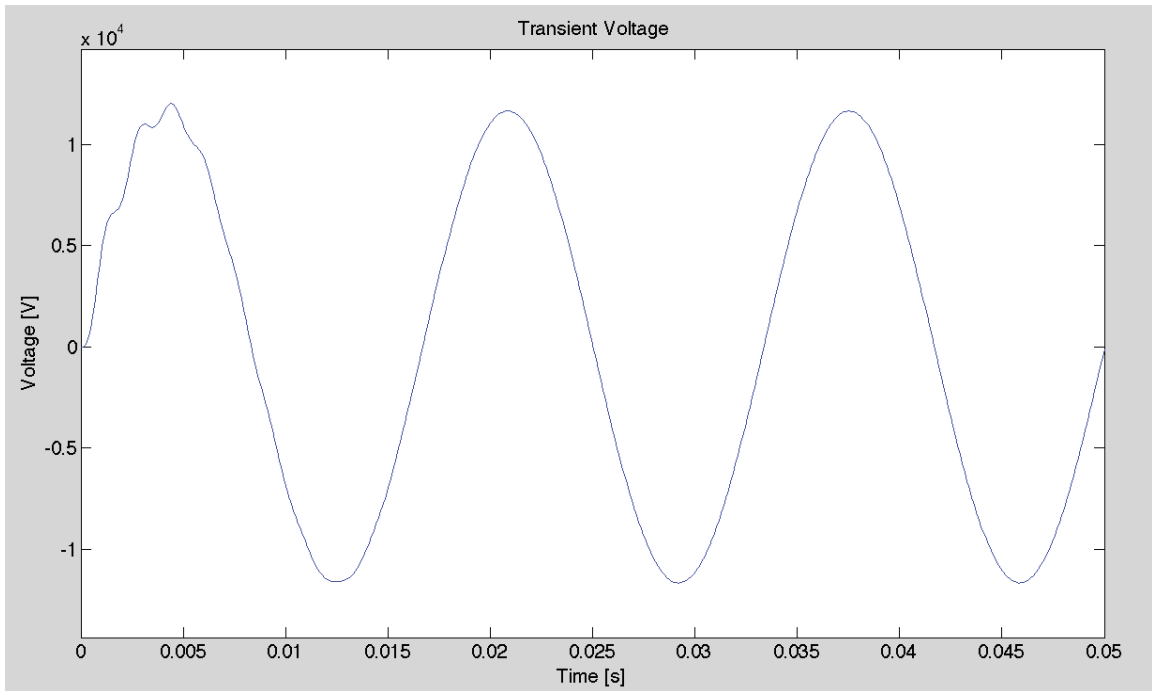


Figure 6-20: Transient Receiving End Voltage at 0° Phase Angle

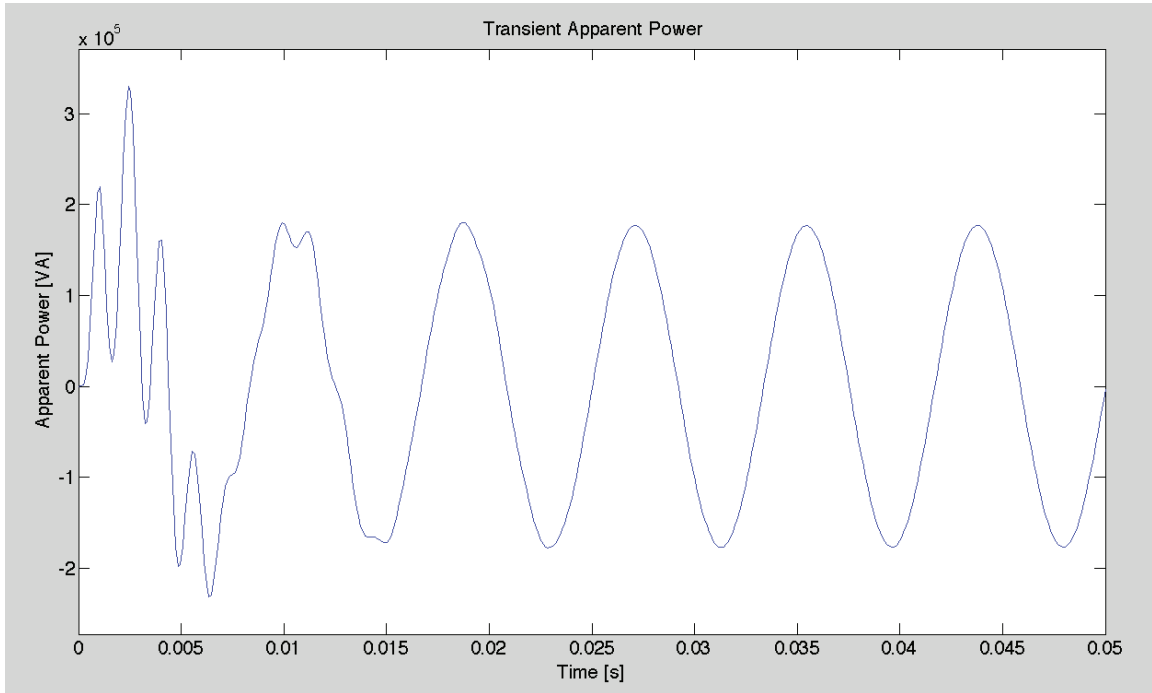


Figure 6-21: Transient Apparent Power at 0° Phase Angle

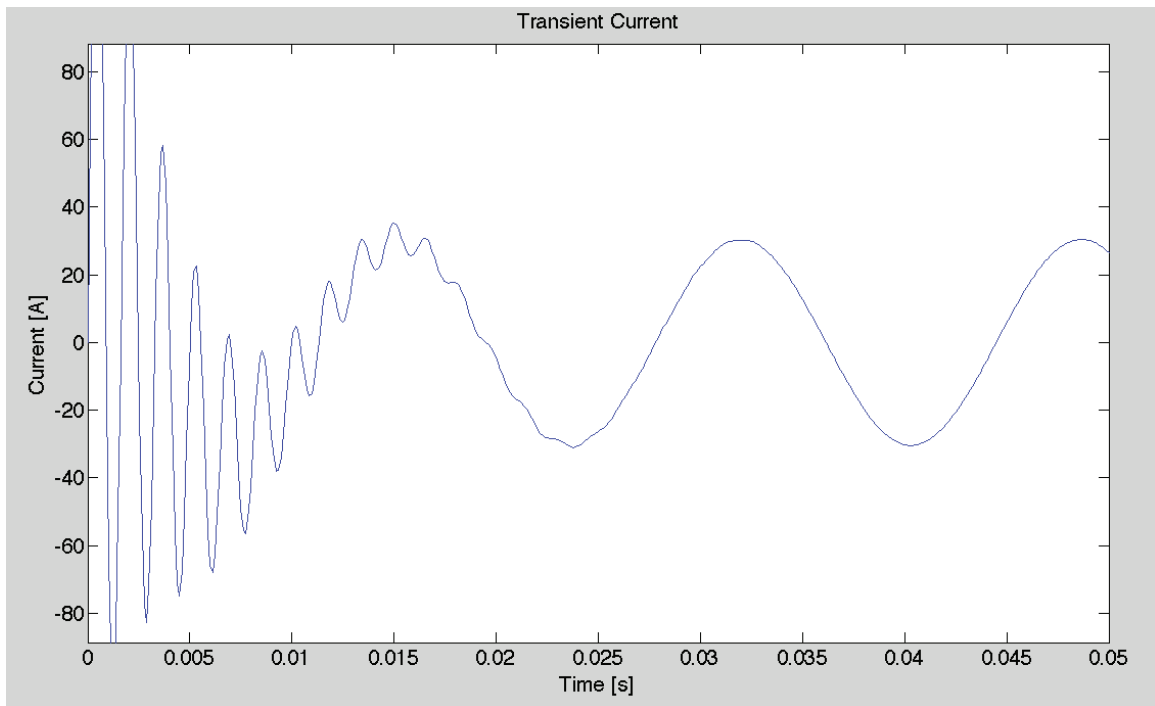


Figure 6-22: Transient Current Flow at 30° Phase Angle

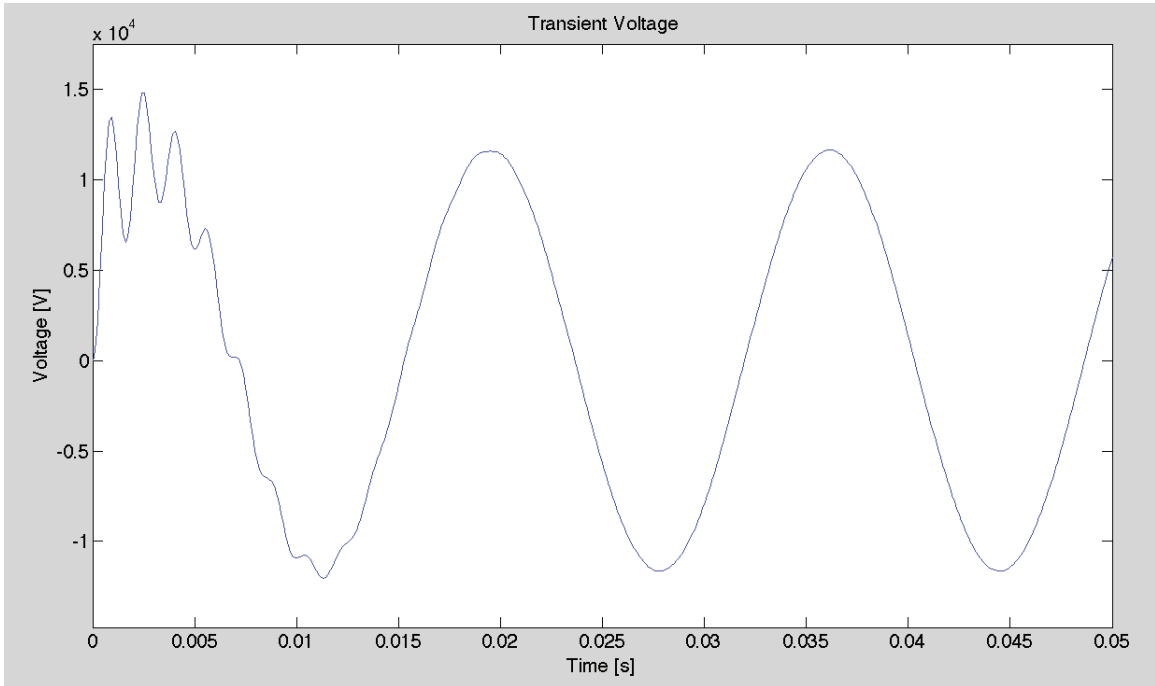


Figure 6-23: Transient Receiving End Voltage at 30° Phase Angle

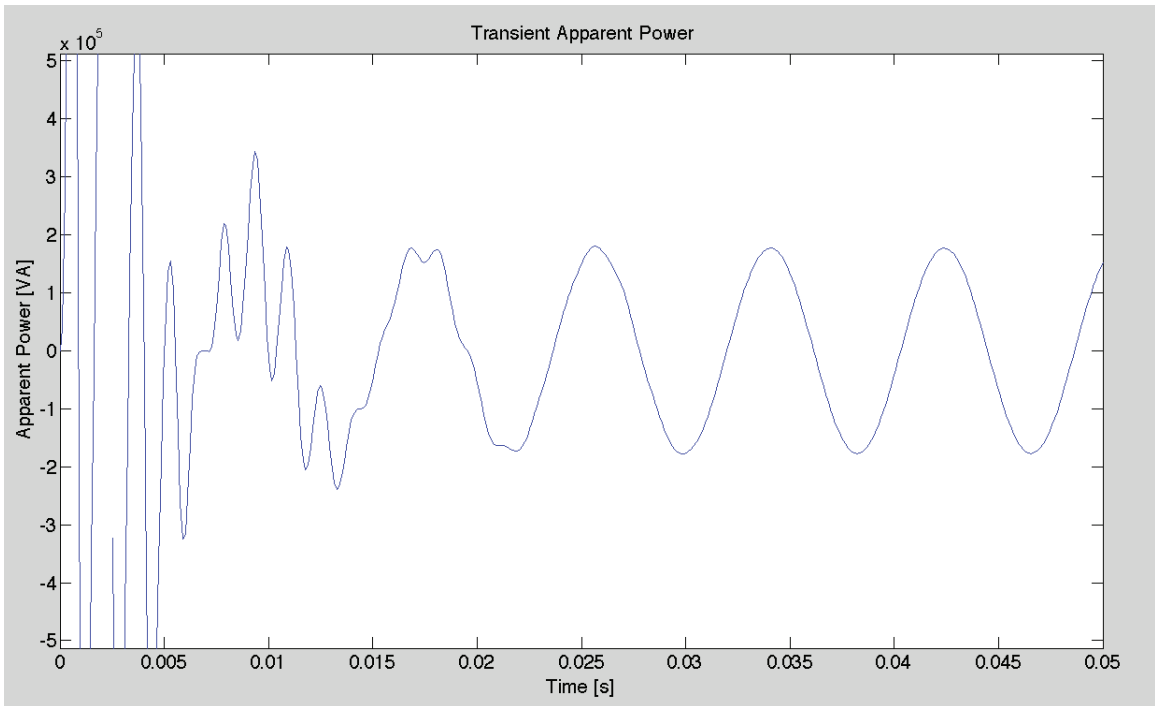


Figure 6-24: Transient Apparent Power at 30° Phase Angle

These results show the transient power flow from the generator along with the voltage overshoot that occurs at the receiving end of the transmission line. The knowledge of the transients is important for determining system protection relay settings, and knowledge about the harmonics that may exist as part of switching. It can be seen from the figures that the receiving end voltage overshoot is larger and more prolonged for greater generator voltage phase angles.

Chapter 7: Conclusion and Future Work

This Chapter summarizes the results obtained in this thesis and the contributions that were made. Future work suggestions are also discussed.

7.1 Conclusions

In this thesis, the transmission line parameters for various submarine cable types have been found and their performance analyzed. In Chapter 2, a discussion about the various submarine cable types was presented, along with a generic geometrical model for the different cable types. In Chapter 3, the electromagnetic field analysis to find line parameters for submarine cables was presented. In Chapter 4, the basics of steady state and transient state performance analysis were presented. In Chapter 5, numerical analysis to find submarine cable line parameters was performed for various cable types. The results obtained revealed the significance that the material type and geometry for the various cable layers have on the line parameters. It was found that for a single core submarine cable, using steel armor instead of copper armor resulted in a larger resistance and inductance. Increasing the insulation thickness causes an increase in inductance, decrease in resistance, and decrease in capacitance. These results for the line parameters are compared with those for overhead transmission lines. This is done to show just how different the two types of transmission media are. In Chapter 6, numerical analysis to determine the performance of various submarine cable types was performed. This analysis provides information about the volatility of the receiving end voltage, the efficiency of the line, and the quality of the received power. This analysis is also performed for overhead transmission lines, again to show how the performance of the

submarine cable is much different from that of an overhead line. Increasing the insulation thickness causes the power factor to increase, voltage regulation increase, efficiency increase, and a receiving end voltage decrease. Changing the armor material from copper to steel results in a decreased power factor, increased voltage regulation, decreased efficiency, and a decreased receiving end voltage.

7.2 Future Work

The findings from this study imply that more work can be done in finding a means to design specific cables for specific applications, and that the inductance and capacitance of the cable can be designed to be a specific value. For future work, a more direct relationship between the line parameter values and geometry of the cable could be formulated. Also, additional layers of material could be added to the cable, which have no purpose besides to change the line parameters of the cable. A means as to how to choose these materials and their geometry could be explored.

References

- [1] “XLPE Submarine Cable Systems Attachment to XLPE Land Cable Systems – User’s Guide”, ABB, 2010
- [2] Worzyk, T, “Submarine Power Cables Design, Installation, Repair, Environmental Aspects”, Springer, Heidelberg, Berlin, 2009
- [3] El-Hawary, M.E, “Electrical Power Systems Design and Analysis”, IEEE Press, New York, NY, 1995
- [4] Sadiku, M.N.O, “Elements of Electromagnetics” Fourth Edition, Oxford University Press, New York, NY, 2007
- [5] Bianchi, G, Luoni, G, “Induced Currents and Losses in Single-Core Submarine Cables”, IEEE Transactions on Power Apparatus and Systems Vol. PAS-95, no. 1, 1976
- [6] Schelkunoff, S.A, “The Electromagnetic Theory of Coaxial Transmission Lines and Cylindrical Shields”, Bell System Technical Journal, vol. XIII (1934), pp. 532-578
- [7] Tranter, C.J, “Bessel Functions with some Physical Applications”, Hart Publishing Company, Inc., New York, NY, 1969
- [8] Carson, John R., Gilbert, J.J., “Transmission Characteristics of the Submarine Cable”, Bell System Technical Journal, Journal of the Franklin Institute, December 1921
- [9] Greenwood, Allan, “Electrical Transients in Power Systems”, Wiley-Interscience, United States, 1971
- [10] Hayt, William H. Jr., Kemmerly, Jack E., Durbin, Steven M., “Engineering Circuit Analysis,” Seventh Edition”, Mc-Graw Hill, New York, NY, 2007
- [11] Zaborszky, John, Rittenhouse, Joseph W., “Electric Power Transmission”, The Ronald Press Company, New York, 1954
- [12] Arrillaga, J., Bradley, D.A., Bodger, P.S., “Power System Harmonics”, Wiley-Interscience, 1985
- [13] Bickford, J.P., Mullineux, N., Reed, J.R., “Computation of Power System Transients”, Peter Peregrinus Ltd., Stevenage, Herts. SG1 1HQ, England, 1976
- [14] Paul, Clayton R., “Introduction to Electromagnetic Compatibility”, Wiley-Interscience, United States, 1992
- [15] Kirtley Jr., James L., “Class Notes 3: Eddy Currents, Surface Impedances and Loss Mechanisms”, Massachusetts Institute of Technology, September 2005

[16] McDonald, Kirk T., “An Off-Center “Coaxial” Cable”, Joseph Henry Laboratories, Princeton University, 1999

[17] Ohman, Marcus C., Sigray, Peter, Wsterberg, Hakan, “Offshore Windmills and the Effects of Electromagnetic Fields on Fish”, Royal Swedish Academy of Sciences, 2007

[18] Tricas, Timothy, Gill, Andrew, “Effects of EMFs From Undersea Power Cables On Elasmobranchs and Other Marine Species”, Normandeau Associates, Inc., 2011